# Influence of Grazing on Vegetation, Surface Energy and Water Balance over the Mongolian Steppe

**January, 2007**

**Hidekazu KATO**

# Influence of Grazing on Vegetation, Surface Energy and Water Balance over the Mongolian Steppe

A Dissertation Submitted to

the Graduate School of Life and Environmental Sciences,

the University of Tsukuba

in Partial Fulfillment of the Requirements

for the Degree of Master of Science

(Doctoral Program in Geoenvironmental Sciences)

**Hidekazu KATO**

# Contents

**Page**

**Abstract** ····· ii

**List of Tables** ····· iv

**List of Figures** ····· v

**Chapter 1 Introduction** ····· 1

1-1. General background

1-2. Previous studies

**Chapter 2 Methods** ····· 4

2-1. Site information

2-2. Measurements

2-2-1. Meteorological and hydrologic measurements

2-2-2. Grazing intensity

2-2-3. Vegetation

2-3. Data processing

2-3-1. Roughness length

2-3-2. Soil heat flux

2-3-3. Radiation

2-3-4. Turbulent flux

2-4. Other data set

**Chapter 3 Results and discussion** ····· 61

3-1. Grazing intensity

3-2. Grazing effect

3-2-1. Soil temperature and soil moisture

3-2-2. Vegetation

3-2-3. Roughness length

3-2-4. Energy and water balance

**Chapter 4 Conclusions** ····· 102

**Acknowledgements** ····· 105

**References** ····· 107

# Influence of Grazing on Vegetation, Surface Energy and Water Balance over the Mongolian Steppe

Hidekazu KATO

**Abstract**

Mongolia in the earthen Eurasia locates in arid to semi-arid area. Since 1990, the social system in Mongolia has changed radically, and resulted in transformation of lifestyle and the way of grazing. The serious influence of such a change is anticipated because Mongolian grassland is a sensible area to the changes of external conditions. In addition to the condition in Mongolian steppe, the interannual variation in precipitation influenced aboveground biomass and increase of air temperature and decrease of precipitation in recent year were reported. Therefore the long-term research is necessary. The object of this study is to assess influence of grazing on vegetation, surface energy balance and water balance over the Mongolian grassland through a three-year research.

The study site is in a steppe grassland at Kherlen Bayaan-Ulaan (KBU), Mongolia. Grazing has been carried on all the year round. In this area, a protected area (200 m by 170 m) was constructed in autumn 2002 in order to study the possible grazing impact. Two measurement stations which employ on eddy correlation method, one in a protected area and the other in a pastoral area, have been installed and operated since March 2003.

The difference of the green biomass values of the two areas appears significantly after July and the values of both areas in 2004 are higher than in 2003 in spite of no significant difference of precipitation in growing season between the two years. The value of dead vegetation biomass in the protected area is constantly bigger than that in

the pastoral area. Therefore the grazing activity appears to have controlled biomass. After July in 2004, the net radiation values of the protected area are higher than those of the pastoral one, which corresponds with changes of biomass and albedo. The increase of the net radiation values in protected area caused the higher values of soil heat flux and sensible heat flux in this area. For the enhanced sensible heat flux values in protected area, the bigger values of roughness length, because of the bigger values of biomass, also contribute to the higher fluxes. There is no significant difference of the annual integrated values of evapotranspiration between the two areas. The result agrees with the simulated one by a previous study which indicates that the reduction of transpiration by grazing in pastoral area is largely compensated by the increase of evaporation.

**Keywords**: semi-arid region, steppe, grazing intensity, energy balance, water balance

# List of tables


Table Page

2-1 Instruments for the observation at the station of pastoral area ····· 17

2-2 Instruments for the observation at the station of protected area ····· 18

2-3 The number of soil moisture data measured around the protected-area station in August of 2005 ····· 19

2-4 The ratio of data removed by data selection ····· 20

2-5 Commonly used animal unit equivalents ····· 21

2-6 The relation NDVI and surface condition ····· 22

3-1 The average of grazing intensity of each district ····· 68

3-2 The average and standard deviation of surface soil temperature ····· 69

3-3 The annual and 5-month average and standard deviation of soil temperature ····· 70

3-4 The average and standard deviation of soil temperature at the depth of 5 cm ····· 71

3-5 The annual and 5-month average and standard deviation of soil moisture ····· 72

3-6 The period divided by the relation between NDVI and AGB ····· 73

3-7 Annual integrated values ····· 74

3-8 The number of major rainfall events ····· 75

3-9 Summer-time integrated values ····· 76

3-10 Annual integrated *G* values measured in TERC ····· 77

# List of figures


| Figure | | Page |
|---|---|---|
| 2-1 | Location of the study area and distribution of vegetation | 23 |
| 2-2 | Annual precipitation and average annual air temperature for a decade | 24 |
| 2-3 | Average monthly precipitation and air temperature | 25 |
| 2-4 | The location of winter camps made for winter grazing in mountain areas | 26 |
| 2-5 | Photograph of the landscape around KBU measurement station | 27 |
| 2-6 | Location of the measurement stations | 28 |
| 2-7 | Photograph of the fence in summer 2005 | 29 |
| 2-8 | Photographs of the landscape around measurement stations in the summer 2003 | 30 |
| 2-9 | Photographs of the landscape around measurement stations in the winter 2004 | 31 |
| 2-10 | Photographs of the landscape around measurement stations in the summer 2005 | 32 |
| 2-11 | Schematic diagram of the observation system of the station of the pastoral area | 33 |
| 2-12 | Schematic diagram of the observation system of the station of the protected area | 34 |
| 2-13 | Photographs of the observation system of the stations | 35 |
| 2-14 | Photographs taken by the digital camera in the pastoral station | 36 |
| 2-15 | Examples of photo taken in the measurement station | 37 |
| 2-16 | The measurement of soil heat flux values by the 11 heat plates in the pastoral area | 38 |
| 2-17 | The measurement of soil heat flux values by the 10 heat plates in the protected area | 39 |
| 2-18 | The diurnal change of soil heat flux values in the pastoral area | 40 |
| 2-19 | A comparison between $G_{pas_station}$ and $G_{pas_avg}$ | 41 |
| 2-20a | A comparison between $G_{pas_station}$ and $G_{pas_avg}$ | 42 |
| 2-20b | A comparison between $G_{pas_station}$ and $G_{pas_avg}$ | 43 |
| 2-21 | The diurnal change of soil heat flux values in the protected area | 44 |

2-22 A comparison between $G_{pro_station}$ and $G_{pro_avg}$ ····· 45
2-23a A comparison between $G_{pro_station}$ and $G_{pro_avg}$ ····· 46
2-23b A comparison between $G_{pro_station}$ and $G_{pro_avg}$ ····· 47
2-24 Radiation of thermal radiation budget on ground surface and observation at sensor height ····· 48
2-25 A photograph of the observation system for the movable measurement of radiation ····· 49
2-26 The observation lines on which movable measurements were carried out ····· 50
2-27 An intercomparison of the components of radiation between those measured by instruments used for the in movable measurement but placed next the station sensor and those measured by sensors ····· 51
2-28 A comparison of the components of the radiation between those measured by movable measurement and those in stations ····· 52
2-29 The horizontal distribution of soil moisture around the pastoral-area station in August of 2003 ····· 53
2-30 The horizontal distribution of soil moisture around the protected-area station in August of 2005 ····· 54
2-31 A Photograph of the observation system of KBU stations installed for intercomparison of the sensors at TERC ····· 55
2-32 Location of TERC ····· 56
2-33 Photographs of the intercomparison-observation system of the pastoral-area station ····· 57
2-34 The comparison of $\overline{w'T'}_{gill}$ and $\overline{w'T'}_{kaijo}$ ····· 58
2-35 The comparison between $\overline{w'q'}_{gill\&OP2}$ and $\overline{w'q'}_{kaijo\&LI7500}$ ····· 59
2-36 The comparison of $\overline{w'q'}$ values between $\overline{w'q'}_{gill}$ and $\overline{w'q'}_{kaijo}$ ····· 60

3-1 The annual change of grazing intensity registered by the State Statistical Office, Mongolia ····· 78
3-2 The distribution of $GI_{\mathrm{statis}}$ in 2003 ····· 79
3-3 The seasonal change of grazing intensity evaluated by photo ····· 80
3-4 The seasonal change of surface temperature ····· 81
3-5 A comparison between $\underline{T_{sa}}$ and $T_{sg}$ of annual data set ····· 82
3-6 A comparison between $\underline{T_{sa}}$ and $T_{sg}$ of 5-month data set ····· 83
3-7 The seasonal change of ST ····· 84

3-8 A comparison between $STa_{-0.05}$ and $STg_{-0.05}$ of annual data set ····· 85
3-9 A comparison between $STa_{-0.05}$ and $STg_{-0.05}$ of 5-month data set ····· 86
3-10 The seasonal change of SM ····· 87
3-11 The seasonal change of AGB ····· 88
3-12 The seasonal change of wind speed in KBU ····· 89
3-13 The seasonal change of NDVI and AGB ····· 90
3-14 The seasonal change of $z_0$ ····· 91
3-15 The seasonal change of $z_0$ ····· 92
3-16 An example of the figure in order to compare the components of the heat balance of the two stations ····· 93
3-17 The seasonal change of *a* of the components of the radiation and heat budget ····· 94
3-18 The seasonal change of *a* of the components of the radiation and heat budget ····· 95
3-19 The seasonal change of *a* of the components of turbulent heat budget ····· 96
3-20 The seasonal change of daily-integrated values of surface heat balance ····· 97
3-21 The annual integrated values of surface energy balance and water balance in the pastoral area ····· 98
3-22 The annual integrated values of surface energy balance and water balance in the protected area ····· 99
3-23 The integrated values of surface energy balance and water balance in the pastoral area ····· 100
3-24 The integrated values of surface energy balance and water balance in the protected area ····· 101

4-1 The annual change of surface energy balance ····· 104

## Chapter 1

# Introduction

## 1-1. General background

Desertification and its influence on regional environmental change have become a research focus of many studies in the past few decades. It has proposed that grassland desertification in the arid semi-arid zones of the worlds is quite serious, and that causes of desertification are not only the climate change but also over-utilization of natural resources and inappropriate management of environment. Deforestation and resulting hydrological changes of land surface affect regional and even global climates (e.g. Shukla *et al*., 1990, Nobre *et al*., 1991, Wright *et al*., 1992). Some GCMs (General Circulation Models) suggest that future global warming will likely exacerbate the degradation of semi-arid grasslands on a large scale in North America and Asia (Manabe and Wetherald, 1986).

Mongolia in the earthen Eurasia locates in arid to semi-arid area, and the grazing has been carried on for more than 2000 years (Nachinshonkhor *et al*., 2003). Mongolia also locates in an ecotone from the Siberian taiga forest to the Gobi Desert of central Asia, so that vegetation of this area is sensible to the changes of eternal conditions (Sugita *et al*., 2006). Under the condition, since 1990, the social system in Mongolia has changed radically, and this change resulted in transformation of lifestyle. In particular, the way of grazing was changed through urbanization and settlement. Thus, impacts on the grassland ecosystem are attributed to overgrazing and settlement (Chuluum and Ojima, 2001). At present, 97.4% of national land area is grassland and about 70% of which is under the overgrazing (National Agency for Meteorology, Hydrology and Environment Monitoring, 2001). Although sheep was the most popular domestic animal for grazing

in the past, the number of goat has increased in the recent years for producing cashmere fabric. Since, goats eat grass from rhizome (Suzuki, 2003), vegetation is easily disappeared and the grassland tends to be in the condition overgrazed. The serious influence of such a change on Mongolian steppe is anticipated (Sugita, 2003).

In addition to the condition in Mongolian steppe, the interannual variation in precipitation influenced aboveground biomass (Fernández-Giménez and Allen-Diaz, 1999) and increase of surface temperature and decrease of precipitation in recent year were reported (Yatagai and Yasunari, 1994). Therefore it is necessary for the environmental assessments of Mongolian steppe to carry out a long-term research.

## 1-2. Previous studies

There have been many studies on the effect of grazing, which is considered as one of the most major impacts on steppe in arid and semi-arid region, as mentioned in section 1-1. Bryant *et al*. (1990) suggested that long term overgrazing in the semi-arid Sonoran Desert caused higher rates of latent heat flux and less amount of soil moisture available for vegetative growth. However, it is reported that grazing reduced seasonal evaporation for a grassland in Kansas by only 6 % (Bremer *et al*., 2001) and negligible affect on carbon dioxide exchange in the mixed grass prairie, Cheyenene (Lecain *et al*., 2000).

In the Horqin Steppe, located in the northeastern China, the problem of desertification is serious, and there have been many studies on its assessments. The desertified grassland area is still expanding due to inappropriate anthropogenic activities such as prolonged overgrazing, poor farmland management and over-lumbering (Zhu and Wang, 1992). Vegetation plays very important roles in mass and heat exchange between land surfaces and the atmosphere (Grace *et al*., 1981). Removal or deterioration of vegetation cover affects water and heat budget of the surfaces. The Horqin Steppe also has been suffering from desertification over the past two decades

primarily because of overgrazing practice experienced in this region (Li *et al*., 2000). Moreover, from studies of the effects of long-term (20 years) grazing, it was suggested that soil organic carbon contents, which shows a level of quality of soil, was sensitive to heavy grazing and it was difficult to recover after a significant decline caused by overgrazing (Cui *et al*., 2005).

There were some researches carried out in Kherlen river basin, our study area, Mongolia. By a half year observation, Kojima (2004) described the relation between grazing and vegetation; the more grazing intensity was, the less the amount of vegetation were. Urano (2005) suggested that the larger grazing intensity caused the steppe to be the source of carbon dioxide flux. From a model analysis, the maximum sustainable grazing intensity was determined to be 0.7 sheep equivalent unit per ha (Chen *et al*., 2006 and Chen *et al*., 2007). If grazing intensity is greater than 0.7, the aboveground biomass keep decreasing. Many studies on the other region of Mongolia have been made on the influence of grazing. For example, the relation between grazing and ecosystem, including soil erosion and vegetation (Batjargal, 1997, Fernández-Giménez and Allen-Diaz, 1999, Komonen *et al*., 2002, Fernández-Giménez and Swift, 2003, Fujita, 2003, Wesche and Retzer, 2005, etc).

As shown above, a lot of studies have been made on the effect of grazing on steppe in semi-arid region. However, there have only been a few studies that tried to study the relation between grazing and energy balance by observation in Mongolian steppe. Therefore the object of this study is to assess influence of grazing on vegetation, surface energy and water balance over the Mongolian steppe.

## Chapter 2

# Methods

## 2-1. Site Information

The study site is in a steppe grassland at Kherlenbayaan-Ulaan (KBU, 47˚ 28' N, 108˚ 78' E, 1235 m above mean sea level), Delgerkhaan district, the Hentiy province of Mongolia, and locates at some 250 km southeast of Ulaanbaatar (Fig. 2-1). The region belongs to the semi-arid zone and has a distinct continental climate. According to the report of the KBU Meteopost Station of the Institute of Meteorology and Hydrology of Mongolia from 1993 to 2002 (Figs. 2-2 and 2-3), mean annual air temperature is 1.2 °C. Mean daily temperature in January and in July are -22.9 and 21.4℃, respectively. From May to September, the monthly mean temperature is above 5℃. Mean annual precipitation (PPT) is 196 mm, with majority of it (88 %) falling between June and September. PPT is quite variable from one year to another and shows strong seasonal variability (Fig. 2-3). Vegetation is summarized as follows by Li *et al*. (2005): frequent drought periods are usually the limiting factor for plant growth in steppe. These dry and temperate climatic conditions favor the development of extensive grass steppe. The growing season usually starts in late April and ends in late October. The vegetation in the study area is typical short-grass steppe. It is dominated by the cool-season $C_3$ species (*Stipa krylovii, Carex duriuscula, Artemisia frigida, Allium mongolicum, Leymus chinensis* and *Caragana microphylla*) and a few $C_4$ species (*Cleistogenes squqrrosa* and *Salsola collina*).

In this area, grazing has been carried on all the year round. The number of domestic animals (horse, cow, camel, sheep and goat) and the area to graze change seasonally (Gerelsuren, 2006, personal communication): between March and October, there is

vegetation throughout KBU ($1.93\times10^5$ ha), and grazing is usually carried out at a flat near the Kherlen river by local people of KBU. In winter, the area of pastureland decreases to nearly $1.30\times10^5$ ha, and the flat area are too cold and snow is falling deeply. Therefore local people move to the mountain and make winter camp at the beginning of wintertime (Fig. 2-4). In winter, moreover, due to milder climate in KBU some people come to KBU mountain area from other area with their animals whose number is between 30000 and 40000. They stay there from 15 November to 15 March and go back to their own district area.

## 2-2. Measurements

### 2-2-1. Meteorological and hydrologic measurements

In study area, a protected area (200 m by 170 m) was constructed in August of 2002 in order to study the possible grazing impact (Figs. 2-5, 2-6 and 2-7). Two measurement stations which employ an eddy covariance (EC) method, one in a protected area and the other in a pastoral area, have been installed and operated since March of 2003 as part of the RAISE (the Rangelands atmosphere–hydrosphere–biosphere Interaction Study Experiment in North-eastern Asia) project (Sugita *et al*., 2007). The details of those stations have been presented in Li *et al*. (2005), and the components and outline of the system are shown in Table 2-1 and 2-2, Fig. 2-11 and 2-12.

We also measured soil temperature (ST) profile by platinum resistance thermometers, soil heat flux ($G$) by soil heat plates and soil moisture (SM) profile by time domain reflectometry probes at both stations (as for depths of those sensors, see Table 2-1 and 2-2). Only at the station in pastoral area, PPT was measured by a tipping bucket rain gauge. They were sampled at 0.1 Hz and the 30 min mean data were logged on CR10X dataloggers. The underground sensors were placed in late September of 2002. Measurements were carried out from March 25 of 2003 and are continued as of the end

of 2006.

### 2-2-2. Grazing intensity

In the station of pastoral area, Digital camera (caplio G4, Ricoh, Japan) was placed in July of 2004 in order to evaluate the grazing intensity at around the measurement stations (Fig. 2-13a). The grazing intensity values ($GI_{photo}$) were calculated as follow:

$$GI_{photo} = LS / A_{camara} / N \quad (1)$$

where $LS$ is the number of the livestock in one photo image (heads), $A_{camera}$ the area taken by the camera (ha), $N$ the number of photo images in daytime. $A$ value was calculated as 4.19 ha ($4.19 \times 10^4$ m$^2$) with the assumption that the area taken by the camera was an isosceles triangle whose altitude and vertex angle were the same as the distance between the camera and the foot of a mountain (318 m) and the angle of the view (45°), respectively (Figs. 2-14 and 2-15).

### 2-2-3. Vegetation

Vegetation measurements (aboveground biomass and canopy height ($h_c$)) were carried out between June and September of 2003, July of 2004 and August of 2005. Four quadrats ($20 \times 20$ m$^2$) and twelve sub-quadrats (three sub-quadrats per quadrat) in each area were used for the measurements. The details of how and where the quadrats and sub-quadrats were constructed are summarized as follows by Kawata *et al*. (2007). After average $h_c$ values in each sub-quadrat were measured, all the amount of vegetation was cut at the height of ground surface and living parts were separated from dead ones. The cut vegetation was dried in an oven and weighed.

## 2-3. Data processing

### 2-3-1. Roughness length

There are several approaches to determine the roughness length for momentum ($z_0$) using single level measurements. In our study, the method to produce $z_0$ values of each term in both stations suggested by Toda and Sugita (2003) was employed, in which (i) $u_*$ values were calculated by applying the profile equation (2) derived on the basis Monin-Obukhov (M-O) similarity theory as

$$u_* = kV \Big/ \left[ \ln\left( \frac{z - d_0}{z_0} \right) - \Psi_m \left( \frac{z - d_0}{L} \right) \right] \tag{2}$$

where $k$ is the von Karman's constant, $z$ the measurement height above ground (3.5 m), $d_o$ value was assumed to be two third of $h_c$. The symbol $\Psi_m$ denotes stability correction function for momentum, which can be obtained by the integration of an experimentally determined function for $\partial V/\partial z$. For example, the integrated form of the Businger-Dyer formulations [e.g., Dyer, 1974; Businger, 1988] can be written as

$$\Psi_m = \ln\left[ \frac{(1+x)^2 (1+x^2)}{(1+x_0)^2 (1+x_0^2)} \right] - 2\arctan(x) + 2\arctan(x_0) \tag{3}$$

where $x = (1 - 16\,y)^{1/4}$, $x_0 = (1 - 16\,z_0/L)^{1/4}$ and $y = (z - d_0)/L$, in which $L$ is the Obukhov length, defined by

$$L = -\frac{u_*^3}{k(g/T_a)(H_v/\rho c_p)} \tag{4}$$

where $g$ is the acceleration of gravity, $T_a$ the air temperature in Kelvin, $H_v = (H + 0.61\,T_a c_p E)$ the virtual sensible heat flux, and the $E$ the rate of evaporation. (ii) $z_0$ value was changed from $10^{-5}$ m to $10^{-1}$ m at $10^{-5}$-m step. (iii) The $z_0$ value was determined when the RMSE (root mean squire error) value of $u_*$ and $u_{*s}$ measured at the stations was the lowest.

### 2-3-2. Soil heat flux

Kustas *et al*. (2000) suggested from observation in the Jarnade Range that variability in soil heat flux from surface heterogeneous area was 200-250 W $m^{-2}$. In KBU vegetation cover is low and clustered (Urano, 2005), and the number of the heat plate in protected area was only one at the time of station setup (Table 1). Moreover the heat plate in pastoral area was constructed within the fence, and there was a strong possibility that the measurement didn't provide pastoral-area-averages. Thus, around each station, ten heat plates were buried at depth of 2 cm in July of 2005 in order to estimate the area-average value (Fig. 2-16 and 2-17). Fig. 2-18 and 2-19 show that the spatial variability of $G$ values in pastoral area was large, and $G$ values inside station fence ($G_{\mathrm{pas_station}}$) were indeed not representative. RMSE between $G_{\mathrm{pas_station}}$ and 11-heat-plate average values ($G_{\mathrm{pas_avg}}$) was 14.83 W $m^{-2}$. No correlation between the comparison of two $G$ values ($G_{\mathrm{pas_station}}$ and $G_{\mathrm{pas_avg}}$) and NDVI (Normalized Difference Vegetation Index, section 2-4), SM, or ST was found. Thus we recalculated the $G$ values by the following equations;

$$G_{pas_corrected} = 1.26 G_{pas_station} - 1.17 \tag{5}$$

$$G_{pas_corrected} = -0.0031 G_{pas_station}^{2} + 1.41 G_{pas_station} + 2.95 \tag{6}$$

where $G_{\mathrm{pas_corrected}}$ is the corrected, recalculated value. RMSE between $G_{\mathrm{pas_corrected}}$ of (6) and $G_{\mathrm{pas_avg}}$ (9.77 W $m^{-2}$) was smaller than that between $G_{\mathrm{pas_corrected}}$ of (5) and $G_{\mathrm{pas_avg}}$ (10.83 W $m^{-2}$). So we used equation (6) for the following analysis. In that same way, the $G_{\mathrm{pro_station}}$ values measured in protected area since March 2003 were recalculated by the following equation;

$$G_{pro_corrected} = 0.83 G_{pro_station} - 2.15 \tag{7}$$

where $G_{\mathrm{pro_corrected}}$ is recalculated values. In the analyses we used the recalculated values till 16 July of 2005 when the measurement values of 10 heat plates buried in July 2005 were judged to have become stable, and average values were used after that.

### 2-3-3. Radiation

Radiation budget was showed by following equation:

$$R_n = K_d - K_u + L_d - L_u \tag{8}$$

where $R_n$ is the net radiation, $K_d$ the downward short wave radiation, $K_u$ the upward short wave radiation, $L_d$ the downward long wave radiation, $L_u$ the upward long wave radiation. In this study, we used the values of $K_d$ and $L_d$ measured in the pastoral station, and $K_u$ and $L_u$ in each station because the short distance between two stations seemed not to cause the difference of the downward radiation.

Kotani and Sugita (in preparation) suggested the necessity of considering atmospheric effects on the measurement of the thermal radiation (long wave radiation) in those radiation measurement systems (Fig. 2-24) and the correct equation;

$$L_{sky} = \tau_a L_{obs\downarrow} + L_a \tag{9}$$

$$L_{obs\uparrow} = \tau_a L_{srf} + \tau_a (1 - \varepsilon_s) L_{sky} + L_a \tag{10}$$

$$L_{srf} = \frac{L_{obs\uparrow} - L_a - \tau_a (1 - \varepsilon_s)(\tau_a L_{obs\downarrow} + L_a)}{\tau_a} \tag{11}$$

where $L_{sky}$ is the radiation emanating from the whole atmosphere, $L_{obs\downarrow}$ the downward long wave radiation observed by the sensor, $L_a$ the radiation emanating from air layer between the ground surface and the sensor height, $L_{srf}$ radiation emanating from the ground surface, $L_{obs\uparrow}$ upward long wave radiation observed by the sensor, $\tau_a$ the transmissivity of the air layer between surface and radiometer, $\varepsilon_s$ emissivity of the ground surface. The values of $\tau_a$ and $L_a$ were calculated by LOWTRAN7 program (Kneizys *et al*., 1988) with the information of profile of air temperature and humidity;

$$\tau_a = -(a_1 T_a + a_2)\ln(RH) - a_3 T_a + a_4 \tag{12}$$

$$L_a = -(b_1 T_a + b_2)\ln(RH) - b_3 T_a + b_4 \tag{13}$$

where $RH$ is relative humidity, $a_i$ and $b_i$ fitting constants ($a_1 = 1.5\times10^{-3}$, $a_2 = 4.2\times10^{-2}$, $a_3 = 5.8\times10^{-3}$, $a_4 = 8.7\times10^{-1}$, $b_1 = 6.2\times10^{-1}$, $b_2$ = 8.90, $b_3$ = 2.14, $b_4$ = 30.59). Using

Recalculated $L_d$ ($L_{srf}$) values, soil surface temperature ($T_s$) was calculated by Stefan-Boltzmann law;

$$T_s^4 = \frac{L_{sky}}{\sigma} \tag{14}$$

where $\sigma$ is Stefan-Boltzmann constant ($5.67 \times 10^{-8}$ W m$^{-2}$ K$^{-4}$).

It was possible that measurement values of radiation at each station may not have been representative of each area as the case of the measurement of soil heat flux. That was why the movable measurement (MV) of radiation was carried out in August of 2005: the instrument of the same model as that in each station and a CR10X datalogger were carried on the back (Fig. 2-25), and were kept moved during measurement (Fig. 2-26). The averaging time for both MV and stations was 30 minutes as well as by the measurements. The numbers of the data set measured in the pastoral and protected area were 14 and 15, respectively. First, those sensors were intercompared by placing the two sensors side by side for an hour at each station. The result is shown in Fig. 2-27. We see from Fig. 2-27 that there was significant difference between the radiation values measured by the instruments of MV and those by the stations, so we corrected the MV values to match with the ones that would have been measured by the instrument in stations. Then we compared the corrected MV values with ones in stations (Fig. 2-28) and a t-test was carried out. From the result, it was found that there was no significant difference between the two data sets. Therefore we concluded that it is appropriate to regard the station data of radiation as regional representative values.

### 2-3-4. Soil moisture

It was possible that measured values of SM at each station may not have been representative of each area as is the case of the measurement of soil heat flux. In August of 2004, the measurement for a comparison between pastoral-area station data and

around-station values was carried out and it was judged appropriate to regard the pastoral-area station data of SM as regional representative values (Kojima, 2004, Fig. 2-29). In the same way, we carried out the measurement for a comparison between protected-area station data and around-station values four times in August of 2005: SM was measured at the depth of 3 cm on the three lines at 5-m intervals to the 100 m distance from each station. The results are shown in Fig. 2-30 and Table 2-3. Fig. 2-30 and Table 2-3 show that there was the partial difference between the around-measurement value ($SM_{around}$) and station-measurement one ($SM_{station}$), and that the many of $SM_{around}$ data were similar to the $SM_{station}$ data. Therefore we concluded that it is appropriate to regard the $SM_{station}$ of protected-area station as regional representative values.

### 2-3-5. Turbulent flux

Sensible heat flux $H$ and latent heat flux $lE$ were calculated by applying the EC method,

$$H = c_p \rho \left( \overline{w'T'} \right) \tag{15}$$

$$lE = l\rho \left( \overline{w'q'} \right) \tag{16}$$

Overbar and prime denote the time averaging and deviation from the average. $w$, $T$ and $q$ represent the vertical wind speed, air temperature and specific humidity, respectively. $l$ is latent heat of evaporation and $c_p$ is the specific heat of the air at constant pressure.

#### <u>(1) Intercomparison-mesurement</u>

Note the difference of the instrumentations of the EC system between the two stations (Table 2-1 and 2-2). For this reason, it is not always appropriate to directly compare those station data, and thus the fluxes data of the protected-area station were corrected by the equations which were derived by an intercomparison experiment. The

intercomparison-measurements were carried out three times: from August to October of 2002 in TERC (the Terrestrial Environment Research Center, the University of Tsukuba), before installation of the stations in KBU, during July of 2004 in KBU, and during August of 2005 in KBU. In TERC, two-station systems were installed side by side (Fig. 2-31). Only those values of $\overline{w'T'}$ and $\overline{w'q'}$ that satisfy the following criteria were used in the intercomparison: (i-i) they should be the daytime ($K_u$ > 10 W m$^{-2}$) measurements without rainfall. (i-ii) no anomalous or spurious spikes found in data. (i-iii) $\overline{w'T'}$ and $\overline{w'q'}$ values were larger than zero. (i-iv) wind came from the direction east through south-southeast, in order to eliminate the effect of the obstruction (e.g. tall trees, convex terrain, other instruments, Fig. 2-32). In KBU, SAT (sonic anemometer-thermometer) which was the same model as was installed in protected-area station, was installed in pastoral-area station side by side (Fig. 2-33). The criteria of data selection was the same as those for the TERC comparison. In criteria (i-iv), wind direction was modified to those except for northeast through southeast. To put it more concretely, the protected-area station system values were corrected to the ones ($\overline{w'T'}_{pro}$ and $\overline{w'q'}_{pro}$) that would have been measured by pastoral-area station system by the equations if it had been placed in the protected area. The equations to correct are (Fig. 2-34~36);

$$\overline{w'T'}_{pro} = 0.89 \times \overline{w'T'}_{pro_obs} + 2.36 \times 10^{-3} \quad (17)$$

$$\overline{w'q'}_{pro} = 1.09 \times \overline{w'q'}_{pro_obs} - 2.95 \times 10^{-3} \text{ (~2004/3)} \quad (18)$$

$$\overline{w'q'}_{pro} = 0.94 \times \overline{w'q'}_{pro_obs} - 8.59 \times 10^{-4} \text{ (2004/4~)} \quad (19)$$

The subscript *pro_obs* designates the values measured at the protected station.

Among the available station data, only those that satisfy the following criteria were used in the analysis: (ii-i) the criteria (i-i) and (i-ii), (ii-ii) $H$ and $lE$ values were larger than 10 W m$^{-2}$. Roughly 47 % and 56 % of the data obtained from our EC system in the pastoral and the protected stations, respectively, were removed and thus the data gaps

were produced (Table 2-4).

**(2) upwind area**

It is quite likely that turbulence flux values measured in the protected-area station consisted of those of not only the protected area but also of the pastoral area because closed area was not large enough. In order to clarify how large influence of the consideration of the upwind source area is, three analyses were carried out: (iii-i) no consideration of the upwind source area, (iii-ii) the consideration of the wind direction, (iii-iii) the consideration of the upwind source area to evaluate the value of only the protected area. In case (iii-i), all the data set selected by criteria (ii-i) and (ii-ii) were used. In case (iii-ii), the data set in only the wind direction in which upwind area was largest was used (from the direction west southwest through northwest, Fig. 2-6). In case (iii-iii), we recalculated the case-(iii-ii) data set by the equation of the effective upwind source area (footprint) sensed by the observation, suggested by Lloyd (1995). The equation can be written as

$$\mathrm{FP}(x) = \frac{1}{Q_0}\frac{dQ}{dx} = \frac{2x_{\max}}{x^2}\phi_m \exp\left[\frac{-2x_{\max}}{x}\phi_m\right] \tag{20}$$

where FP ($x$) is the relative source strength at a distance $x$ in upwind direction, $Q_0$ the measured value of the turbulence flux, $Q$ the turbulence flux value at a distance $x$. $x_{\max}$, the position of the peak of FP, and $\varphi_{\mathrm{m}}$, a similarity function of stability, are (Dyer, 1974):

$$x_{\max} = \frac{V(z-d_0)}{u_* 2k} \tag{21}$$

$$\phi_m = \left[1 - 16\frac{z-d_0}{L}\right]^{-1/4} \tag{22}$$

The integrated value of (20) from 0 to $X$ m is the fractional flux from upwind area $X$ m

as measured from the point of observation, "cumulative footprint (CF)", as follow:

$$\mathrm{CF}(X) = \frac{Q}{Q_0} = \exp\left[\frac{-2x_{\max}}{X}\phi_m\right] \tag{23}$$

$X$ values were a distance between protected station and a fence. In case (iii-iii), $X$ was 205 m, because the data set was used when wind came from the direction west southwest through northwest. CF values were calculated every 30 minutes. The value of protected area $F_{protected}$ only was calculated as follow:

$$F_{pro_obs} = \mathrm{CF} \times F_{protecred} + (1 - \mathrm{CF}) \times F_{pastoral} \tag{24}$$

$$F_{protecred} = \frac{F_{pro_obs} - (1 - \mathrm{CF}) \times F_{pastoral}}{\mathrm{CF}} \tag{25}$$

**(3) Gap filling**

For the calculation of the daily and annual sums the fluxes, these gaps (made by criteria (i-ii)) were filled following strategy suggested by Falge *et al*. (2001a) and Falge *et al*. (2001b): (iv-i) a linear interpolation was used to fill the gaps that were less than 2 hours, (iv-ii) the other data gaps were filled using the empirical relationships ("look-up tables", which we will explain in the next paragraph), and (iv-iii) if there remained gaps by these two ways because too many or long-term meteorological data were missing, we used mean daily variations to fill the gaps.

The "look-up tables" (criteria (iv-ii)) are suggested by Falge *et al*. (2001a) and Falge *et al*. (2001b): tables were created for each station so that missing values of $H$ and $lE$ could be "looked-up" based on the environmental conditions associated with the missing data. Tables were created to represent changing environmental conditions based on six bimonthly periods. Seasons were assigned as periods ranging from 1 April to 31 May, 1 June to 31 July, 1 August to 30 September, 1 October to 30 November, 1 December to 31 January, and 1 February to 31 March. For look-up tables average $H$ and

$lE$ were compiled for a maximum of six seasonal periods × 23 $Q_{\mathrm{PPFD}}$-classes × 35 $T_a$-classes ($Q_{\mathrm{PPFD}}$ denotes photosynthetic photon flux density ($\mu\mathrm{mol\,m^{-2}\,s^{-1}}$)). $Q_{\mathrm{PPFD}}$-classes consisted of 100 $\mu\mathrm{mol\,m^{-2}\,s^{-1}}$ intervals from 0 to 2200 with a separate class for $Q_{\mathrm{PPFD}} = 0$. Similarly, $T_a$-classes were defined through 2 ºC intervals ranging from −19 ºC to 49 ºC. This procedure produced tables of $H$ and $lE$ means and standard deviations for each class. Gaps in the look-up tables (classes with no mean assigned) were interpolated linearly.

We calculated evapotranspiration values $E$ from the gap-filled $lE$ values;

$$E_{daily} = \sum \frac{lE}{l\rho} \tag{26}$$

where $E_{daily}$ is integrated $E$ value.

### 2-4. Other data set

There was another data set of grazing intensity evaluated from the statistics showing the number of registered animal by the State Statistical Office, Mongolia ($GI_{\mathrm{statis}}$). In that data set, $LS$ in every district and every animal was registered. There was variability in the ratio of 5 animals among districts, so it was necessary to convert $LS$ value in every district into animal unit equivalents. USDA National Range and Pasture Handbook (1997) suggested the animal unit equivalents of the 800 lbs of forage on a dry weight basis (Table 2-5). On the basis of the animal unit equivalents, we introduce the equation to calculate sheep equivalent unit ($SEu$).

$$SEu = 8.15 \times HD_{camel} + 6.25 \times HD_{horse} + 5.00 \times HD_{cow} + 0.75 \times HD_{goat} + HD_{sheep} \tag{27}$$

where HD is Heads, subscripts show the sort of animals. $GI_{\mathrm{statis}}$ value of each district was calculated as follow:

$$GI_{statis} = SEu / A \tag{28}$$

where $A$ is the area of a district (ha) obtain from Saander and Sugita (2004). In the data set of KBU village, the number of animals staying in KBU village throughout the year ($LS_{\mathrm{local}}$) and that migrating from outside of KBU village in winter ($LS_{\mathrm{mig}}$), reported by KBU local government (Gerelsuren, 2006, personal communication, cited from RAISE homepage) were taken (Section 2-1). The former data set between 1992 and 2002 was not available, and those values were estimated by the relation between KBU and Delgerkhaan (of which KBU village is a part) values;

$$LS_{KBUes} = \overline{\left(\frac{LS_{local}}{LS_{DGH}}\right)} \times LS_{DGH} \tag{29}$$

where $LS_{KBUes}$ is estimated $LS_{local}$ values between 1992 and 2002, $LS_{DGH}$ $LS$ values in Delgerkhaan. Overbar denotes averaging from 1984 to 1991 and 2003. The values in winter ($LS_{\mathrm{winter}}$) were the sum of $LS_{\mathrm{local}}$ and $LS_{\mathrm{mig}}$, and $A$ values of KBU in winter and summer were $1.30 \times 10^5$ ha and $6.29 \times 10^4$ ha, respectively (section 2-1).

We also used the NDVI (Normalized Difference Vegetation Index) data set measured by Free VEGETATION products (cited from Free VEGETATION products homepage). NDVI was calculated on the basis of vegetation response to radiation that the wavelength region of red and blue visible band ($VIS$) was absorbed and near-infrared region ($NIR$) was reflected strongly by green leaf;

$$NDVI = \frac{NIR - VIS}{NIR + VIS} \tag{30}$$

The data set was available as 10-day averages. Relation between NDVI values and the surface condition is shown Table 2-6 (Kondo, 1994). Kojima (2004) suggested the relation between NDVI and leaf area index (LAI) in KBU steppe;

$$LAI = 1.39 NDVI - 2.12 \times 10^{-2} \tag{31}$$

Table 2-1 Instruments for the observation at the station of pastoral area. (Kotani, 2006)

| Component | Instrument | Model / Manufacturer (location) | Height / depth |
|---|---|---|---|
| Relative humidity / Air temperature | Capacitance hygrometer | HMP45A / Vaisala Oy. (Helsinki, Finland) | 2.5 m |
| | Platinum resistance thermometer in ventilation shelter | PVC-02-AC / Prede Co. Ltd. (Tokyo, Japan) | |
| Surface temperature | Infrared thermometer | 303F / Konica Minolta Holdings, Inc. (Tokyo, Japan) | 2.5 m |
| Sensible / latent heat flux | Sonic aemometer-thermometer | SAT550/ Kaijo Sonic Co. (Tokyo, Japan) | 3.0 m |
| | $CO_2$/$H_2O$ Infrared gas analyser | Li7500 / Li-cor Inc. (Lincoln, U.S.) | |
| Short-wave radiation | Pyranometers[*1] | CM3 / Kipp and Zonen B.V. (Delft, Netherlands) | 2.5 m |
| Long-wave radiation | Pygrometers[*1] | CG3 / Kipp and Zonen B.V. (Delft, Netherlands | 2.5 m |
| Air pressure | Barometer | PTB210 / Vaisala Oy. (Helsinki, Finland) | 1.3 m |
| Precipitation | Tipping bucket rain gauge | 52202 / R. M. Young Inc. (Traverse, U.S.) | |
| Soil heat flux | Heat flux plate | HFT1.1 / REBS[*2] Inc. (Seattle, U.S.) | -0.02, -0.1m |
| Soil temperature | Platinum resistance thermometer | C-PTG / Climatec Inc. (Tokyo, Japan) | -0.05, -0.1, -0.2, -0.3, -0.5, -0.7, -1.0, -1.5m |
| Volumetric water content | TDR[*3] sensor | CS616 / Cambel Scientific Inc. (Logan, U.S.) | -0.1, -0.2, -0.3, -0.7, -1.0, -1.5m |

*1: Included in Net-radiometer (CNR1, Kipp and Zonen, B.V.)

*2: Radiation and Energy Balance Systems

*3: Time Domain Reflectometry

Table 2-2 Instruments for the observation at the station of protected area.

| Component | Instrument | Model / Manufacturer (location) | Height / depth |
|---|---|---|---|
| Relative humidity / Air temperature | Capacitance hygrometer | HMP45A / Vaisala Oy. (Helsinki, Finland) | 2.5 m |
| | Platinum resistance thermometer in ventilation shelter | PVC-02-AC / Prede Co. Ltd. (Tokyo, Japan) | |
| Surface temperature | Infrared thermometer | 303F / Konica Minolta Holdings, Inc. (Tokyo, Japan) | 2.5 m |
| Sensible / latent heat flux | Sonic aemometer-thermometer | R3A / Gill instruments Ltd. (Hampshire, U.K) | 3.0 m |
| | $CO_2$/$H_2O$ Infrared gas analyser [until March 2004] | OP2 / ADC BioSientific Inc. (Hoddesdon, U.K.) | |
| | $CO_2$/$H_2O$ Infrared gas analyser [since April 2004] | Li7500 / Li-cor Inc. (Lincoln, U.S.) | |
| Short-wave radiation | Pyranometers[*1] | CM3 / Kipp and Zonen B.V. (Delft, Netherlands) | 2.5 m |
| Long-wave radiation | Pygrometers[*1] | CG3 / Kipp and Zonen B.V. (Delft, Netherlands | 2.5 m |
| Air pressure | Barometer | PTB210 / Vaisala Oy. (Helsinki, Finland) | 1.3 m |
| Precipitation | Tipping bucket rain gauge | 52202 / R. M. Young Inc. (Traverse, U.S.) | |
| Soil heat flux | Heat flux plate | HFT1.1 / REBS[*2] Inc. (Seattle, U.S.) | -0.02, -0.1m |
| Soil temperature | Platinum resistance thermometer | C-PTG / Climatec Inc. (Tokyo, Japan) | -0.05, -0.1, -0.2, -0.3, -0.5, -0.7, -1.0, -1.5m |
| Volumetric water content | TDR[*3] sensor | CS616 / Cambel Scientific Inc. (Logan, U.S.) | -0.1, -0.2, -0.3, -0.7, -1.0, -1.5m |

*1: Included in Net-radiometer (CNR1, Kipp and Zonen, B.V.)

*2: Radiation and Energy Balance Systems

*3: Time Domain Reflectometry

Table 2-3 The number of soil moisture (SM) data measured around the protected-area station in August of 2005. Circles denote the SM values measured at the protected-area station.

| SM (%) | the number of data | | | |
|---|---|---|---|---|
| | 8/1 7:20 | 8/2 7:30 | 8/4 7:54 | 8/4 10:37 |
| 4~5 | 0 | 0 | 0 | 1 |
| 5~6 | 0 | 0 | 0 | 2 |
| 6~7 | 0 | 0 | 8 | 13 |
| 7~8 | 0 | 6 | ○ **24** | ○ **29** |
| 8~9 | 0 | 14 | 14 | 12 |
| 9~10 | 2 | ○ **26** | 13 | 4 |
| 10~11 | 3 | 10 | 2 | 0 |
| 11~12 | 9 | 4 | 0 | 0 |
| 12~13 | ○ **12** | 1 | 0 | 0 |
| 13~14 | 19 | 0 | 0 | 0 |
| 14~15 | 9 | 0 | 0 | 0 |
| 15~16 | 6 | 0 | 0 | 0 |
| 16~ | 1 | 0 | 0 | 0 |

Table 2-4 The ratio (%) of the three-year data removed by data selection.

| crreteria | pastoral | protected |
|---|---|---|
| daytime & no rainfall | 52 | 64 |
| > 10 W m-2 | 47 | 56 |
| Wind direction | 23 | 30 |

Table 2-5 Commonly used animal unit equivalents (USDA National Range and Pasture Handbook, 1997)

| Class of animal | Animal Unit Equivalent |
|---|---|
| Cow, 1000 lb, with calf | 1.00 |
| Horse, mature | 1.25 |
| Sheep, mature | 0.20 |
| goat, mature | 0.15 |

Table 2-6 The relation NDVI and surface condition (Kondo, 1994).

| NDVI | Suface condition |
|---|---|
| -0.1~0.1 | water, snow and ice (clouds) |
| 0.1 | dead vegetaion |
| 0.2~0.7 | green vegetation |

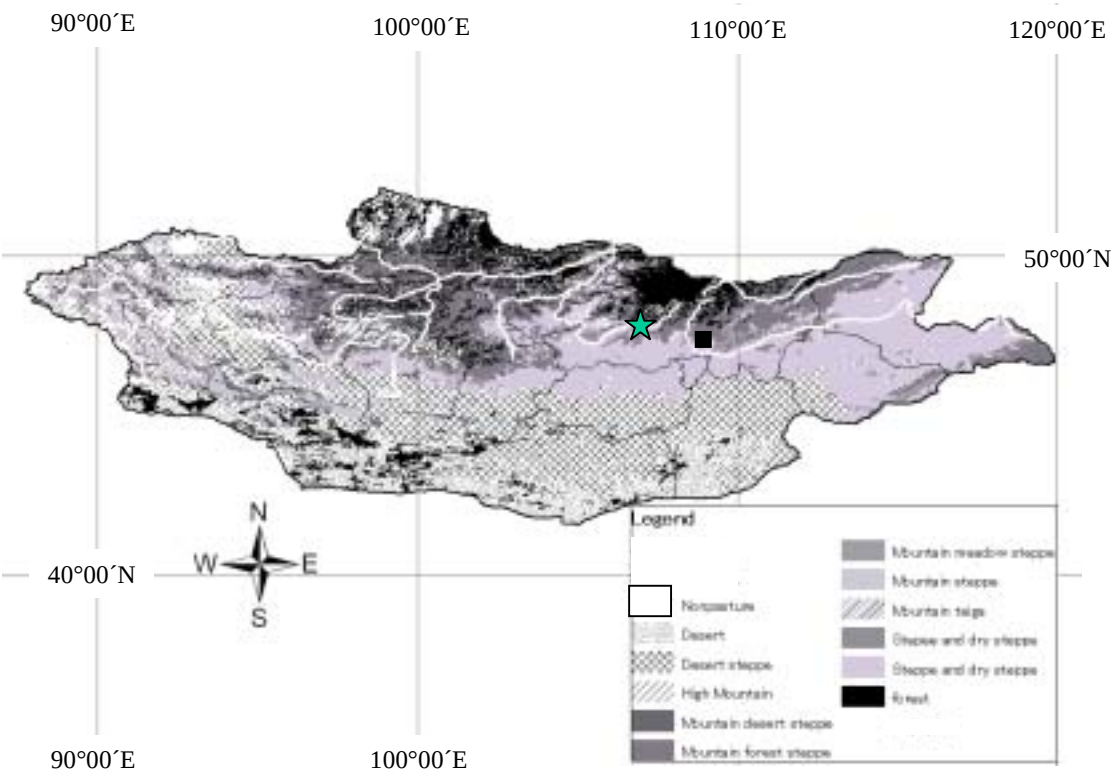


Fig. 2-1 Location of the study area and distribution of vegetation. A star and square show the Ulaanbaatar city and KBU, respectively. The data was obtained from Saandar and Sugita (2004).

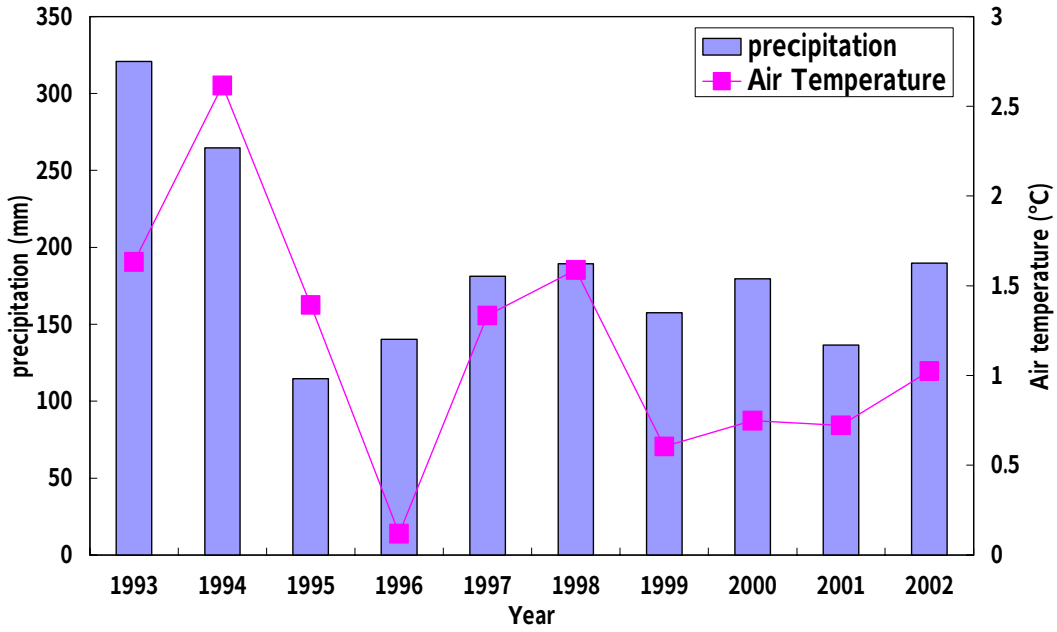


Fig. 2-2 Annual precipitation and average annual air temperature for a decade. The data set was measured in KBU Meteopost managed by the Institute of Meteorology and Hydrology, Mongolia

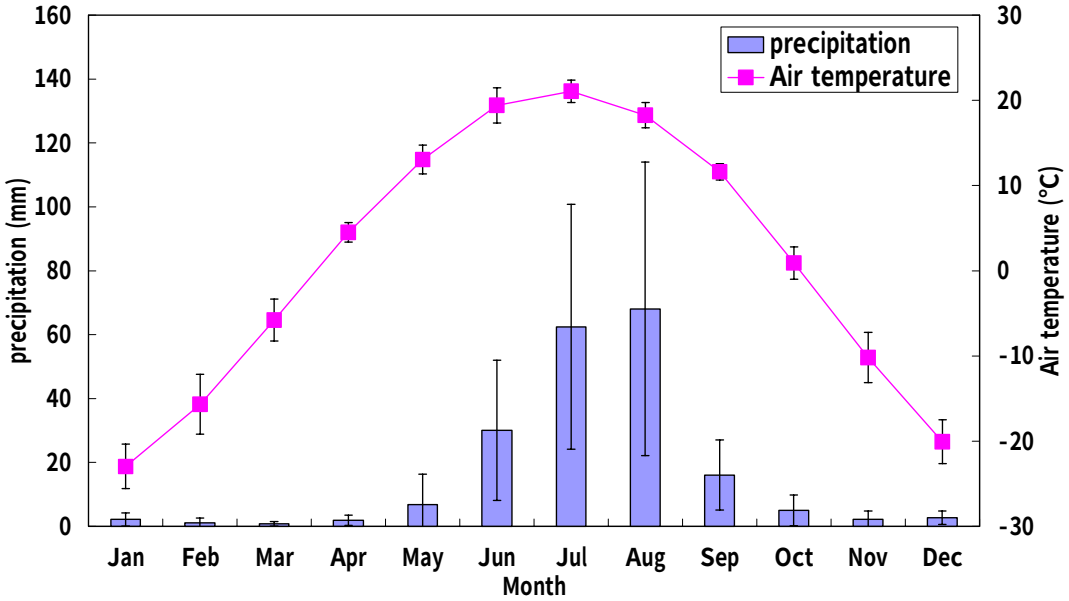


Fig. 2-3 Average monthly precipitation and air temperature. The data set was measured in KBU Meteopost managed by the Institute of Meteorology and Hydrology, Mongolia

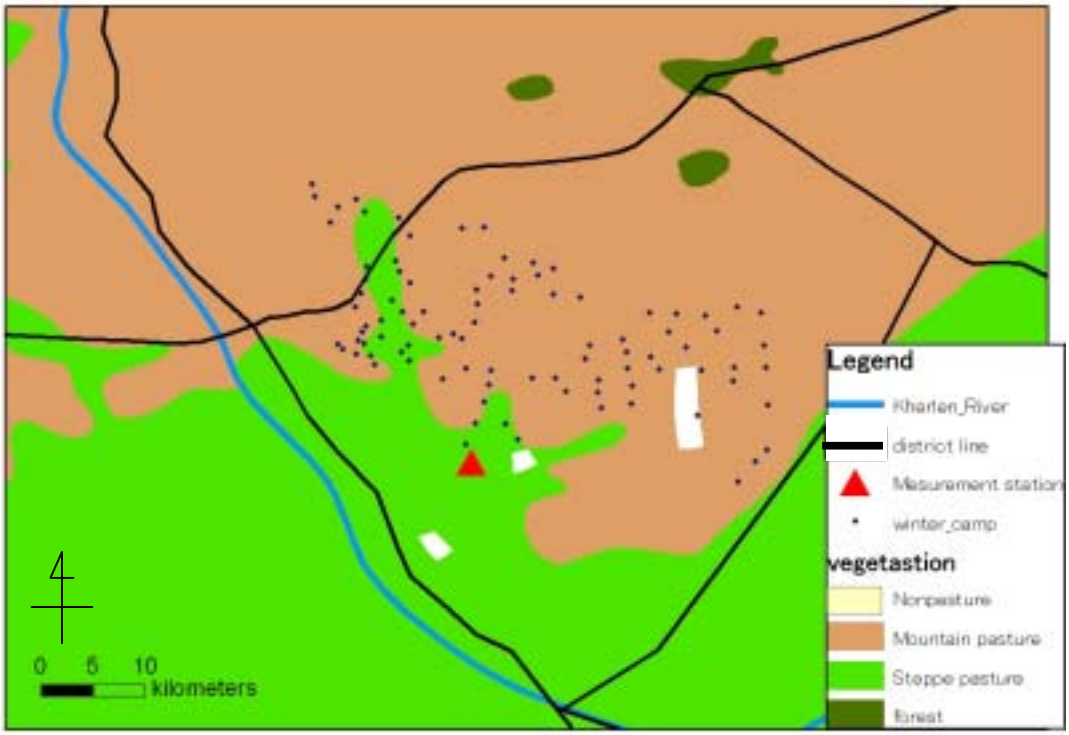


Fig. 2-4 The location of winter camps made for winter grazing in mountain areas. (Gerelsuren, 2006, personal communication)

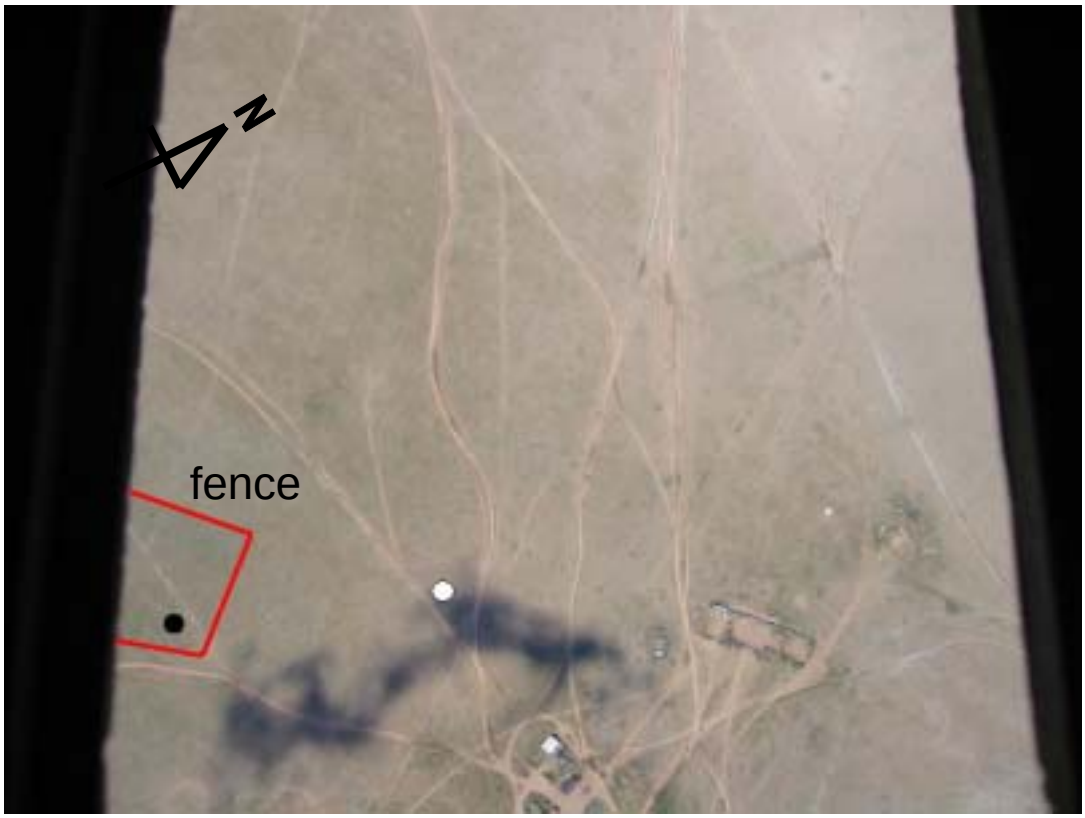


Fig. 2-5 Photograph of the landscape around KBU measurement station. Two circles show the measurement stations. (http://erc3.suiri.tsukuba.ac.jp/~raise/)

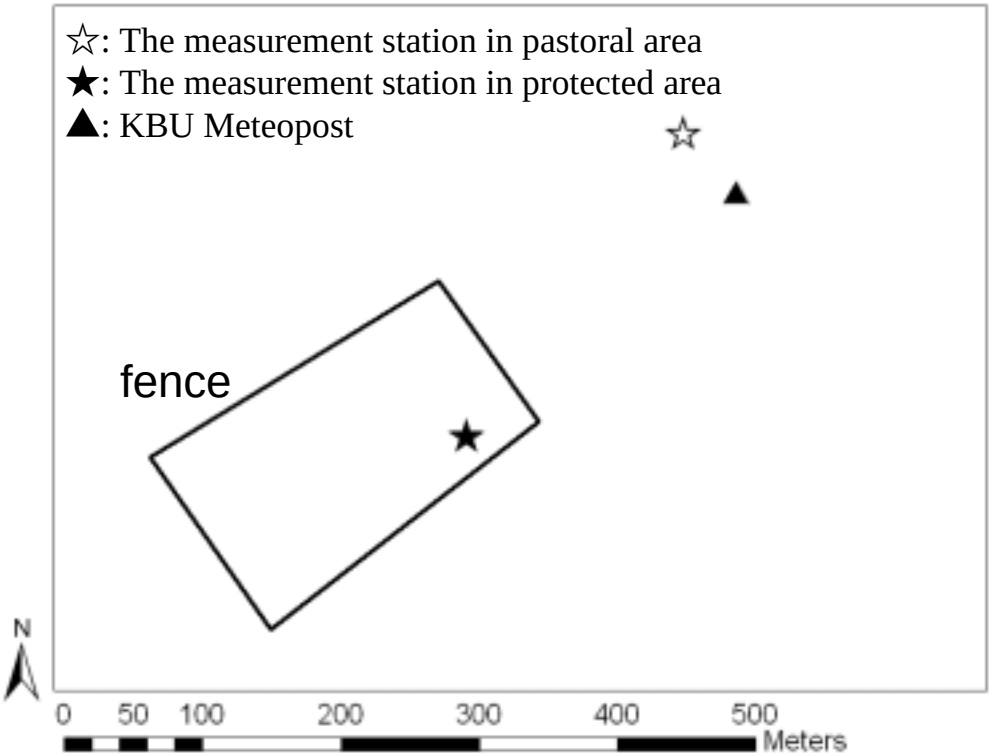


Fig. 2-6 Location of the measurement stations. Fence was constructed in August of 2002 in order to study possible grazing impact. KBU Meteopost is managed by the Institute of Meteorology and Hydrology, Mongolia.

Fig. 2-7 Photograph of the fence in the summer of 2005.

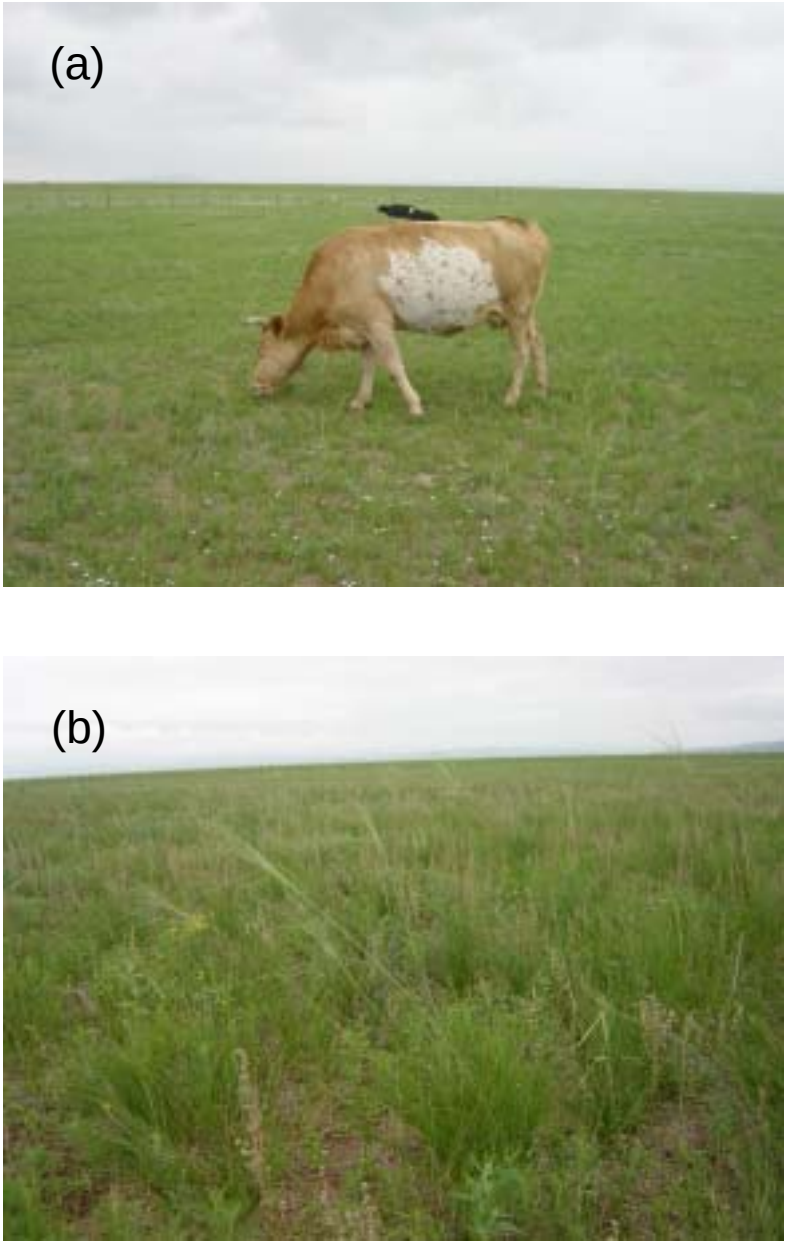


Fig. 2-8 Photographs of the landscape around measurement stations in the summer of 2003. (a): pastoral area, (b): protected area. (Urano, 2005)

Fig. 2-9 Photographs of the landscape around measurement stations in the winter of 2004. (a): pastoral area, (b): protected area. (photograph by Mr. Gombold of the Institude of Meteorology and Hydrology, Mongolia)

Fig. 2-10 Photographs of the landscape around measurement stations in the summer of 2005. (a): pastoral area, (b): protected area.

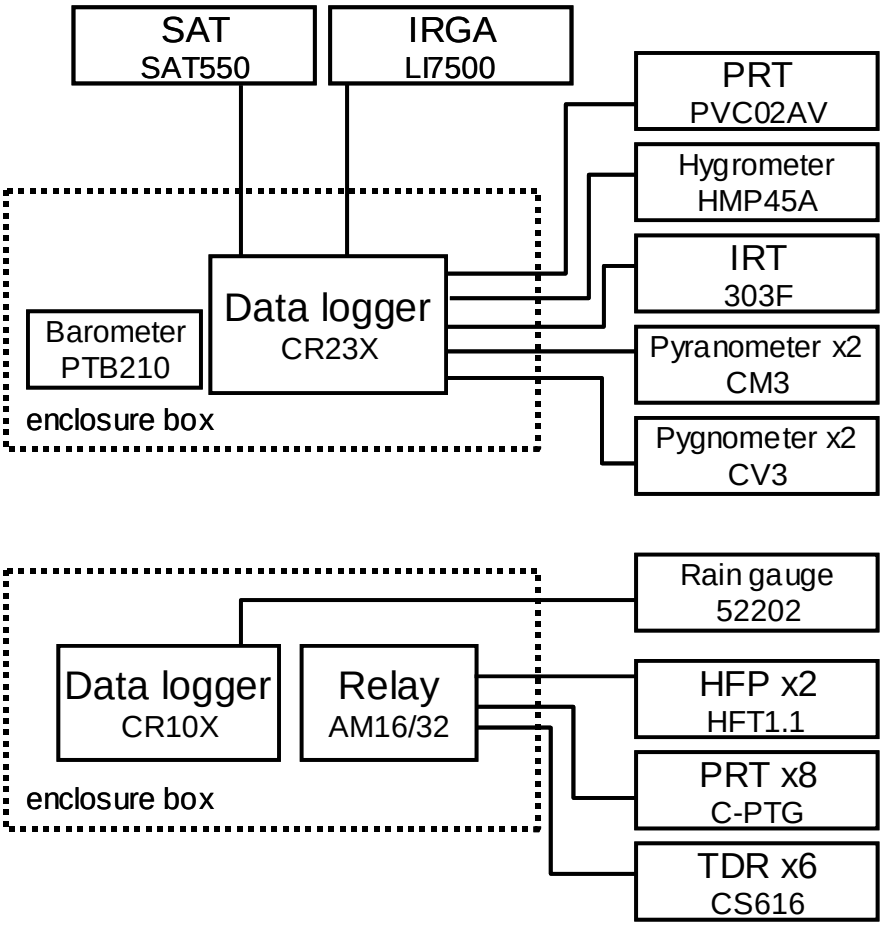


Fig. 2-11 Schematic diagram of the observation system of the station of pastoral area. (measurement system only) SAT: sonic anemometer-thermometer, IRGA: infrared gas analyzer, PRT: platinum resistance thermometer, IRT: infrared thermometer, HFP: heat flux plate, TDR: time domain reflectmetry. (Kotani, 2006)

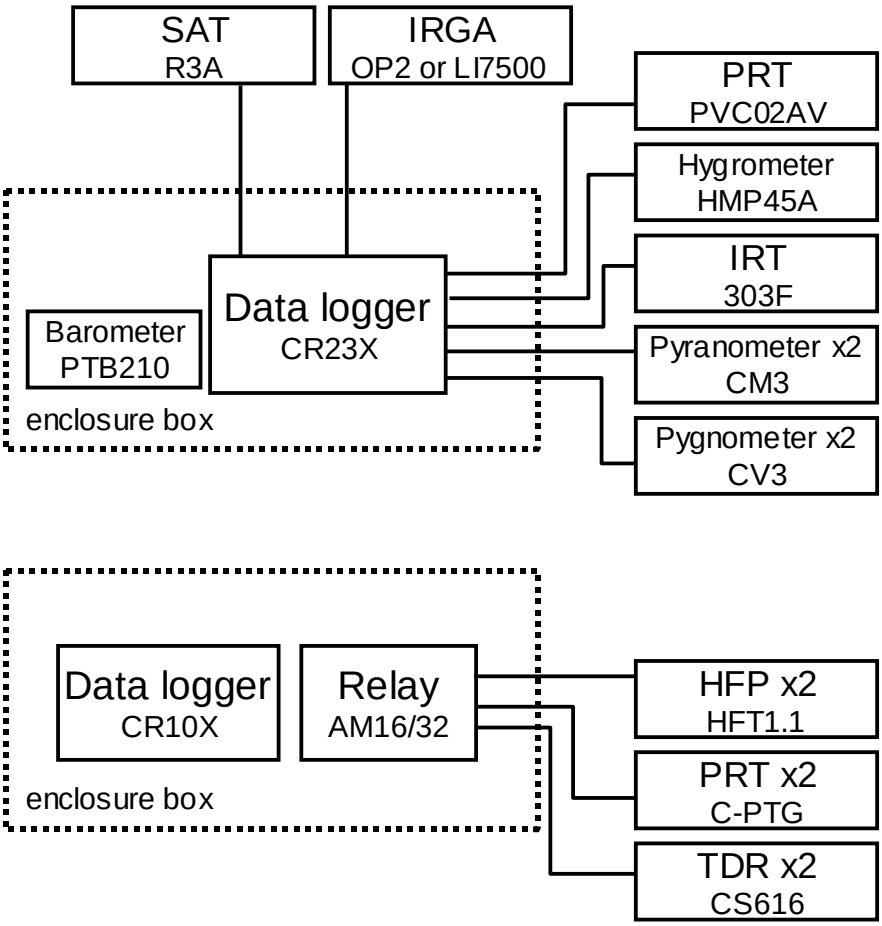


Fig. 2-12 Schematic diagram of the observation system of the station of proteted area. (measurement system only) SAT: sonic anemometer-thermometer, IRGA: infrared gas analyzer, PRT: platinum resistance thermometer, IRT: infrared thermometer, HFP: heat flux plate, TDR: time domain reflectmetry.

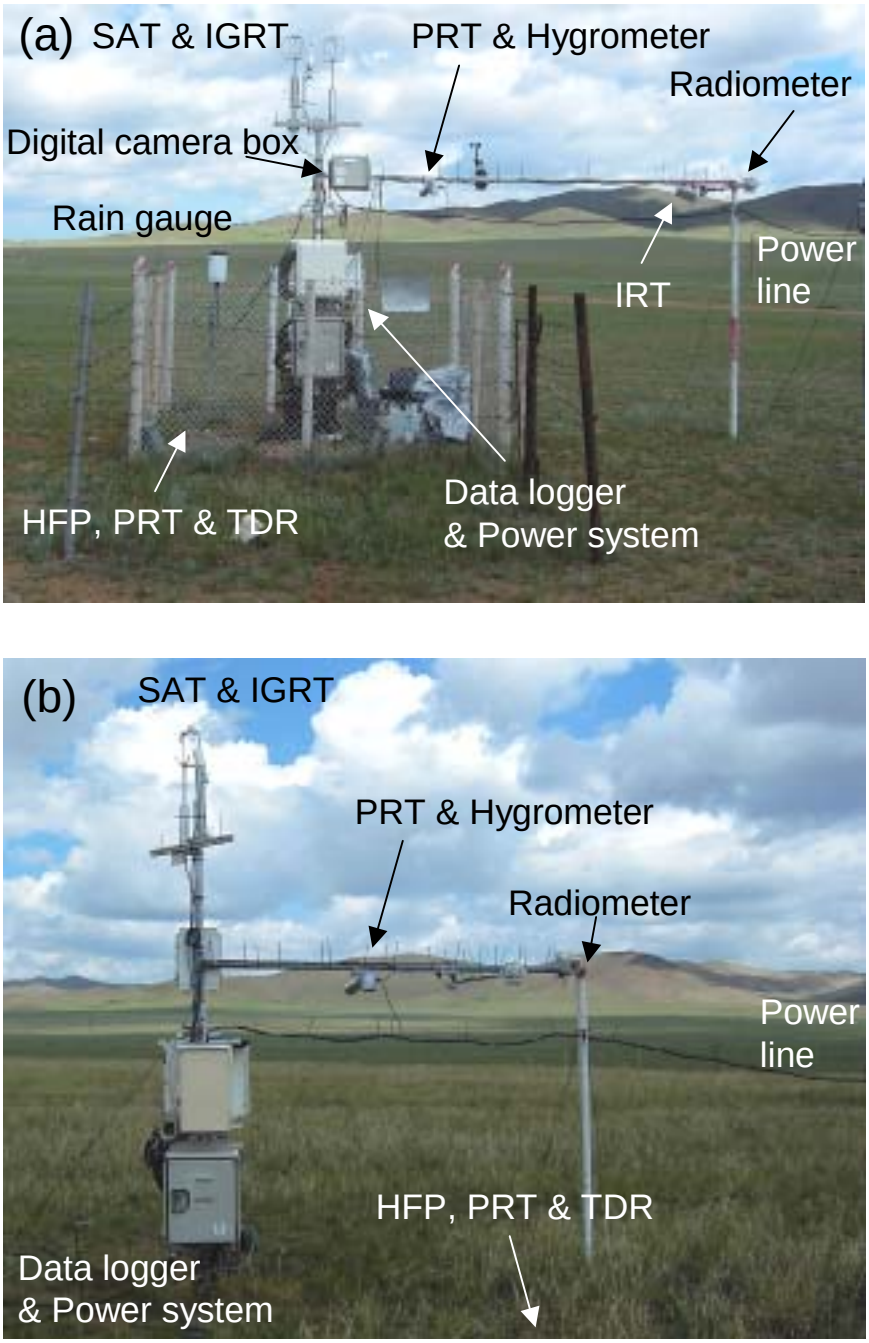


Fig. 2-13 Photographs of the observation system of the stations. (a): pastoral area, (b): protected area. SAT: sonic anemometer-thermometer, IRGA: infrared gas analyzer, PRT: platinum resistance thermometer, IRT: infrared thermometer, HFP: heat flux plate, TDR: time domain reflectmetry.

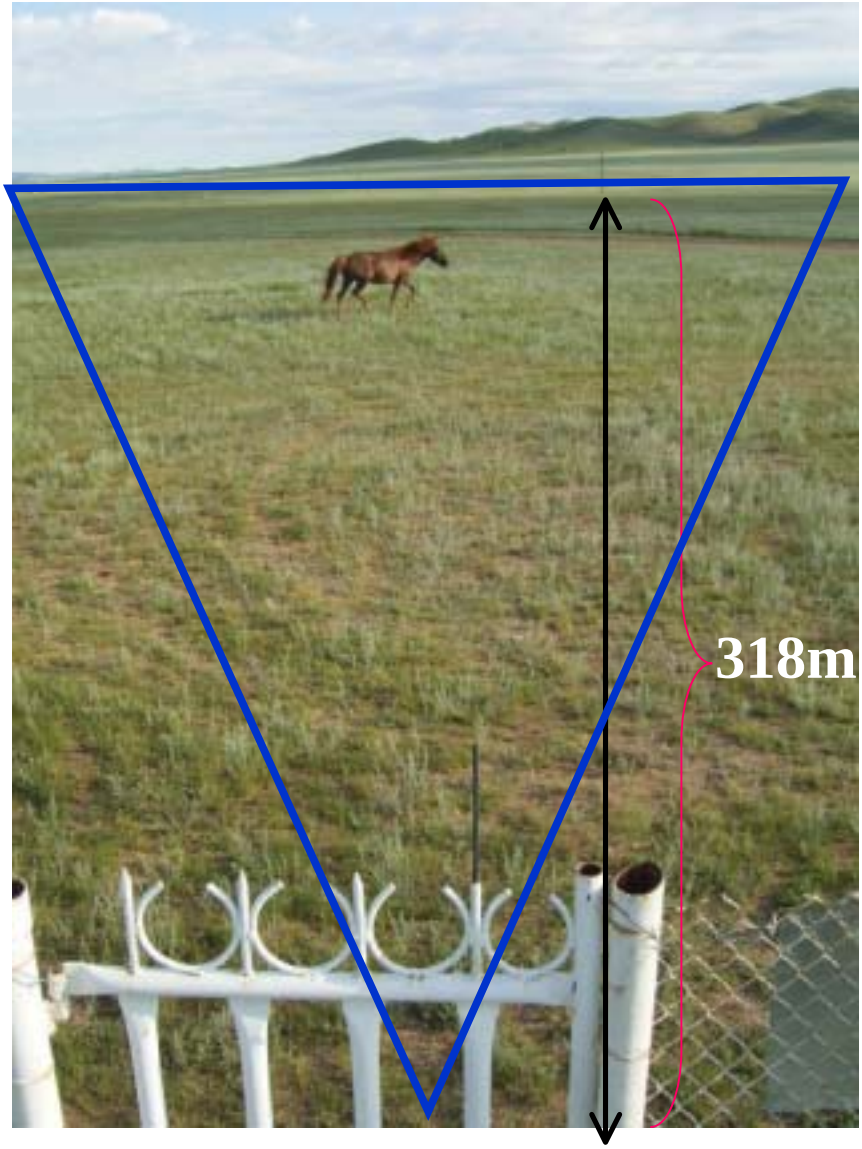


Fig. 2-14 Photographs taken by the digital camera of the pastoral station

Fig. 2-15 Examples of photo taken in the measurement station. (a) 2005/7/27 18:27 (b) 2005/7/27 18:57 (c) 2005/7/27 19:27 (d) 2005/7/27 19:57 (e) 2005/7/27 20:27 (f) 2005/7/27 20:57

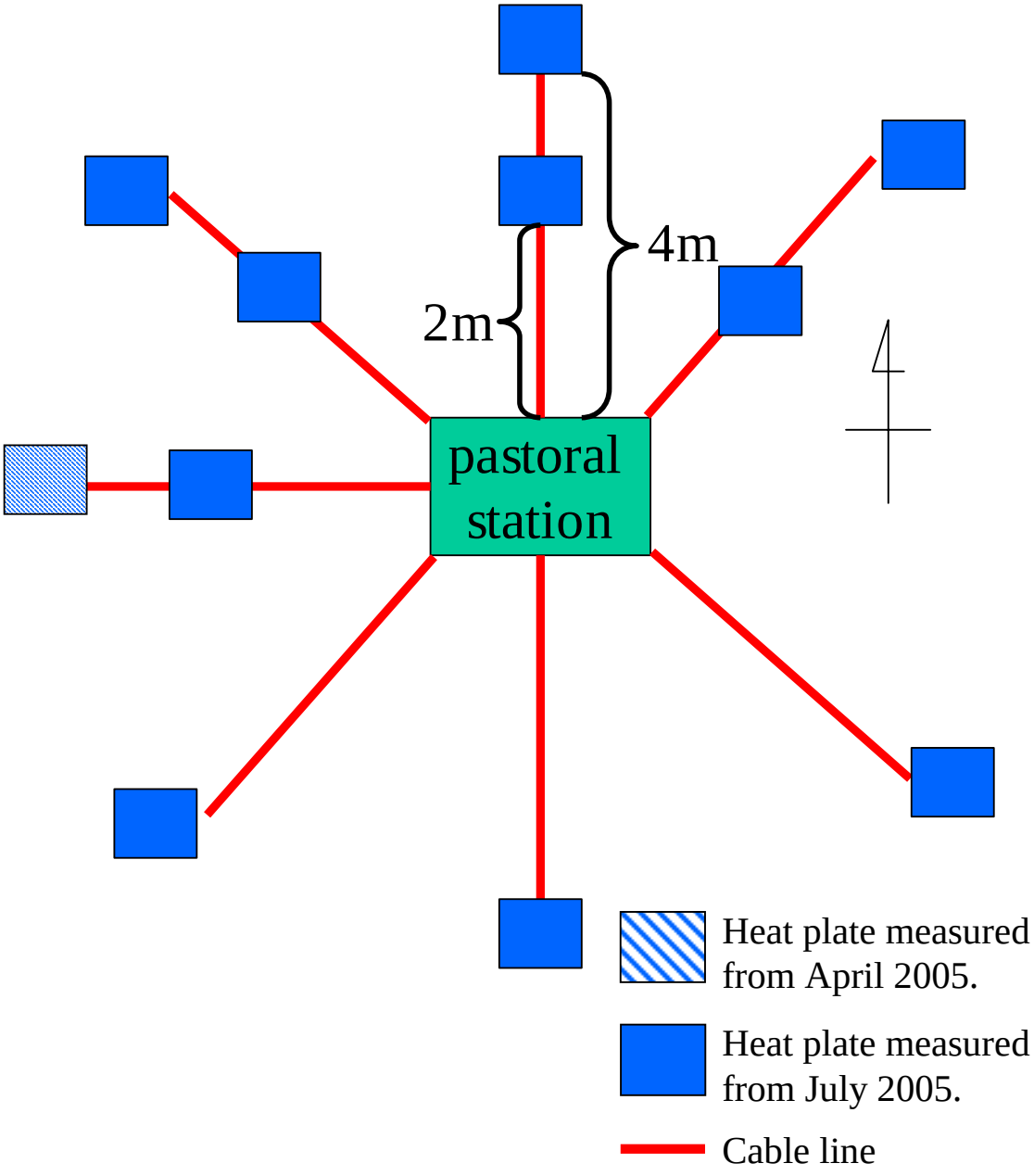


Fig. 2-16 The measurement of soil heat flux (*G*) values by the 11 heat plates in the pastoral area.

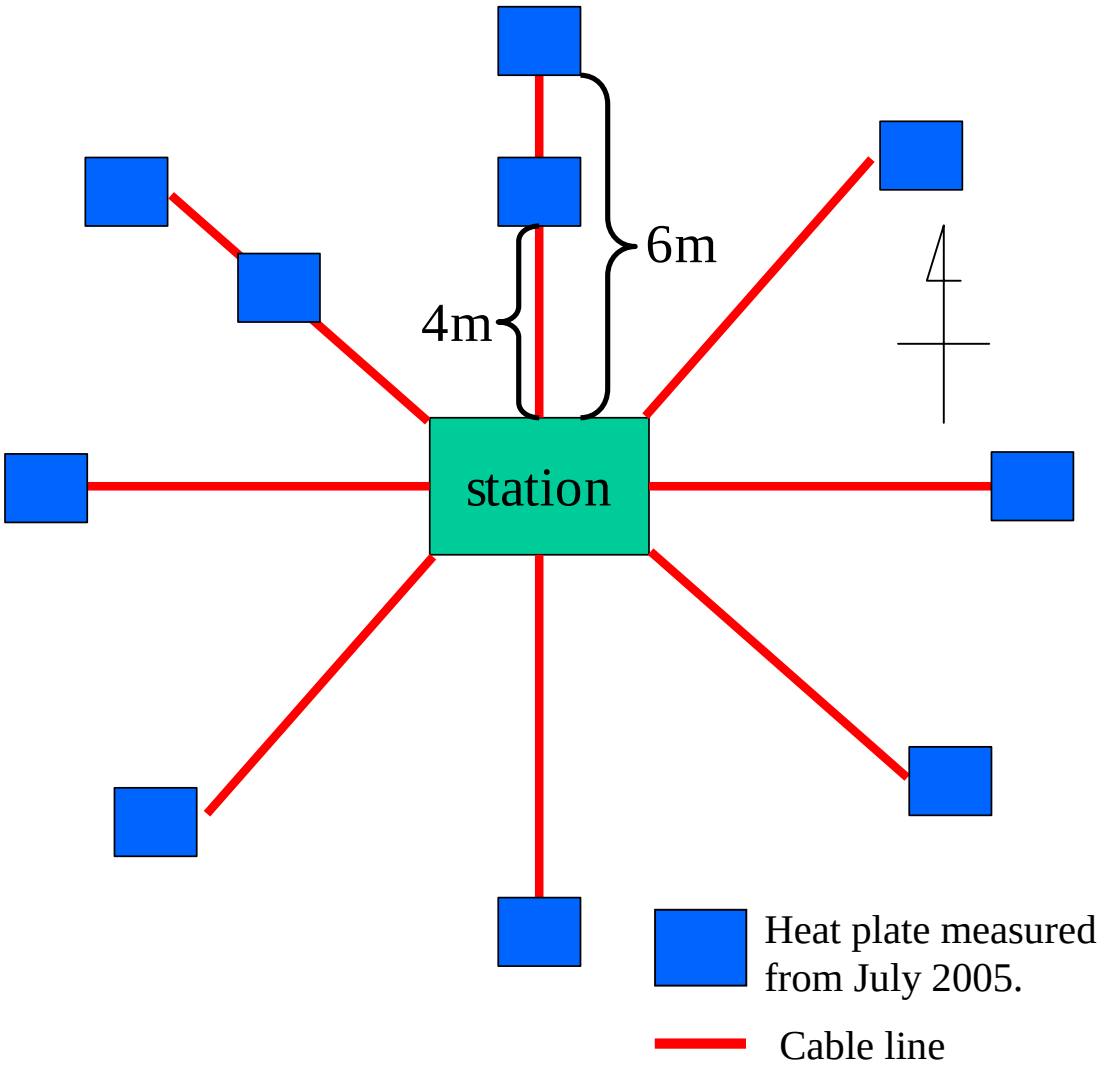


Fig. 2-17 The measurement of soil heat flux (*G*) values by the10 heat plates in the protected area.

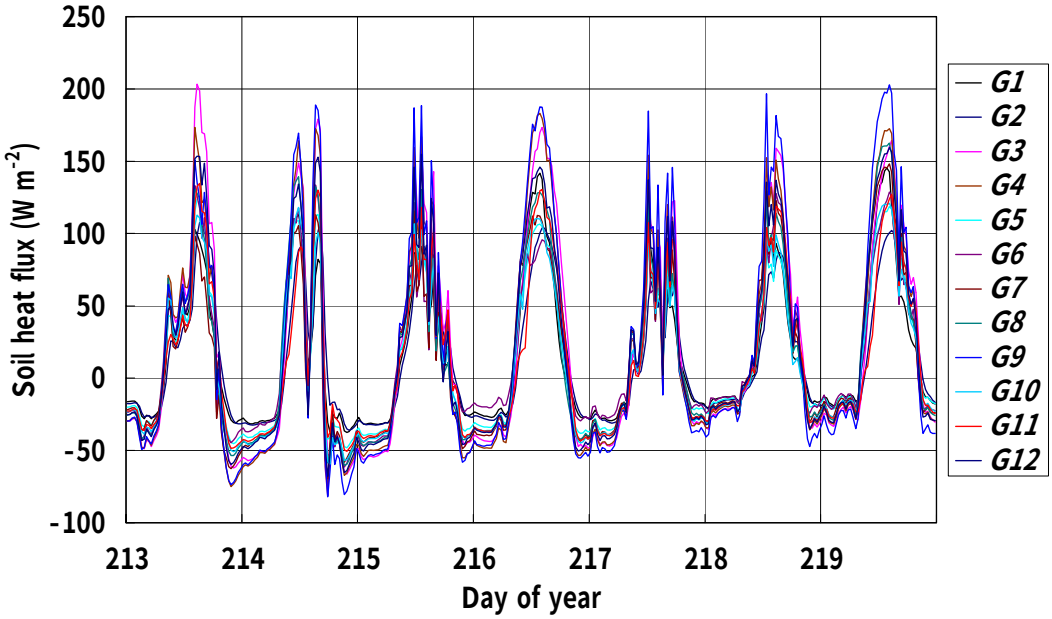


Fig. 2-18 The diurnal change of soil heat flux (*G*) values in the pastoral area. *G1*: the value measured inside station fence, *G2~12*: the values measured outside of station fence.

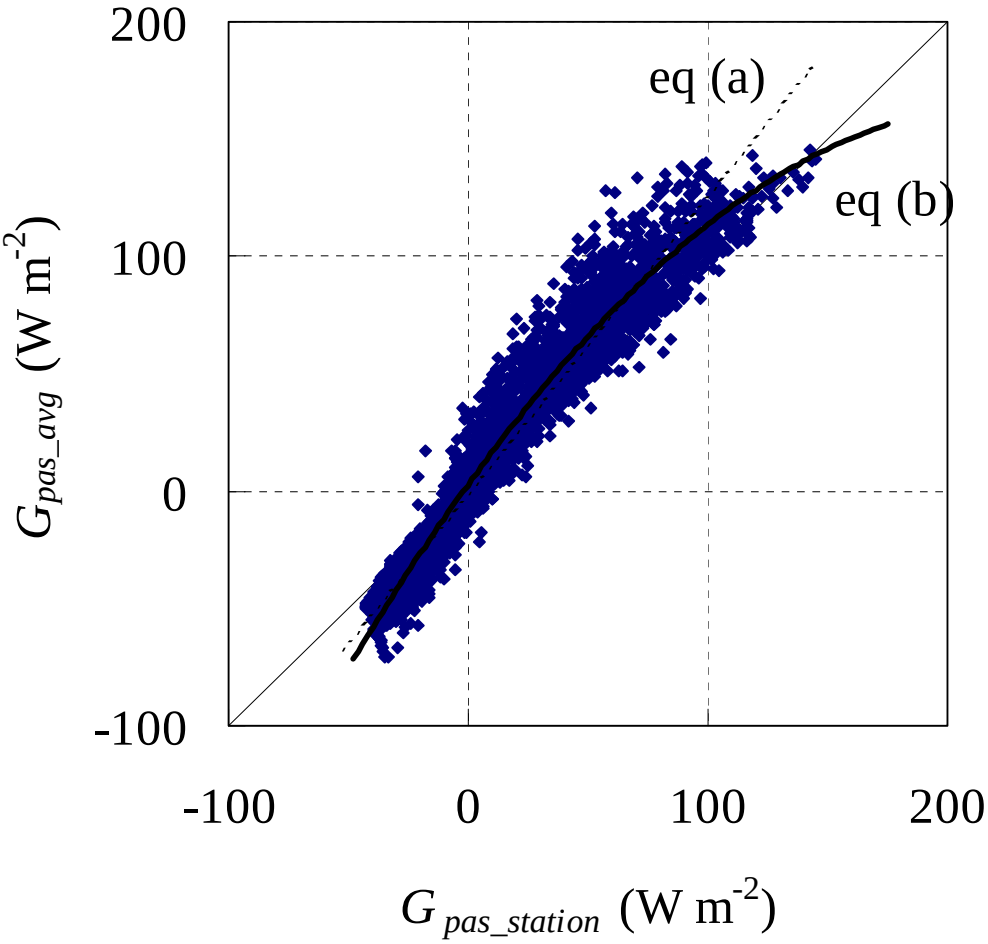


Fig. 2-19 A comparison between $G_{pas_station}$ and $G_{pas_avg}$. $G_{pas_station}$: the $G$ values measured in pastoral station, $G_{pas_avg}$: the average of the $G$ values measured by the 11 heat plates. The data set was 30-average values. The measurement period was from July to October 2005. A straight line and a curve are the following regression lines, eq (a): $G_{pas_avg} = 1.26\ G_{pas_station} - 1.17$ ($R^2 = 0.95$), eq (b); $G_{pas_avg} = -0.0031 G_{pas_station}^2 - +1.41 G_{pas_station} + 2.95$ ($R^2 = 0.96$).

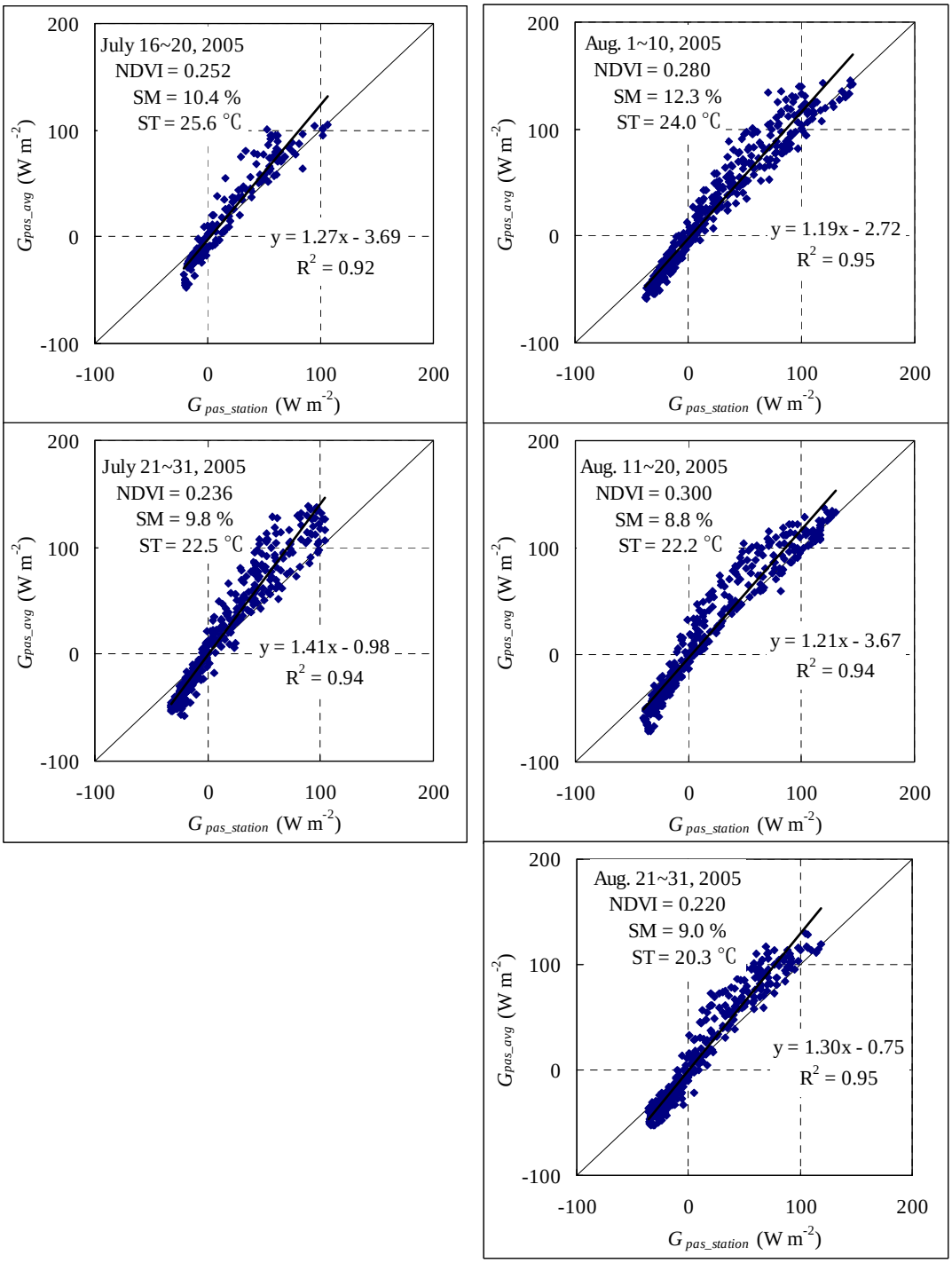


Fig. 2-20a A comparison between $G_{pas_station}$ and $G_{pas_avg}$. $G_{pas_station}$: the $G$ values measured in pastoral station, $G_{pas_avg}$: the average of the $G$ values measured by the 11 heat plates. The data set was 30-average values. The straight lines are regression lines. NDVI, SM and ST were average values in the periods written in each graph. NFVI: Normalized Difference Vegetation Index, SM: soil moisture at –0.10 cm, ST: soil temperature at –0.05 cm.

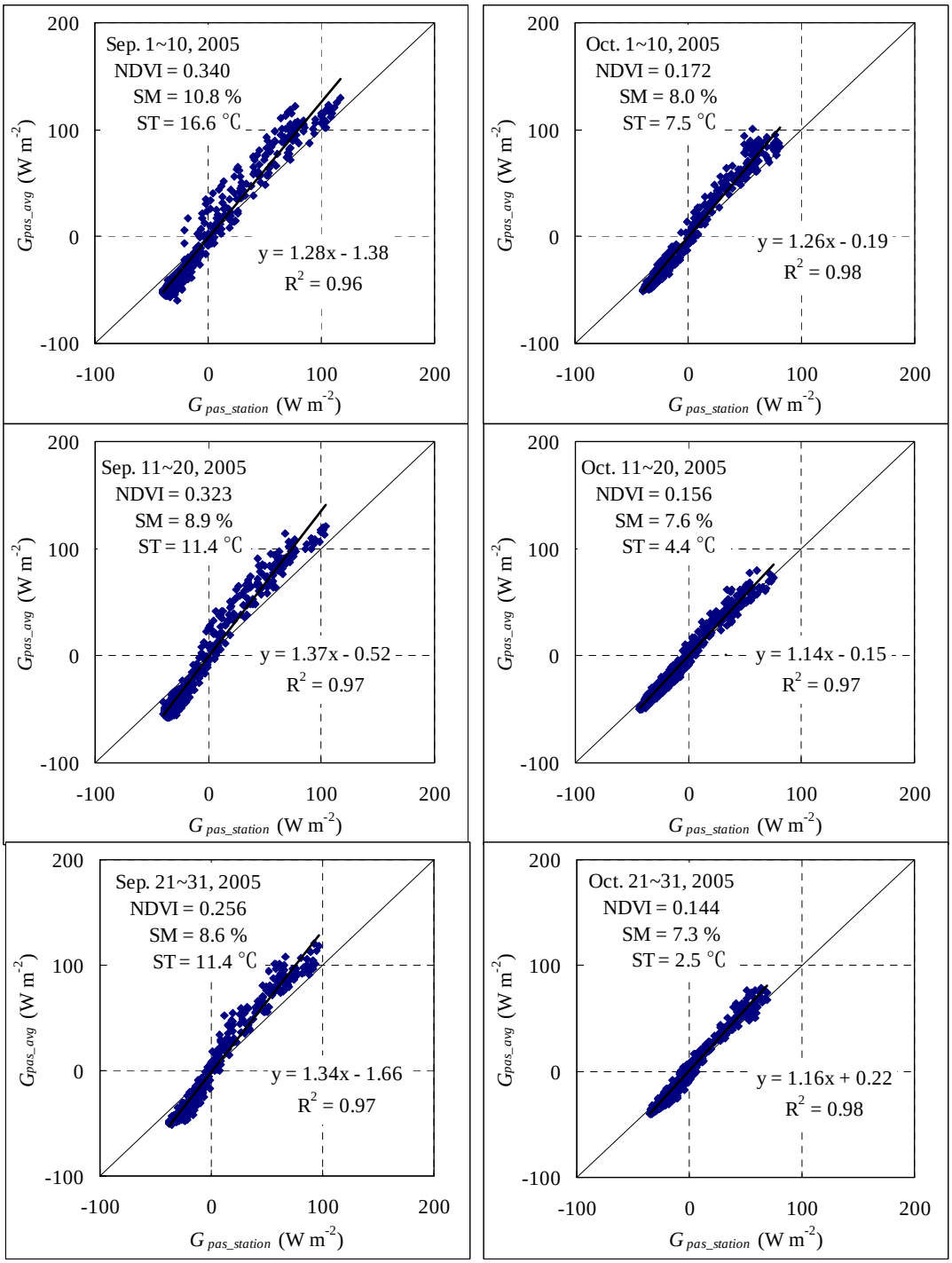


Fig. 2-20b The comparison between $G_{pas_station}$ and $G_{pas_avg}$. $G_{pas_station}$: the $G$ values measured in pastoral station, $G_{pas_avg}$: the average of the $G$ values measured by the 11 heat plates. The data set was 30-average values. The straight lines are regression lines. NDVI, SM and ST were average values in the periods written in each graph. NFVI: Normalized Difference Vegetation Index, SM: soil moisture at –0.10 cm, ST: soil temperature at –0.05 cm.

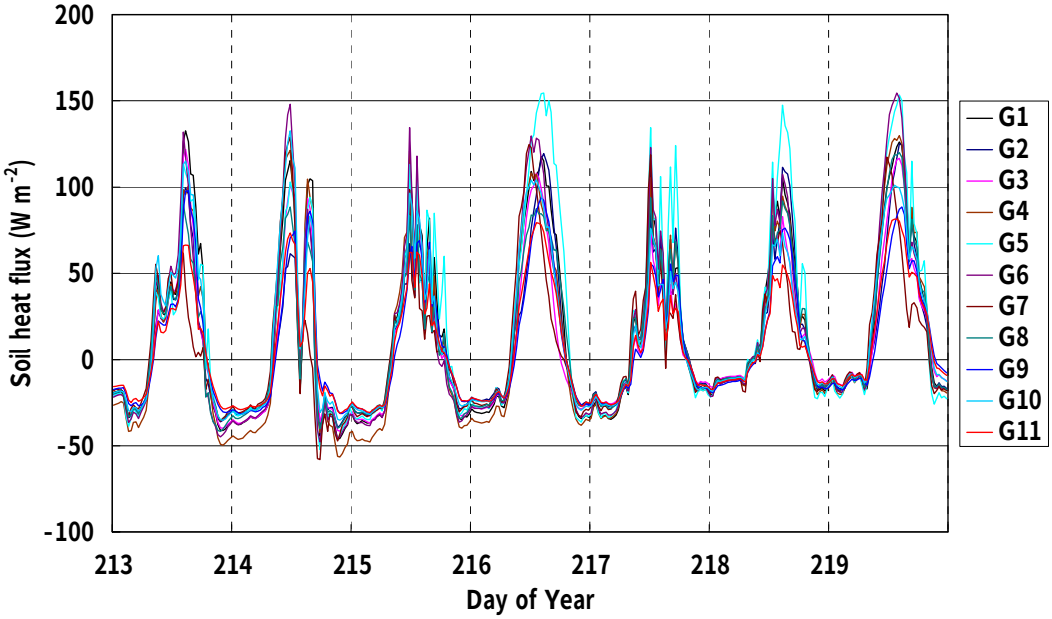


Fig.2-21 The diurnal change of soil heat flux (*G*) values in the protected area. *G1*: the value measured since March of 2003, *G2~11*: the value measured since July of 2005.

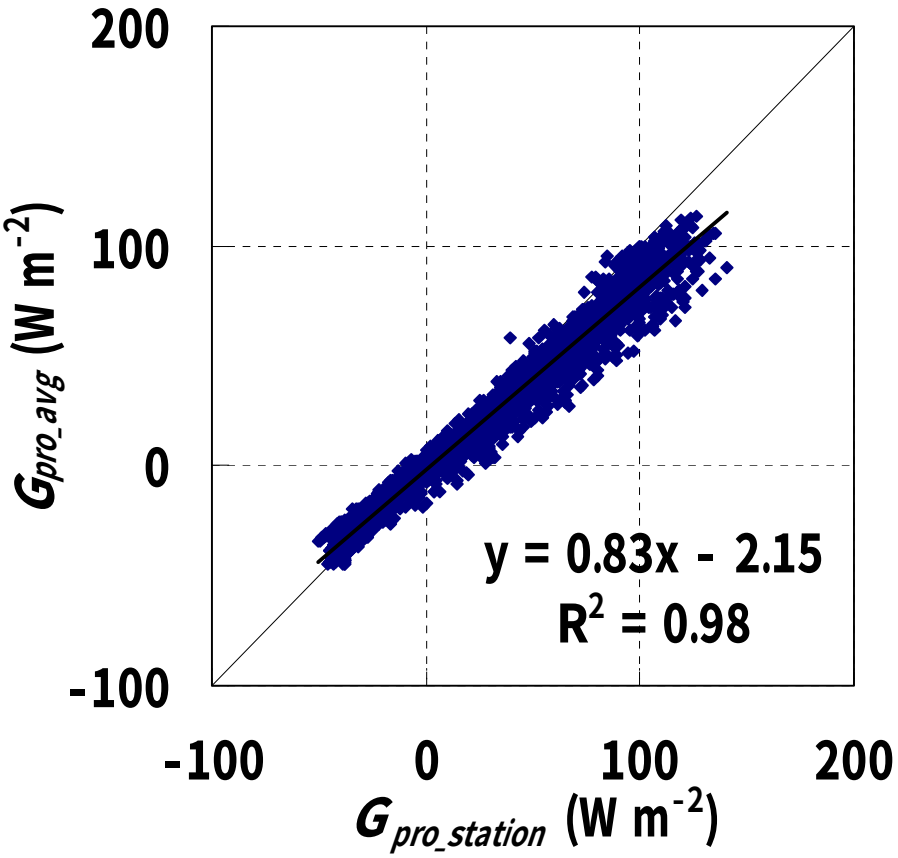


Fig. 2-22 A comparison between $G_{pro_station}$ and $G_{pro_avg}$. $G_{pro_station}$: the $G$ values measured in protected station, $G_{pro_avg}$: the average of the $G$ values measured 10 heat plates. The data set was 30-average values. The straight line is regression line. The measurement period was from July to October 2005.

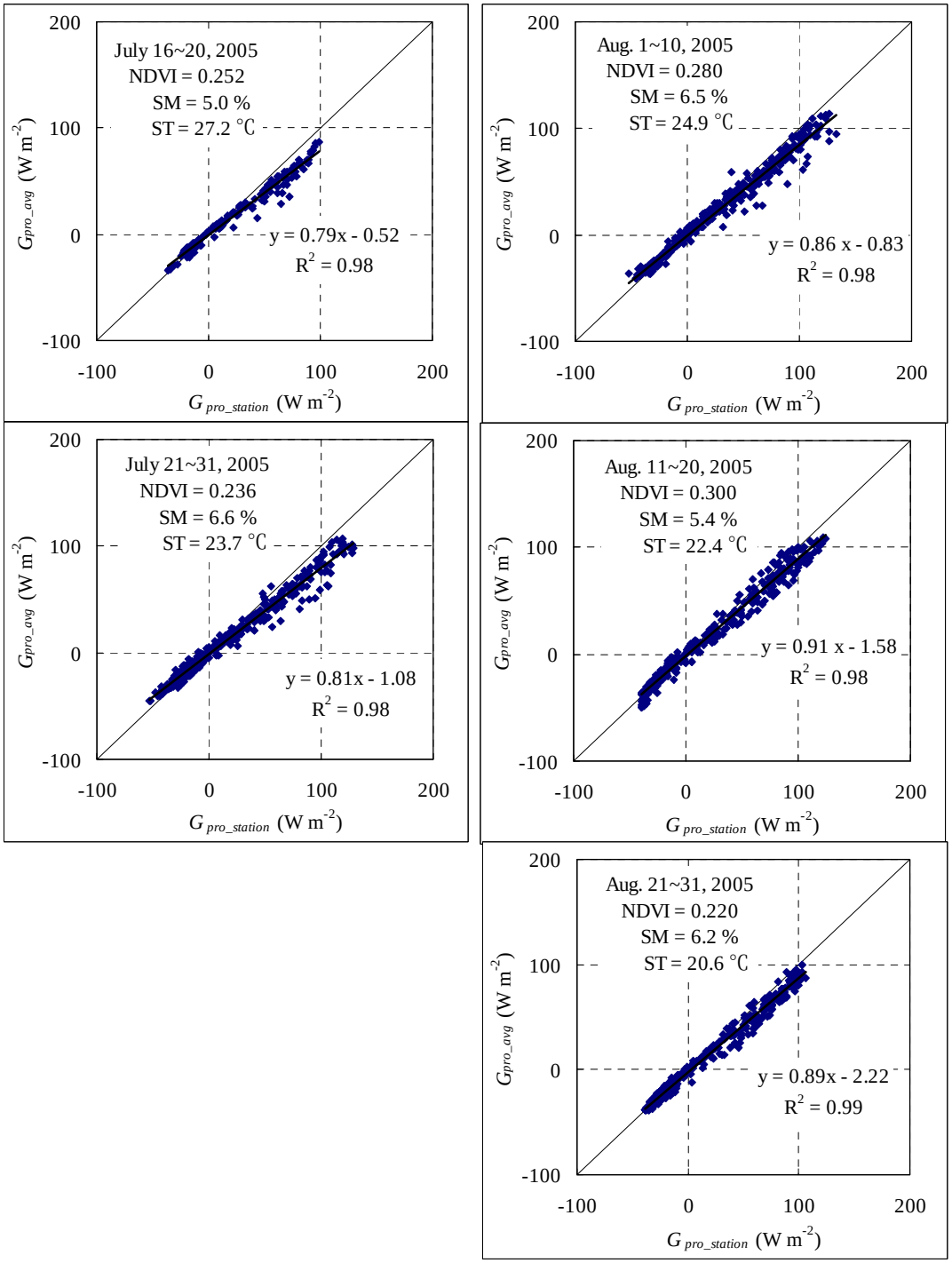


Fig. 2-23a A comparison between $G_{pro_station}$ and $G_{pro_avg}$. $G_{pro_station}$: the $G$ values measured in the protected station, $G_{pro_avg}$: the average of the $G$ values measured by the 10 heat plates. The data set was 30-average values. The straight lines are regression lines. NDVI, SM and ST were average values in the periods written in each graph. NFVI: Normalized Difference Vegetation Index, SM: soil moisture at –0.10 cm, ST: soil temperature at –0.05 cm.

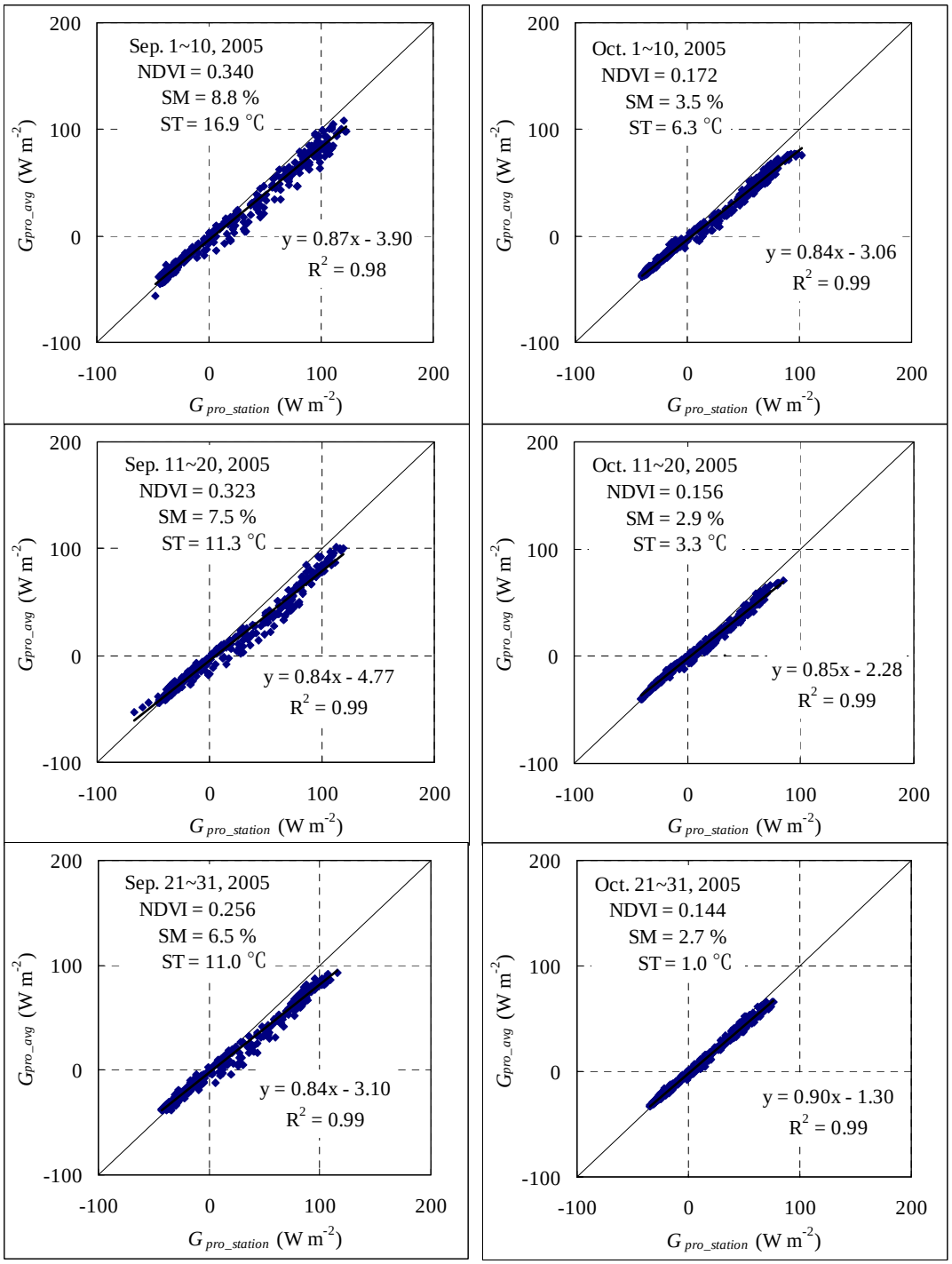


Fig. 2-23b A comparison between $G_{pro_station}$ and $G_{pro_avg}$. $G_{pro_station}$: the $G$ values measured in the protected station, $G_{pro_avg}$: the average of the $G$ values measured by the 10 heat plates. The data set was 30-average values. The straight lines are regression lines. NDVI, SM and ST were average values in the periods written in each graph. NDVI: Normalized Difference Vegetation Index, SM: soil moisture at –0.10 cm, ST: soil temperature at –0.05 cm.

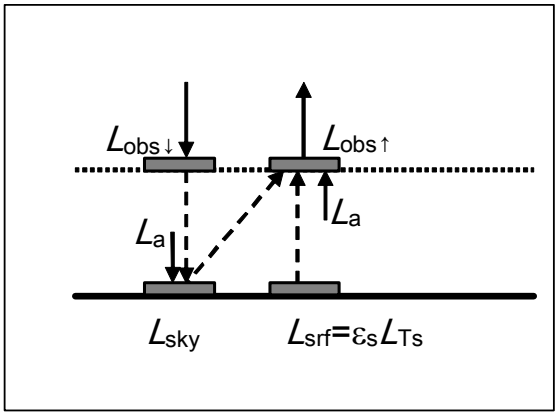


Fig. 2-24. Radiation of thermal radiation budget on ground surface and observation at sensor height. (Kotani and Sugita, in preparation) $L_{sky}$: radiation emanating from the whole atmosphere, $L_{obs\downarrow}$: downward long wave radiation observed by the sensor, $L_a$: radiation emanating from air layer between the ground surface and the sensor height, $L_{srf}$: radiation emanating from the ground surface, $L_{obs\uparrow}$: upward long wave radiation observed by the sensor,

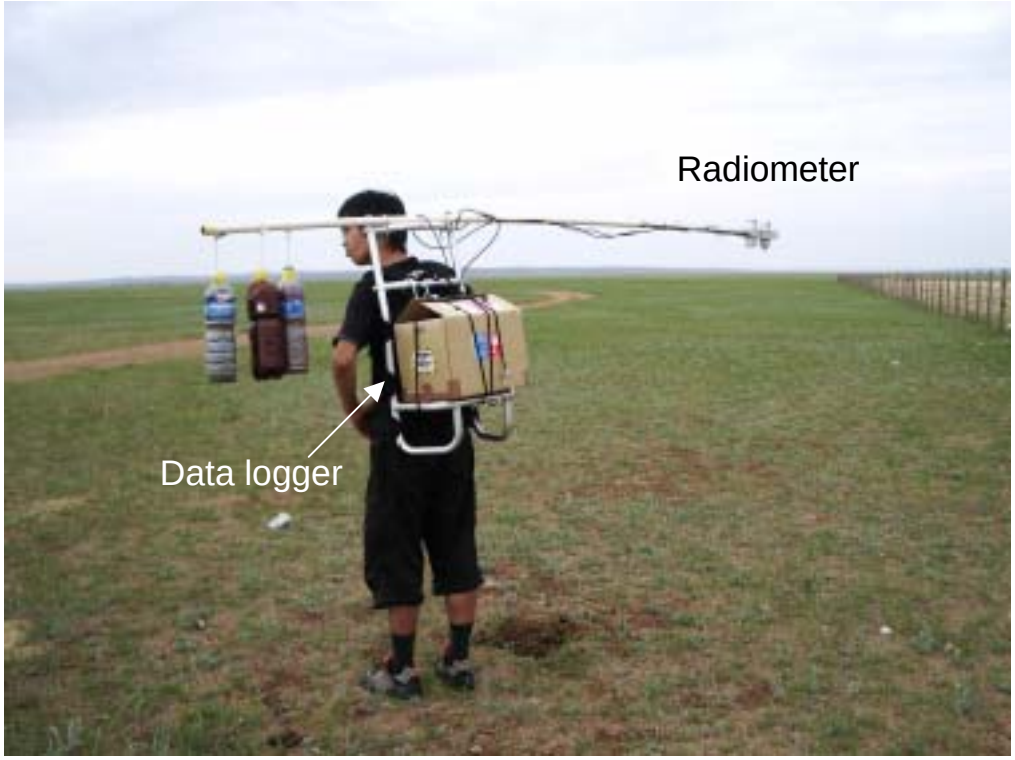


Fig. 2-25 A photograph of the observation system for the movable measurement of radiation.

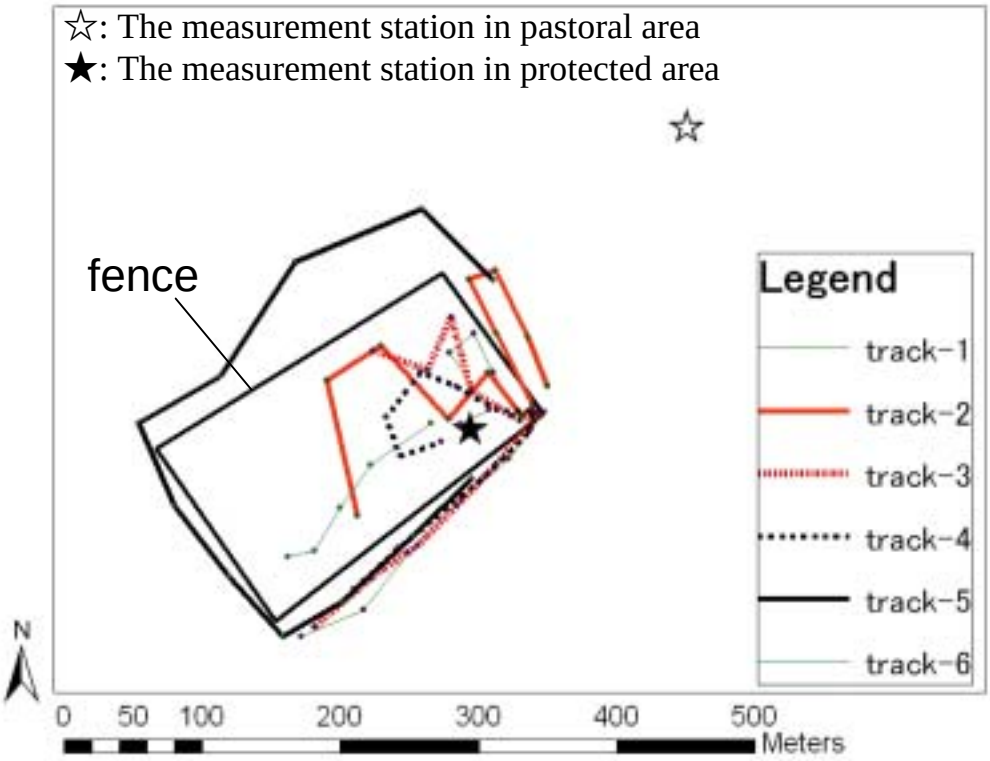


Fig. 2-26 The observation lines on which movable measurements were carried out.

Track-1. August 3, 14:30~15:30

Track-2. August 3, 18:30~19:30

Track-3. August 4, 19:00~20:00

Track-4. August 4, 20:30~21:30

Track-5. August 5, 17:30~18:30

Track-6. August 5, 19:00~19:30

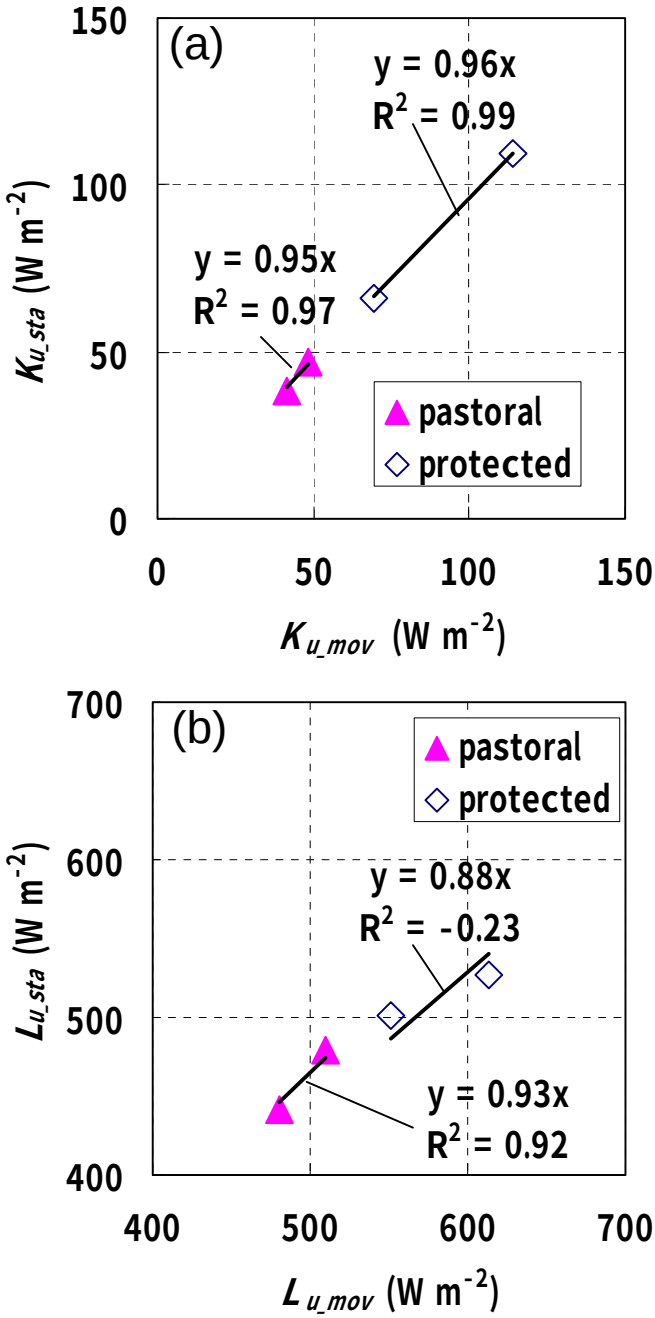


Fig. 2-27 An intercomparison of the components of radiation between those measured by instruments used for the movable measurement but placed nest the station sensor and those measured by station sensors.(a): upward shortwave radiation, (b) upward longwave radiation. $K_{u_mov}$ : upward shortwave radiation measured by moving measurement, $K_{u_sta}$ : upward shortwave radiation measured in stations, $L_{u_mov}$ : upward longwave radiation measured by moving measurement, $L_{u_sta}$ : upward longtwave radiation measured in stations. The straight lines are regression lines on an intercepts are zero.

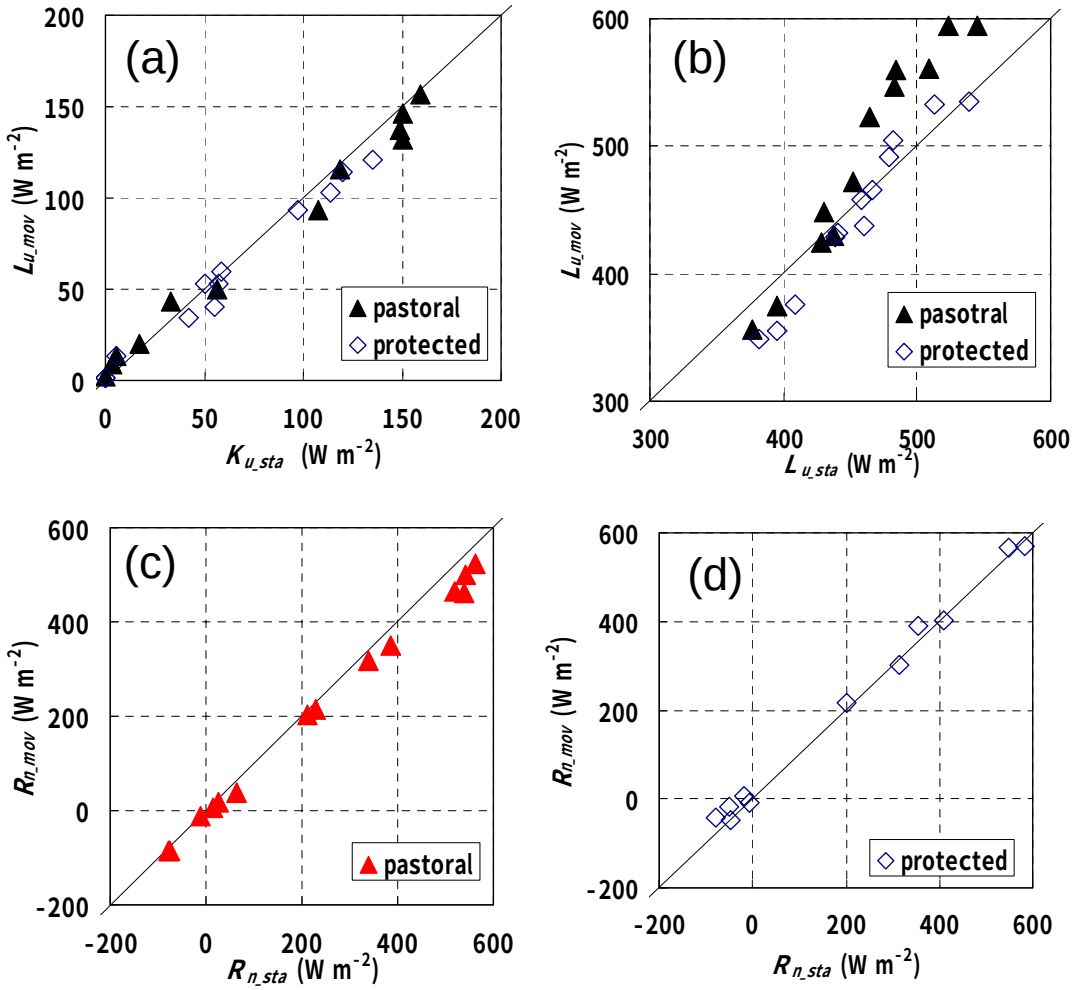


Fig. 2-28 A comparison of the components of the radiation between those measured by the movable measurement and in stations. (a): upward shortwave radiation, (b) upward longwave radiation. (c): net radiation in pastoral area, (d): net radiation in protected area. $K_{u_mov}$ : upward shortwave radiation measured by moving measurement, $K_{u_sta}$ : upward shortwave radiation measured in stations, $L_{u_mov}$ : upward longwave radiation measured by moving measurement, $L_{u_sta}$ : upward longtwave radiation measured in stations. $R_{n_mov}$ : net radiation measured by moving measurement, $R_{n_sta}$ : net radiation measured in stations.

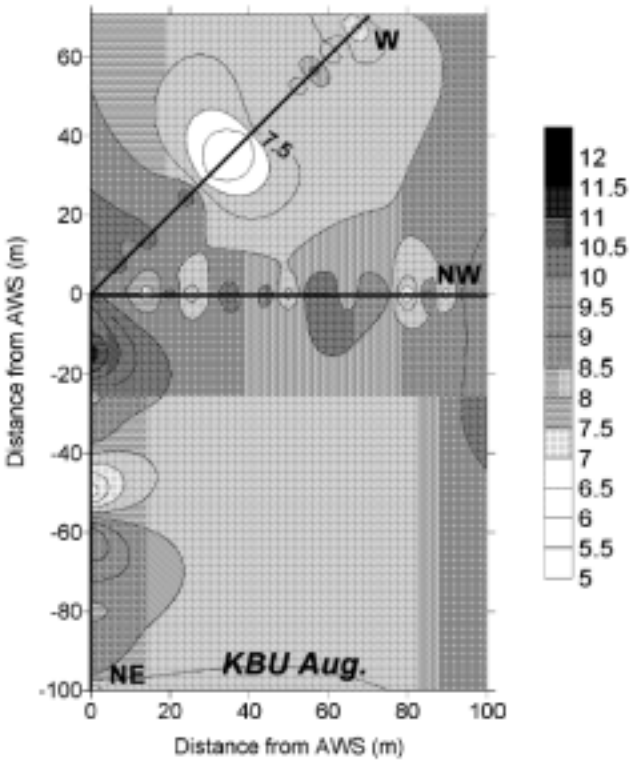


Fig. 2-29 The horizontal distribution of soil moisture around the pastoral-area station (AWS) in August of 2003. (Kojima, 2004)

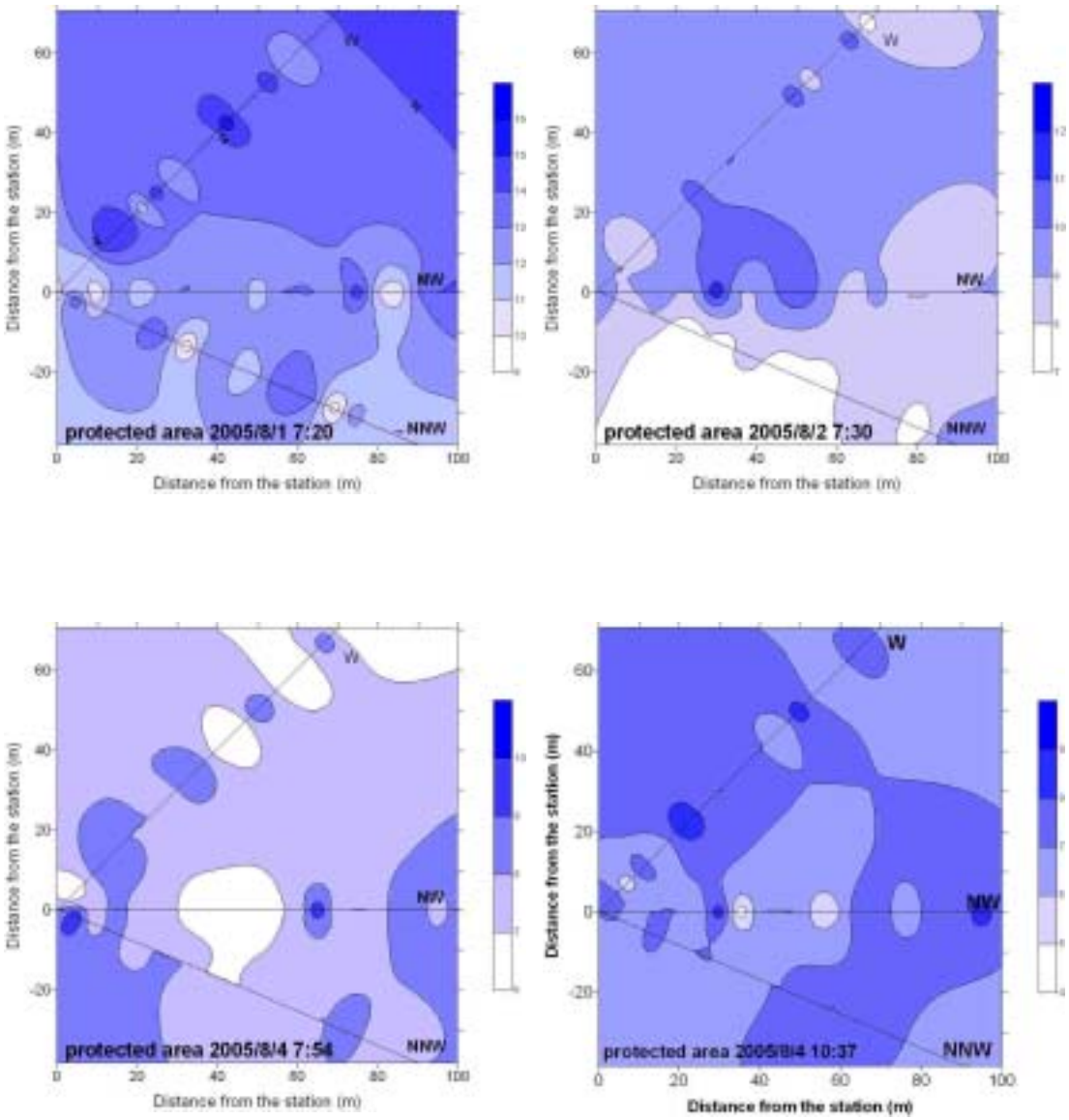


Fig. 2-30 The horizontal distribution of soil moisture around the protected-area station in August of 2005.

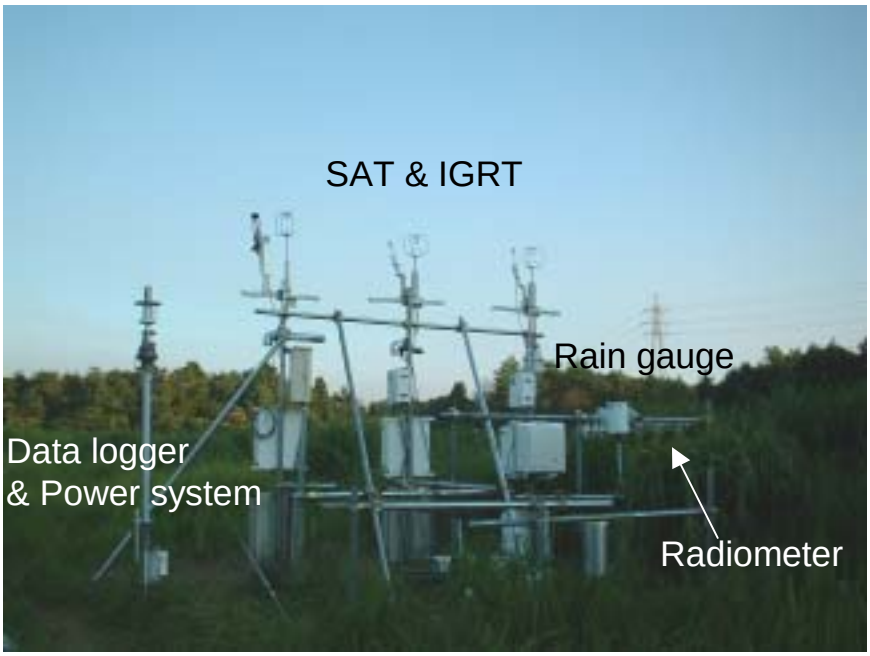


Fig. 2-31 A Photograph of the observation system of KBU stations installed for intercomparison of the sensors at TERC, Tsukuba Japan. SAT: sonic anemometer-thermometer, IRGA: infrared gas analyzer, PRT: platinum resistance thermometer, IRT: infrared thermometer, HFP: heat flux plate, TDR: time domain reflectmetry.

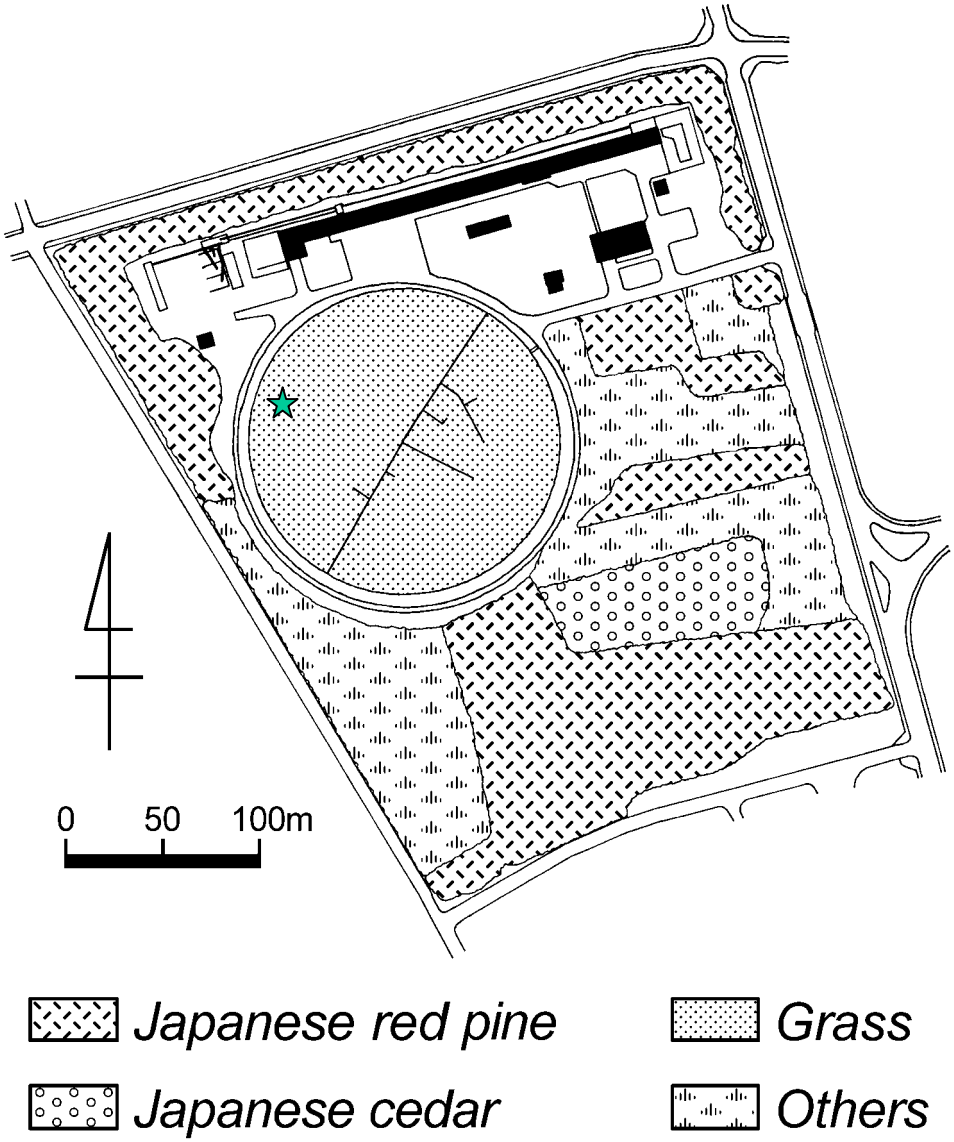


Fig. 2-32 Location of TERC (the Terrestrial Environment Research Center, the University of Tsukuba). A star is the measurement point. (Iida, 2000)

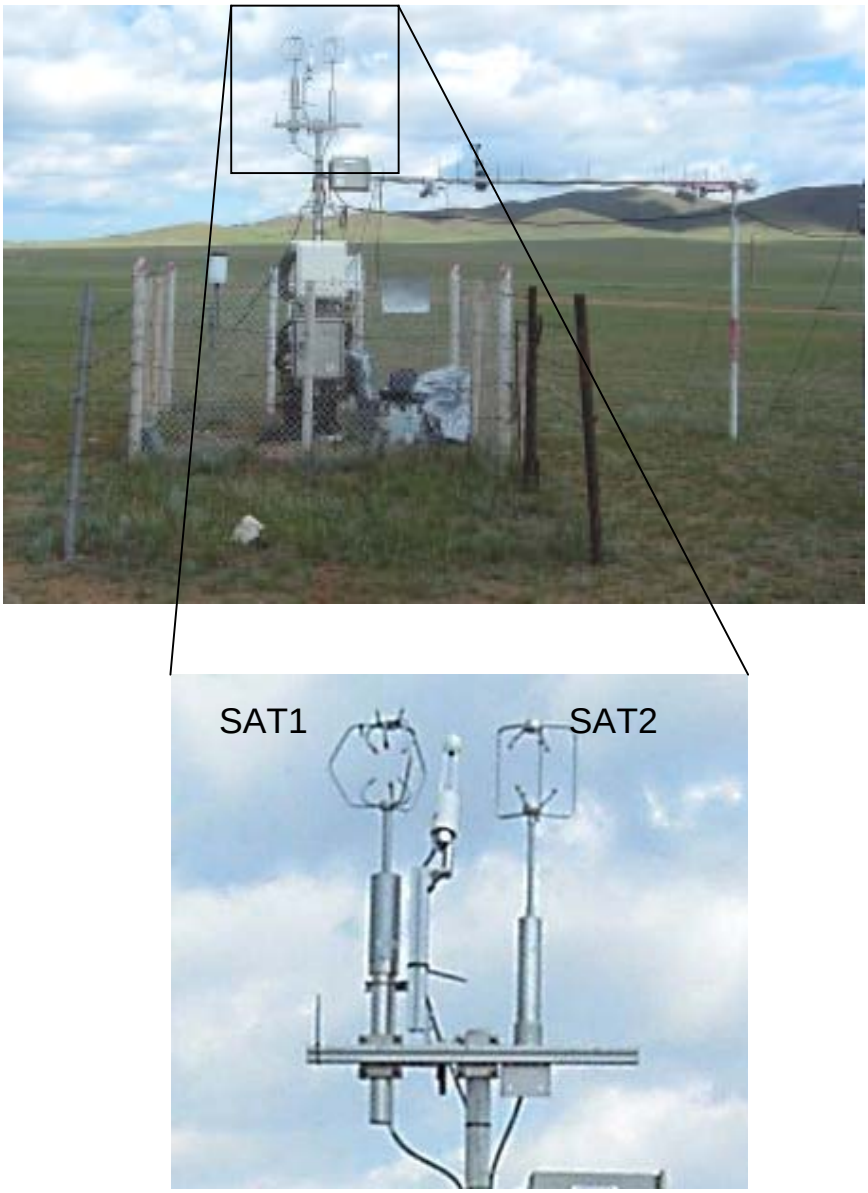


Fig. 2-33 Photographs of the intercomparison-observation system of the pastoral-area station. SAT1: initially installed sonic anemometer-thermometer. SAT2: sonic anemometer-thermometer which is the same model installed in the protected-area station.

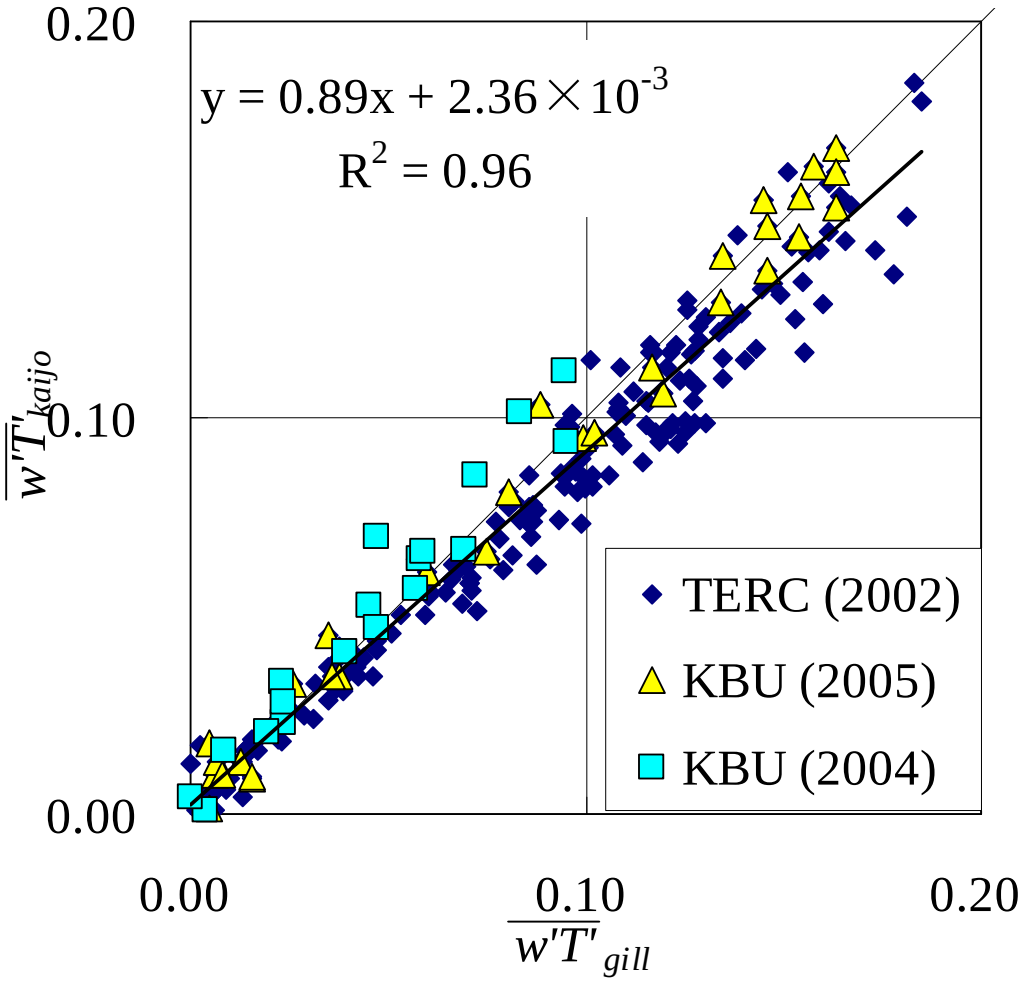


Fig. 2-34 The comparison between $\overline{w'T'}_{gill}$ and $\overline{w'T'}_{kaijo}$. Overbar and prime denote the time averaging and deviation from the average. *w* and *T* represent the vertical wind speed and air temperature, respectively. Subscripts are the name of instruments. The names of symbols and the number show measurement place and year, respectively.

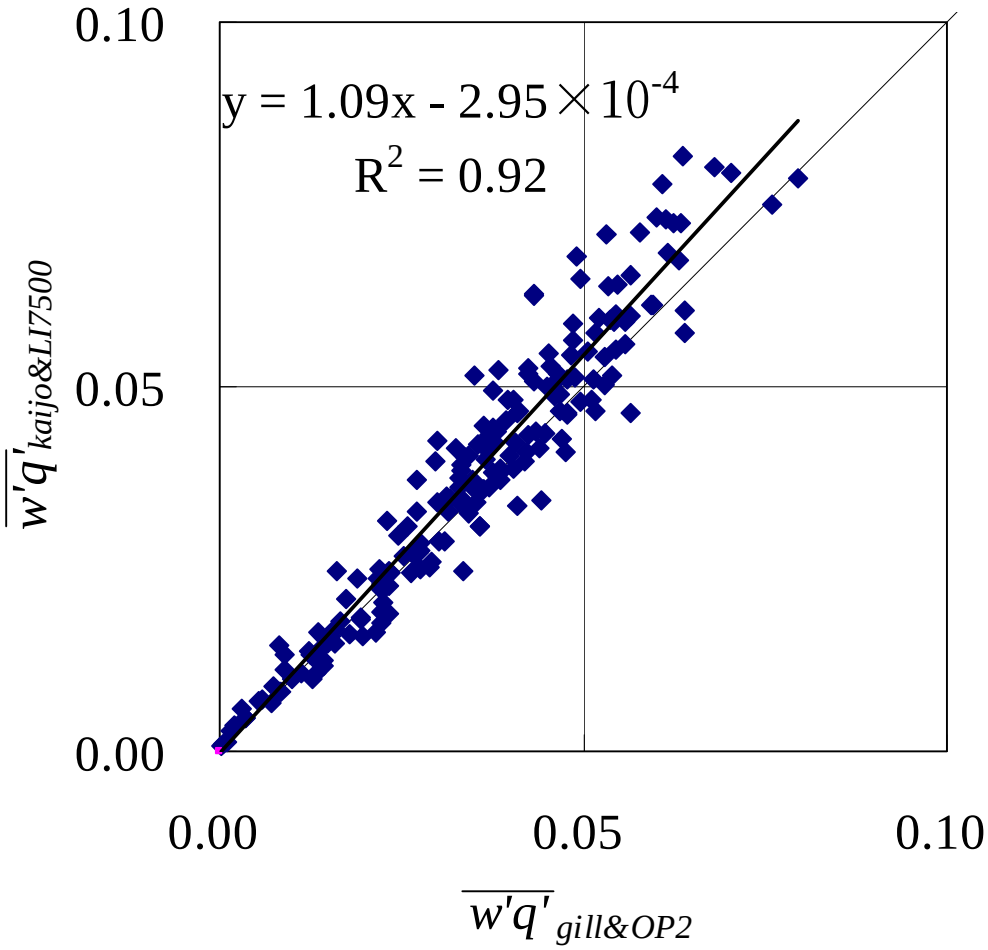


Fig. 2-35 The comparison between $\overline{w'q'}_{gill\&OP2}$ and $\overline{w'q'}_{kaijo\&LI7500}$ measured at TERC between August and October of 2002. Overbar and prime denote the time averaging and deviation from the average. *w* and *q* represent the vertical wind speed and specific humidity, respectively. Subscripts denote the names of the instruments.

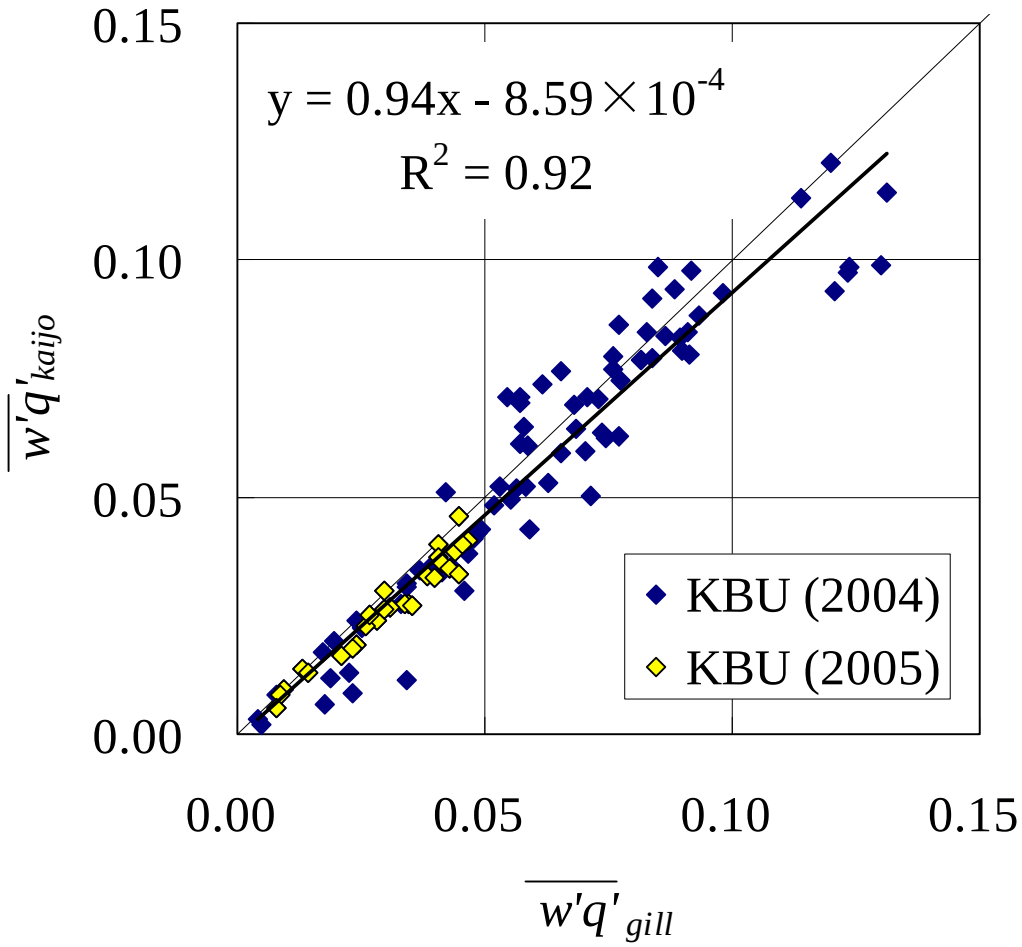


Fig. 2-36 The comparison between $\overline{w'q'}_{gill}$ and $\overline{w'q'}_{kaijo}$ . Overbar and prime denote the time averaging and deviation from the average. *w* and *q* represent the vertical wind speed and specific humidity, respectively. Subscripts are the names of instruments. The names of symbols and the number show measurement place and year, respectively.

## Chapter 3

# Results and Discussion

### 3-1. Grazing intensity

In Kherlen river basin, the number of livestock has increased drastically in the past two decades or so (Fig. 3-1), as a result of the introduction of the so-called market oriented economy in 1990-91 after the change of the political system in Mongolia. The average $GI_{statis}$ of Delgerkhaan district, where KBU village belongs to, was as large as that of the other districts, 0.57±0.12SD *SEu* $ha^{-1}$ from 1984 to 2003 (Table 3-1 and Fig. 3-2). A simulation study by Chen *et al*. (2006) suggested that the maximum sustainable grazing intensity was 0.7 *SEu* per ha at KBU. Fig. 3-1 shows $GI_{statis}$ of KBU in summer, when livestock was grazed at the flat area near the measurement stations, was lower than 0.7. Therefore the steppe of KBU is expected to be sustainable if *GI* doesn't become higher than that of now. Though $GI_{statis}$ of KBU in winter was too high, in this study those aren't so important because little livestock are grazed at flat area in winter. This was also confirmed by the photo record of grazing activities. $GI_{photo}$ values show that around measurement station, grazing intensity in summer was large while in winter it was smaller (Fig. 3-3). The result agrees with the fact that local people move to the mountain area and stay at winter camps when wintertime begins (section 2-1). From that fact, $GI_{photo}$ of summer can be expected to be equal to $GI_{statis}$ of KBU in summer, but $GI_{photo}$ of summer was a little smaller. Two reasons can be inferred as follows. One is that *LS* is not in *SEu* but the total number without consideration of the animal type. One cow is calculated as 8.15 *SEu* by the equation (27), $GI_{photo}$ of summer may be equal to $GI_{statis}$ of KBU in summer if *LS* was calculated into *SEu*. The other is that the area

taken by the camera was on the side of the mountain area (Figs. 2-4 and 2-14) which was not necessarily representative whole area for grazing (Section 2-1).

## 3-2. Grazing effect.

### 3-2-1. Surface soil temperature, soil temperature and soil moisture

The trampling by animal renders the soil compact, so the grazing effect on $T_s$, ST and SM can be expected (Li *et al.*, 2000, Brayant *et al.*, 1990). However, Figs. 3-4, 3-5 and Table 3-2 show that the difference of daily-average $T_s$ ($T_{sa}$) between the two areas didn't appear significantly. For diurnal fluctuation of $T_s$ ($T_{sg}$) of May through September in which $T_s$ was not less than 0 ºC, there was not a significant difference (Fig. 3-6). In spite of the results of $T_s$, a significant difference and clear annual change of daily average and diurnal fluctuation of ST of the two areas appeared (Figs. 3-7~3-9, Tables 3-3 and 3-4). $T_s$ was regarded as area-average value because $T_s$ was calculated from $L_u$ (equation (14)) measured by the instrument whose field of view was wide enough (150º), and because it was appropriate to regard $L_u$ values as regional representative values (section 2-3-3). On the other hand, ST was measured by one sensor at each depth, and there was a possibility that the measured values are not quite area-averages as was the case of soil heat flux (section 2-3-2). Besides, for SM, it is not easy to show the significant difference of the two areas (Fig. 3-10 and Table 3-5) because the depths of sensors of the two stations were different (Table. 2-1 and 2-2). Further researches are necessary, but from the result of $T_s$, it can be inferred that *GI* in KBU is not heavy enough to cause underground heat regime.

### 3-2-2. vegetation

Fig. 3-11 shows that the grazing activity appears to have controlled biomass: the difference of aboveground green biomass (AGB) values of the two areas appears

significantly after July. The AGB values of July of both areas in 2004 are higher than in 2003, in spite of the insignificant difference of PPT until July between the two years. Therefore, protection of the area caused the favorable condition for vegetation growth. The aboveground dead-vegetation biomass (ADB) values of the protected area were always higher than those of the pastoral area, because vegetation in the protected area could not be consumed by grazing and remains in standing-dead state. ADB value in July of 2004 decreased, which was caused by not only the decomposition but also by the common strong wind in spring (Fig. 3-12). ADG value in August of 2005, however, was large. This is because the large amount of dead-vegetation became litter, lying on the ground, which is hard to blow away. Moreover, Fig. 3-11 shows that too much dead-vegetation might have disturbed the vegetation growth in 2005, but there is no cogent reason for insisting on that point because of the short of data sets; aboveground biomass data of 2005 was measured at only 3 times each at both areas. From Fig. 3-11, we divided period of seven months (from April to October) into three seasons; during April through June, July and August, September and October.

We also divided period by the seasonal changes of NDVI and AGB data appeared in Fig. 3-13: the seasonal changes of both data were similar to one another. There is usually strong correlation between NDVI and LAI since NDVI was calculated on the basis of vegetation characteristics of reflectance of radiation. Kojima (2004) suggested the linear correlation between AGB and LAI in this area (Section 2-4). From Fig. 3-13, we divided period; the period in NDVI > 0.3 was growing season (GR), the one before GR and after GR were pre-GR and post-GR, respectively. The detail of period in each year is summarized in Table 3-6.

### 3-2-3. Roughness length $z_0$

Figs. 3-14 and 3-15 plots the seasonal change of $z_0$, along with the aboveground total

biomass (ATB = AGB + ADB) and vegetation height $h_c$. After GR, $z_0$ values of the protected area were always larger than those of the pastoral area. In addition, in post-GR of 2004 and 2005, $z_0$ values of the protected area were as large as those in GR, while $z_0$ values of the pastoral area decreased. Those agree with the facts that the difference of ATB and $h_c$ values of two areas appears significantly after July in 2003 because vegetation in the protected area could not be consumed and remained in standing-dead state. The $z_0$ values in the spring in both areas are small possibly because the standing dead-vegetation was removed and tumbles down by a strong wind (Fig. 3-12).

### 3-2-4. Energy and water balance

**(1) 30-minute average data set**

To compare the components of the heat balance ($H$, $lE$, $G$ and $R_n$) and the radiation ($K_u$ and $L_u$) in the two areas, the regression coefficient $a$ in a linear equation was evaluated ($F_{\text{protected}} = a\ F_{\text{pastoral}}$, $F$: energy flux, e.g. Fig. 3-16), and the seasonal change of $a$ values was studied. Fig. 3-17 and 3-18 plots the seasonal change of $a$ of the components. When $a$ value is larger (smaller) than one, the flux values of the protected area are larger (smaller) than those of the pastoral area. We see from the figure that $a$ values of $K_u$ were smaller than 1.0. On the other word, the $K_u$ values of protected area were smaller than those of the pastoral, and the difference became larger as time goes by. This corresponds with results of the biomass changes. The smaller $K_u$ values caused the higher values of $R_n$ in the protected area. Moreover, the larger $R_n$ values in protected area contributed to the larger $a$ values of $G$, because the amount of the increased $R_n$ values increased $G$ values. $H$ values in the protected area were larger than those in the pastoral area during GR and post-GR. This agrees with the result of the roughness length changes (Fig. 3-15). The effect of $z_0$ on $lE$ values was expected, but $a$ values of $lE$ didn't show clearly the seasonal change, because of small magnitude of

evapotranspiration.

Note that we carried out the same analyses with the entire data set which weren't subjected to the data selection by the wind direction and the correction to consider the upwind area (Fig. 3-19). The seasonal change was a little less clear than that by the selected data set, but the general trend of two results is similar. This was probably because wind direction used for data selection was 30-minute averages, and probably wind direction is not always the same during the 30 minutes. From the same reason, the correction to consider the upwind area was not always valid. Therefore we can safely say that the data selection by the wind direction and the correction to consider upwind area were not so important for the present purpose of the study.

**(2) Integrated values**

From the discussion given above, it was decided that the data set used to calculate the integrated values was not subjected to the data selection by the wind direction and the correction to consider upwind area.

First, we will describe the seasonal change of the daily-integrated values of the surface heat balance. Fig. 3-20 shows that *lE* values are larger than *H* values at the pastoral area in rainy season of 2003 and 2004, and that *lE* values of the protected area are larger than those of the pastoral area in summer of 2004.

Second, the annual budget was considered (Figs. 3-21, 3-22 and Table 3-7). In 2004 and 2005, *E* values were almost the same as PPT. This result is in agreement with Batima and Dagvadori (2000) who reported that in Mongolian steppe 90.1% of the annual precipitation was evaporated. In 2003, the infiltration $I_G$ (the difference between *E* and PPT) was higher. There can be two reasons, regarding those $I_G$ results; one is larger number of major rainfall events (> 10 mm) (Table 3-8). Fig. 3-7 shows that strong rainfall caused infiltration to the deeper layers and that the number of infiltration

in 2003 is indeed larger when $I_G$ values was high. The other is the unseasonable strong rainfall in September of 2003. It is suspected that the low temperature and potential evapotranspiration made it difficult to evapotranspirate. In order to eliminate the effect of irregular strong rainfall events, we will consider the budget from June throughout August in what follows. We see from Figs. 3-23, 3-24 and Table 3-9 that the difference of values among the 3 periods was small, but larger $I_G$ values coincide with the number of major rainfall events. Thus the amount of infiltration was mainly effected by the timing of rainfall, and that the number of major rainfall events was a minor effect. Besides Figs. 3-23 and 25 show that the $G/R_n$ (fraction of $G$ in $R_n$) of the pastoral area was larger than that of the protected area. Larger $G/R_n$ values seemed to be caused by larger diurnal fluctuations of the surface soil temperature due to smaller vegetation coverage by the grazing. However, the difference of $T_s$ of the two areas didn't appear significantly (section 3-2-1). Generally, annually integrated $G$ value should be zero (Kayane, 1980), but the values were far from zero (Table 3-7). This might show that the corrected of $G$ values were still not quit satisfactory. In TERC data set, however, annually integrated $G$ value was not also always zero (Table 3-10); thus there is a possibility that annual also $G$ value in Mongolian steppe should tend to zero if long-term averages were evaluated. This calls for further examination.

Finally, in addition to the results mentioned above, there is no significant difference of the annual integrated $E$ values between the two areas. Bremer *et al*. (2001) reported that grazing reduced seasonal evapotranspiration for grassland in Kansas by only 6 %, and that younger leaves in regrowth on the pastoral area likely had lower stomatal resistance, and thus higher transpiration per unit leaf area were observed as compared with their counterparts on protected area. Moreover, the result of $E$ agrees with the simulated study by a plant ecological model applied to the KBU pastoral area for different grazing intensity by Chen *et al*. (2007); the reduction of transpiration by

grazing in pastoral area is largely compensated by the increase of evaporation. However there is a possibility that *E* values were too small to clarify the difference, because the amount of PPT in this area was small.

Table 3-1 The average of the number of livestock and grazing intensity (*SEu* $ha^{-1}$) of each district (1984~2003). *SEu*: Sheep Equivalent unit.

| district | livestock (*SEu*) | Area (ha) | grazing intensity | Standard deviation |
|---|---|---|---|---|
| Delgerkhaan | $1.68\times10^5$ | $2.97\times10^5$ | 0.57 | 0.12 |
| Underhaan | $1.77\times10^5$ | $2.54\times10^5$ | 0.70 | 0.19 |
| Darhan | $1.86\times10^5$ | $4.41\times10^5$ | 0.42 | 0.08 |
| Mongenmorit | $9.27\times10^4$ | $6.75\times10^5$ | 0.14 | 0.01 |
| Jargaltkhaan | $1.50\times10^5$ | $3.05\times10^5$ | 0.49 | 0.09 |
| Baganuur | $1.88\times10^5$ | $2.35\times10^5$ | 0.80 | 0.22 |
| Ulaanbaatar city | $4.35\times10^5$ | $3.16\times10^5$ | 1.37 | 0.39 |

Table 3-2 The average and standard deviation of surface soil temperature. Max, and min represent annual and 5-month (from May to September) average of daily maximum and minimum, respectively, of 30-minute average data set. avg: annual and 5-month average values. defferece: the annual and 5-month average of difference between daily maximum and minimum.

| pastoral area | 2003 | | | | 2004 | | | | 2005 | | | |
|---|---|---|---|---|---|---|---|---|---|---|---|---|
| | annual | | 5~9 | | annual | | 5~9 | | annual | | 5~9 | |
| | avg | SD | avg | SD | avg | SD | avg | SD | avg | SD | avg | SD |
| max | -1.08 | 17.25 | 16.40 | 4.71 | -0.95 | 19.12 | 17.13 | 6.10 | 0.10 | 16.90 | 17.31 | 6.34 |
| min | -9.93 | 15.90 | 6.19 | 4.91 | -10.57 | 17.34 | 6.00 | 6.09 | -10.40 | 15.45 | 5.42 | 6.86 |
| avg | 11.86 | 19.75 | 31.03 | 7.81 | 12.78 | 21.94 | 32.70 | 8.81 | 15.66 | 19.07 | 34.25 | 8.09 |
| difference | 21.79 | 7.20 | 24.83 | 8.08 | 23.35 | 7.44 | 26.70 | 8.11 | 26.06 | 7.05 | 28.82 | 7.16 |

| protected area | 2003 | | | | 2004 | | | | 2005 | | | |
|---|---|---|---|---|---|---|---|---|---|---|---|---|
| | annual | | 5~9 | | annual | | 5~9 | | annual | | 5~9 | |
| | avg | SD | avg | SD | avg | SD | avg | SD | avg | SD | avg | SD |
| max | -1.17 | 17.68 | 16.66 | 4.95 | -1.38 | 19.57 | 17.07 | 6.23 | -0.61 | 17.18 | 16.78 | 6.45 |
| min | -10.95 | 16.38 | 5.58 | 5.13 | -12.09 | 18.12 | 5.24 | 6.24 | -11.83 | 16.04 | 4.52 | 7.12 |
| avg | 13.27 | 20.55 | 32.93 | 8.52 | 13.67 | 22.22 | 33.70 | 9.29 | 15.31 | 19.04 | 33.71 | 8.08 |
| difference | 24.22 | 7.96 | 27.35 | 8.86 | 25.76 | 7.65 | 28.46 | 8.70 | 27.14 | 6.87 | 29.19 | 7.07 |

Table 3-3 The annual and 5-month (from May to September) average and standard deviation of soil temperature.

| pastoral area | 2003 | | | | 2004 | | | | 2005 | | | |
|---|---|---|---|---|---|---|---|---|---|---|---|---|
| | annual | | 5~9 | | annual | | 5~9 | | annual | | 5~9 | |
| **depth** | avg | SD | avg | SD | avg | SD | avg | SD | avg | SD | avg | SD |
| -0.05 cm | **8.50** | **18.72** | **27.12** | **6.35** | **7.04** | **18.93** | **25.77** | **7.07** | **7.85** | **16.87** | **25.58** | **6.66** |
| -0.10 cm | **2.87** | **14.05** | **17.23** | **4.15** | **2.59** | **14.91** | **17.51** | **4.76** | **2.10** | **14.14** | **17.10** | **5.26** |
| -0.20 cm | **2.81** | **13.33** | **16.48** | **3.92** | **2.78** | **14.00** | **16.79** | **4.41** | **2.29** | **13.31** | **16.43** | **5.03** |
| -0.30 cm | **2.55** | **12.82** | **15.68** | **3.82** | **2.68** | **13.36** | **16.04** | **4.19** | **2.22** | **12.74** | **15.75** | **4.92** |
| -0.50 cm | **2.16** | **11.40** | **13.71** | **3.70** | **2.87** | **11.91** | **14.65** | **3.97** | **2.31** | **11.31** | **14.19** | **4.78** |
| -0.70 cm | **2.25** | **10.06** | **12.15** | **3.86** | **3.21** | **10.63** | **13.46** | **4.00** | **2.58** | **10.04** | **12.79** | **4.91** |
| -1.00 cm | **2.11** | **8.83** | **10.37** | **4.10** | **3.07** | **9.39** | **11.69** | **4.26** | **2.52** | **8.90** | **11.06** | **5.08** |

| protected area | 2003 | | | | 2004 | | | | 2005 | | | |
|---|---|---|---|---|---|---|---|---|---|---|---|---|
| | annual | | 5~9 | | annual | | 5~9 | | annual | | 5~9 | |
| **depth** | avg | SD | avg | SD | avg | SD | avg | SD | avg | SD | avg | SD |
| -0.05 cm | **8.76** | **16.61** | **25.08** | **5.38** | **8.78** | **19.63** | **27.89** | **7.12** | **9.01** | **18.28** | **28.04** | **7.14** |
| -0.25 cm | **2.95** | **13.35** | **16.54** | **3.84** | **3.05** | **14.25** | **17.34** | **4.51** | **2.39** | **13.72** | **17.07** | **4.98** |

Table 3-4 The average and standard deviation of soil temperature at the depth of 5 cm. Max, and min represent annual and 5-month (from May to September) average of daily maximum and minimum, respectively, of 30-minute average data set. avg: annual and 5-month average values. defferece: the annual and 5-month average of difference between daily maximum and minimum.

| pastoral area | 2003 | | | | 2004 | | | | 2005 | | | |
|---|---|---|---|---|---|---|---|---|---|---|---|---|
| | annual | | 5~9 | | annual | | 5~9 | | annual | | 5~9 | |
| | avg | SD | avg | SD | avg | SD | avg | SD | avg | SD | avg | SD |
| max | 2.89 | 14.83 | 17.96 | 4.63 | 2.27 | 15.89 | 18.16 | 5.45 | 1.72 | 15.23 | 17.79 | 5.76 |
| min | -1.48 | 12.13 | 10.90 | 4.36 | -1.54 | 13.64 | 12.13 | 4.80 | -3.07 | 14.02 | 11.60 | 5.58 |
| avg | 8.50 | 18.72 | 27.12 | 6.35 | 7.04 | 18.93 | 25.77 | 7.07 | 7.85 | 16.87 | 25.58 | 6.66 |
| difference | 9.97 | 7.64 | 16.21 | 5.08 | 8.58 | 6.06 | 13.64 | 4.36 | 10.93 | 4.19 | 13.98 | 3.54 |

| protected area | 2003 | | | | 2004 | | | | 2005 | | | |
|---|---|---|---|---|---|---|---|---|---|---|---|---|
| | annual | | 5~9 | | annual | | 5~9 | | annual | | 5~9 | |
| | avg | SD | avg | SD | avg | SD | avg | SD | avg | SD | avg | SD |
| max | 3.09 | 14.56 | 17.79 | 4.26 | 2.67 | 16.39 | 18.93 | 5.62 | 1.75 | 15.94 | 18.66 | 6.01 |
| min | -1.51 | 13.01 | 11.66 | 4.26 | -2.17 | 13.99 | 11.77 | 5.13 | -3.81 | 14.24 | 11.24 | 5.78 |
| avg | 8.76 | 16.61 | 25.08 | 5.38 | 8.78 | 19.63 | 27.89 | 7.12 | 9.01 | 18.28 | 28.04 | 7.14 |
| difference | 10.27 | 5.53 | 13.42 | 4.48 | 10.95 | 6.64 | 16.12 | 4.77 | 12.82 | 5.57 | 16.80 | 4.07 |

Table 3-5 The annual and 5-month (from May to September) average and standard deviation of soil moisture.

| pastoral area | 2003 | | | | 2004 | | | | 2005 | | | |
|---|---|---|---|---|---|---|---|---|---|---|---|---|
| | annual | | 5~9 | | annual | | 5~9 | | annual | | 5~9 | |
| **depth** | avg | SD | avg | SD | avg | SD | avg | SD | avg | SD | avg | SD |
| -0.10 cm | **8.84** | **3.69** | **11.60** | **3.21** | **8.15** | **4.05** | **10.72** | **3.62** | **8.24** | **3.33** | **10.64** | **1.84** |
| -0.20 cm | **5.31** | **1.94** | **6.25** | **1.83** | **5.42** | **2.28** | **7.12** | **1.87** | **5.16** | **1.50** | **6.46** | **0.82** |
| -0.30 cm | **4.17** | **1.66** | **4.44** | **1.64** | **4.76** | **2.10** | **6.43** | **1.70** | **4.08** | **0.98** | **5.13** | **0.29** |
| -0.70 cm | **3.65** | **0.43** | **4.05** | **0.18** | **4.19** | **0.81** | **4.94** | **0.58** | **4.34** | **0.71** | **5.04** | **0.24** |
| -1.00 cm | **5.87** | **0.63** | **6.44** | **0.21** | **6.08** | **0.73** | **6.70** | **0.31** | **6.40** | **0.91** | **7.19** | **0.56** |

| protected area | 2003 | | | | 2004 | | | | 2005 | | | |
|---|---|---|---|---|---|---|---|---|---|---|---|---|
| | annual | | 5~9 | | annual | | 5~9 | | annual | | 5~9 | |
| **depth** | avg | SD | avg | SD | avg | SD | avg | SD | avg | SD | avg | SD |
| -0.05 cm | **6.32** | **3.91** | **8.58** | **4.39** | **5.01** | **3.52** | **6.60** | **3.82** | **4.54** | **3.13** | **6.30** | **2.46** |
| -0.25 cm | **5.28** | **2.29** | **6.23** | **2.46** | **5.35** | **2.18** | **6.81** | **1.74** | **5.23** | **1.95** | **6.20** | **1.35** |

Table 3-6 The period divided by the relation between NDVI and AGB. AGB: aboveground green biomass. GR: growing season (NDVI > 0.3), pre-GR: the period before GR, post-GR: the period after GR.

| | pre-GR | GR | post-GR |
|---|---|---|---|
| 2003 | ~6/30 | 7/1~9/20 | 9/21~ |
| 2004 | ~6/30 | 7/1~9/10 | 9/11~ |
| 2005 | ~8/10 | 8/10~9/20 | 9/21~ |

Table 3-7 Annual integrated values (MJ year$^{-1}$ m$^{-2}$). $K_d$: downward shortwave radiation, , $K_u$: upward shortwave radiation, $L_u$: upward longwave radiation, $L_d$: downward longwave radiation, $R_n$: net radiation, $G$: soil heat flux, $H$: sensible heat flux, $lE$: latent heat flux. Subscript "corrected" denotes corrected values calculated by Twine et al. (2000).

| | pastoral | | | protected | | |
|---|---|---|---|---|---|---|
| | 2003/4~2004/3 | 2004/4~2005/3 | 2005/4~2006/3 | 2003/4~2004/3 | 2004/4~2005/3 | 2005/4~2006/3 |
| $K_d$ | 5565 | 5791 | 5810 | 5577 | 5786 | 5850 |
| $K_u$ | 1506 | 1794 | 1461 | 1430 | 1690 | 1310 |
| $L_d$ | 7472 | 7558 | 7609 | 7472 | 7558 | 7609 |
| $L_u$ | 10545 | 10574 | 10797 | 10557 | 10535 | 10726 |
| $R_n$ | 987 | 981 | 1161 | 1062 | 1119 | 1423 |
| $H$ | 800 | 744 | 1039 | 796 | 879 | 1141 |
| $lE$ | 403 | 417 | 387 | *403* | 340 | 271 |
| $G$ | -45 | 89 | 69 | -58 | -20 | 35 |
| $H_{corrected}$ | 714 | 611 | 871 | 757 | 839 | 1129 |
| $lE_{corrected}$ | 317 | 282 | 221 | *364* | 300 | 259 |

Table 3-8 The number of major rainfall events. PPT: precipitation.

| period | PPT | |
|---|---|---|
| | 4mm < | 10 mm < |
| 2003/4~2004/3 | 12 | 11 |
| 2004/4~2005/3 | 9 | 5 |
| 2005/4~2006/3 | 9 | 1 |

| period | PPT | |
|---|---|---|
| | 4mm < | 10 mm < |
| 2003/6~8 | 7 | 7 |
| 2004/6~8 | 8 | 5 |
| 2005/6~8 | 8 | 1 |

Table 3-9 Summer-time integrated values (MJ three-month$^{-1}$ m$^{-2}$). Summer time is defined as the period from July to August. $K_d$: downward shortwave radiation, , $K_u$: upward shortwave radiation, $L_u$: upward longwave radiation, $L_d$: downward longwave radiation, $R_n$: net radiation, $G$: soil heat flux, $H$: sensible heat flux, $lE$: latent heat flux. Subscript "corrected" denotes corrected values calculated by Twine et al. (2000).

| | pastoral | | | protected | | |
|---|---|---|---|---|---|---|
| | 2003 | 2004 | 2005 | 2003 | 2004 | 2005 |
| $K_d$ | 2019 | 1991 | 2003 | 2019 | 1991 | 2003 |
| $K_u$ | 413 | 385 | 416 | 383 | 359 | 391 |
| $L_d$ | 2532 | 2600 | 2607 | 2532 | 2600 | 2607 |
| $L_u$ | 3423 | 3502 | 3537 | 3442 | 3503 | 3541 |
| $R_n$ | 716 | 703 | 657 | 726 | 728 | 678 |
| $H$ | 332 | 299 | 415 | 316 | 360 | 423 |
| $lE$ | 261 | 284 | 246 | *261* | 293 | 189 |
| $G$ | 55 | 98 | 105 | 29 | 33 | 63 |
| $H_{corrected}$ | 366 | 310 | 359 | 376 | 381 | 425 |
| $lE_{corrected}$ | 295 | 296 | 193 | *321* | 314 | 191 |

Table 3-10 Annual integrated *G* (soil heat flux) values measured in (Terrestrial) Environment Research Center, the University of Tsukuba (MJ year$^{-1}$ m$^{-2}$).

| year | $G_{annual}$ |
|---|---|
| 1989 | 22.41 |
| 1990 | 12.02 |
| 1991 | -10.93 |
| 1992 | 0.04 |
| 1993 | -80.65 |
| 1994 | -24 |
| 1995 | -27.1 |
| 1996 | -21.2 |
| 1997 | -8.79 |
| 1998 | -30.22 |
| 1999 | -30.22 |
| 2000 | -25.36 |
| 2001 | -25.43 |
| 2002 | -20.91 |
| 2003 | -17.76 |
| avg | -19.21 |
| SD | 23.06 |

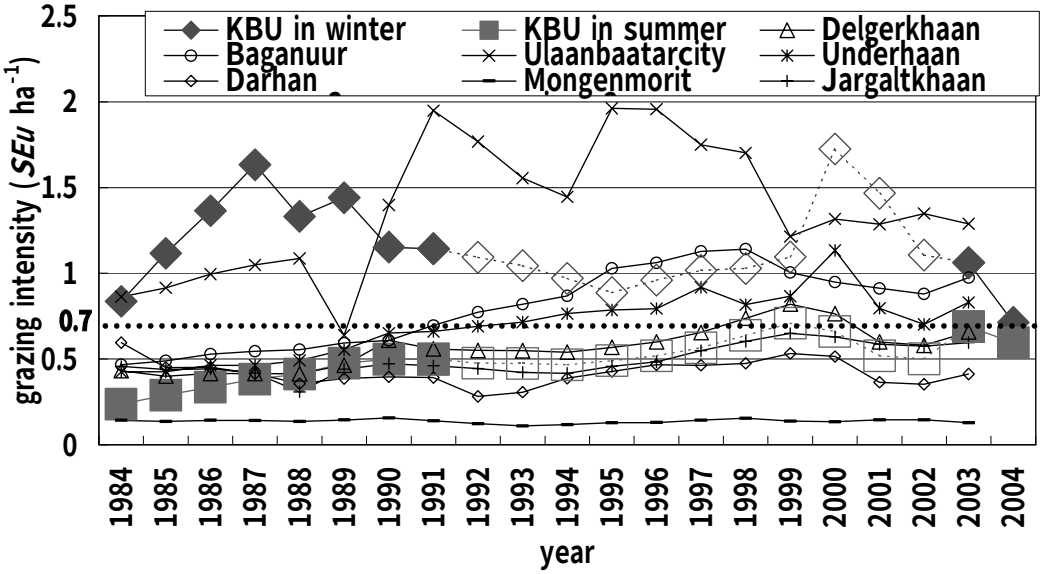


Fig. 3-1 The annual change of grazing intensity registered by the State Statistical Office, Mongolia ($GI_{statis}$). The values except for KBU are Sheep Equivalent unit (SEu) per each district area. For KBU village, which is a part of Delgerkhaan district, the values in summer and winter are given as SEu per KBU grazing area in summer (62856 ha) and in winter (130000 ha), respectively. The KBU values between 1992 and 2002 are estimated by those form the other years.

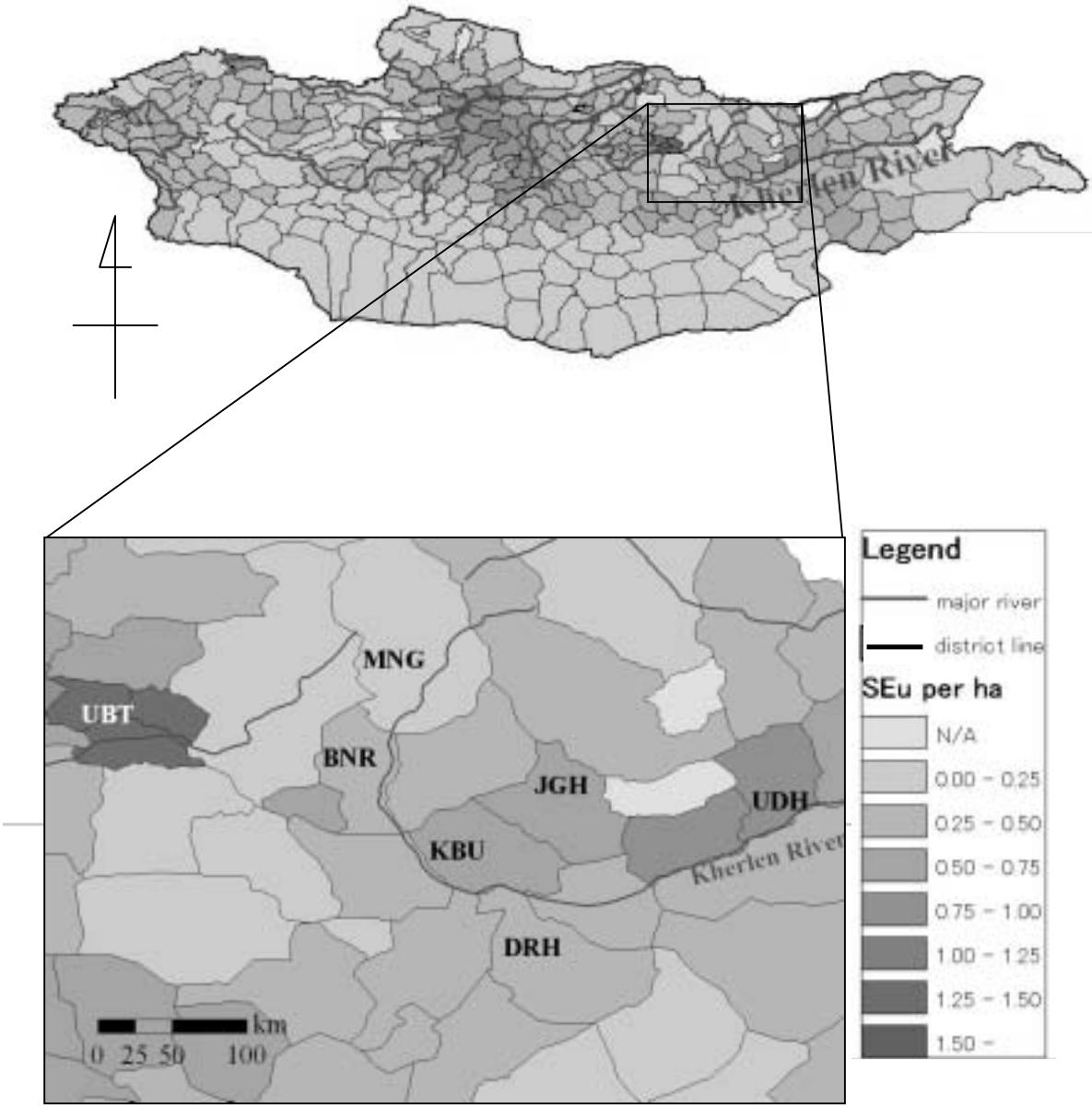


Fig. 3-2 The distribution of $GI_{statis}$ in 2003. $GI_{statis}$: grazing intensity registered by the State Statistical Office, Mongolia. UBT: Ulaanbaatarcity, BNR: Baganuur, MNG: Mongenmorit, JGH: Jargaltkhaan, KBU: Kherlenbayaan-Ulaan, DRH: Darhan, UDH: Underhaan

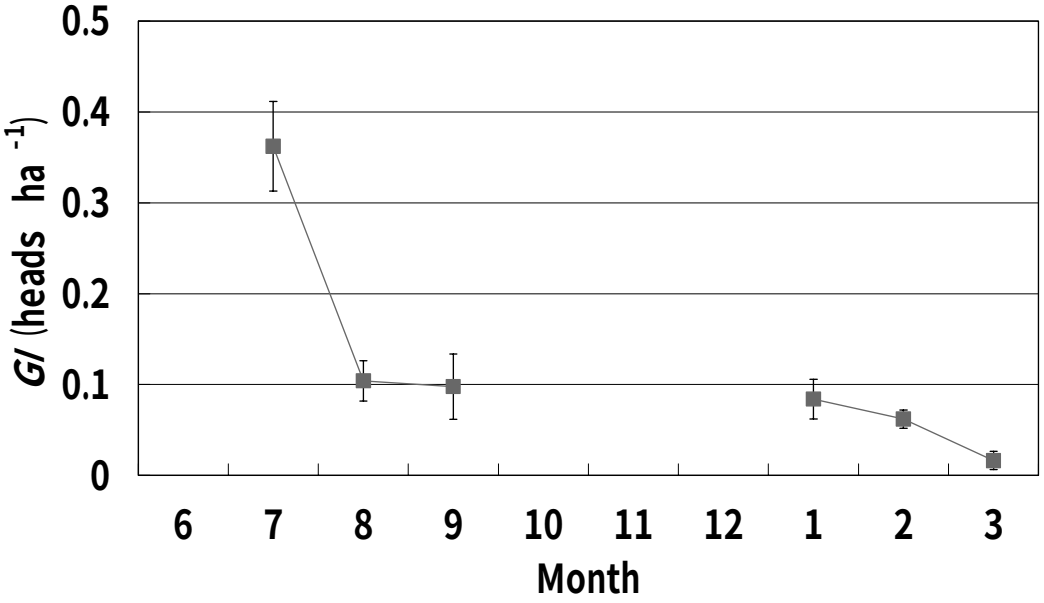


Fig. 3-3 The seasonal change of grazing intensity evaluated by photo ($GI_{photo}$). The values were averaged data set of 2004 and 2005.

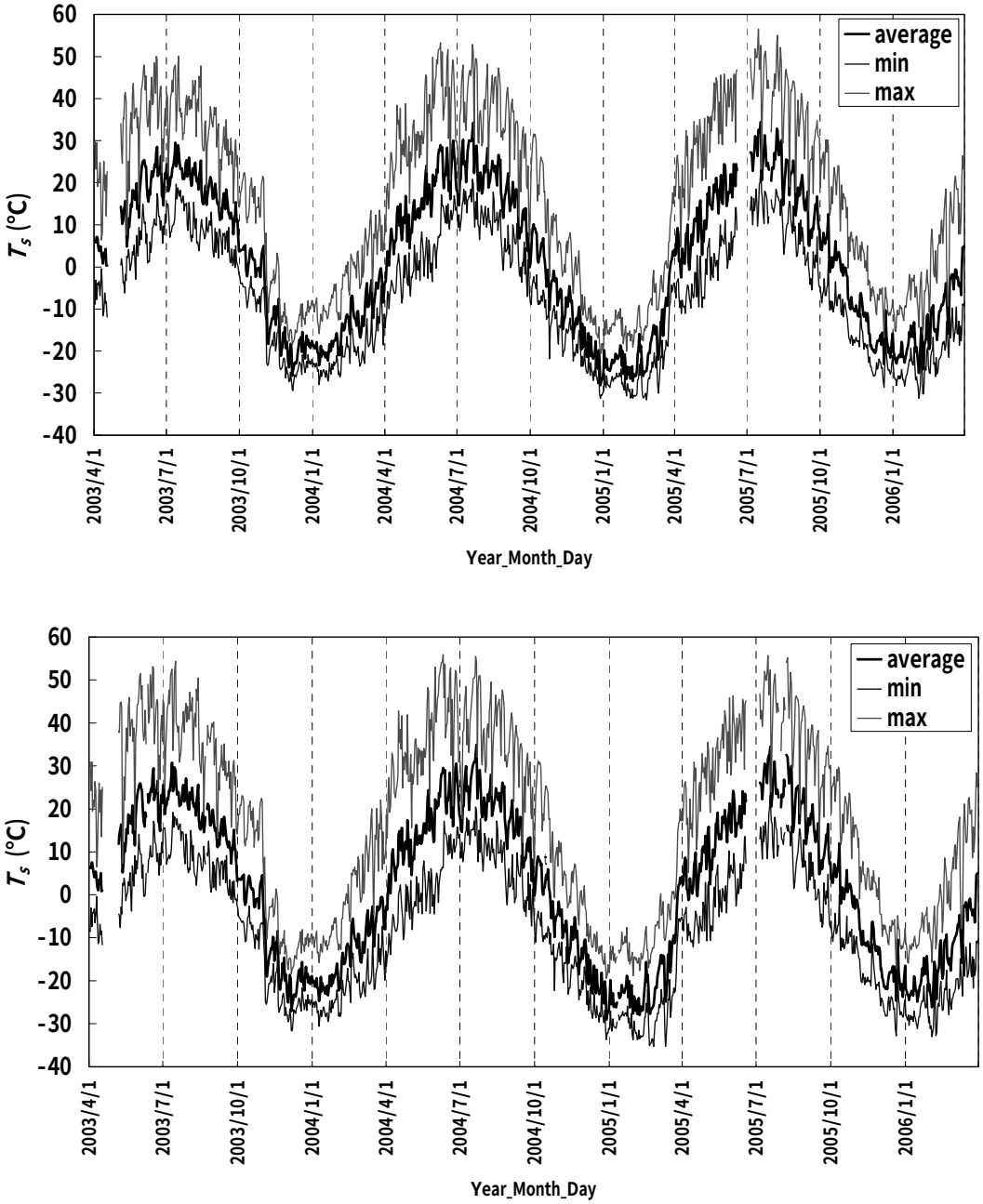


Fig. 3-4 The seasonal change of surface temperature. (a): pastoral station, (b): protected station. average: daily average value, min: daily minimum value, max: daily maximum value,

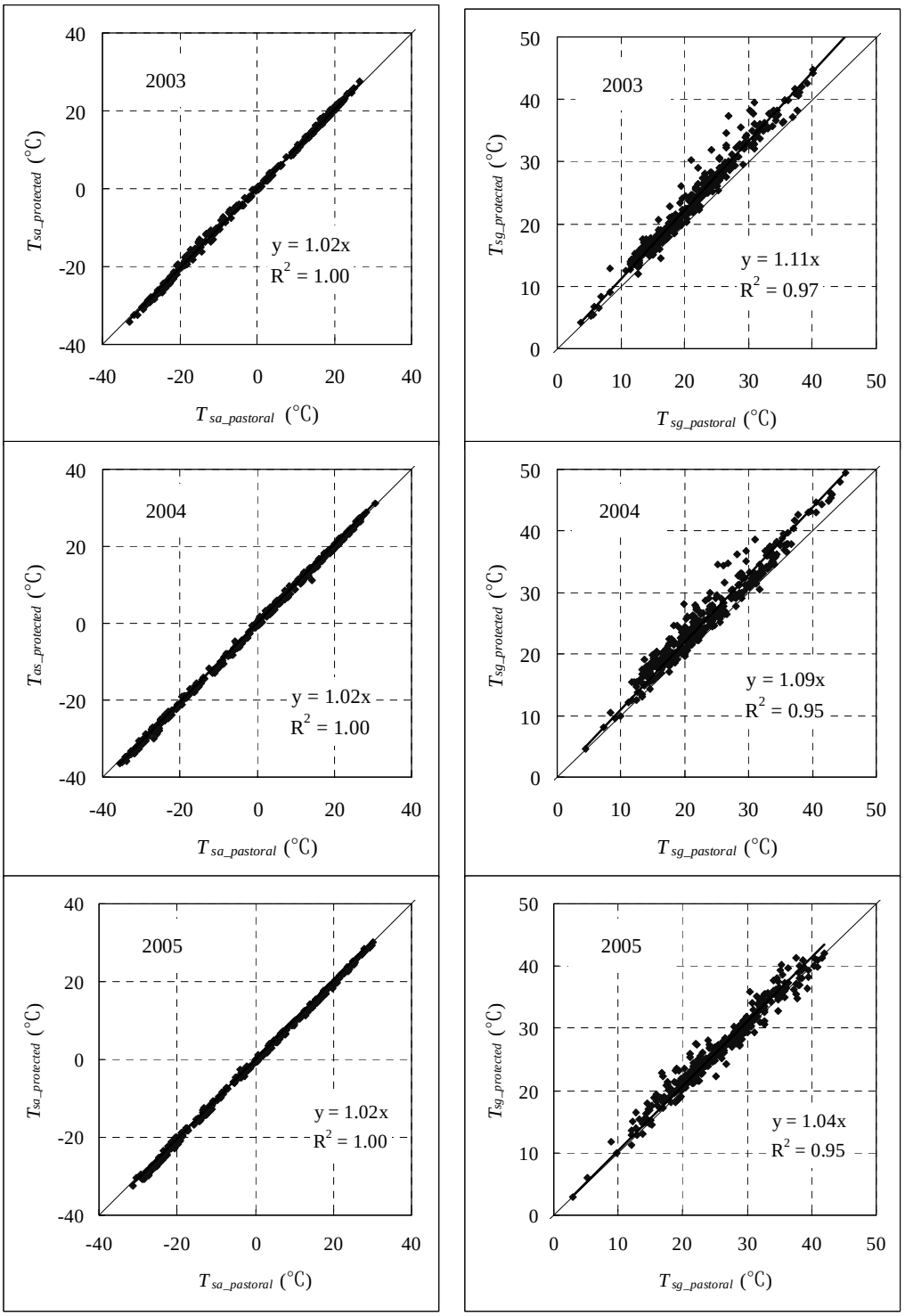


Fig. 3-5 A comparison between $\underline{T_{sa}}$ and $T_{sg}$ of annual data set. $\underline{T_{sa}}$: daily-average surface soil temperature, $T_{sg}$: the difference of 30-minute average surface soil temperature values between daily-maximum and daily-minimum. Subscripts denote measurement areas. The straight lines are regression lines.

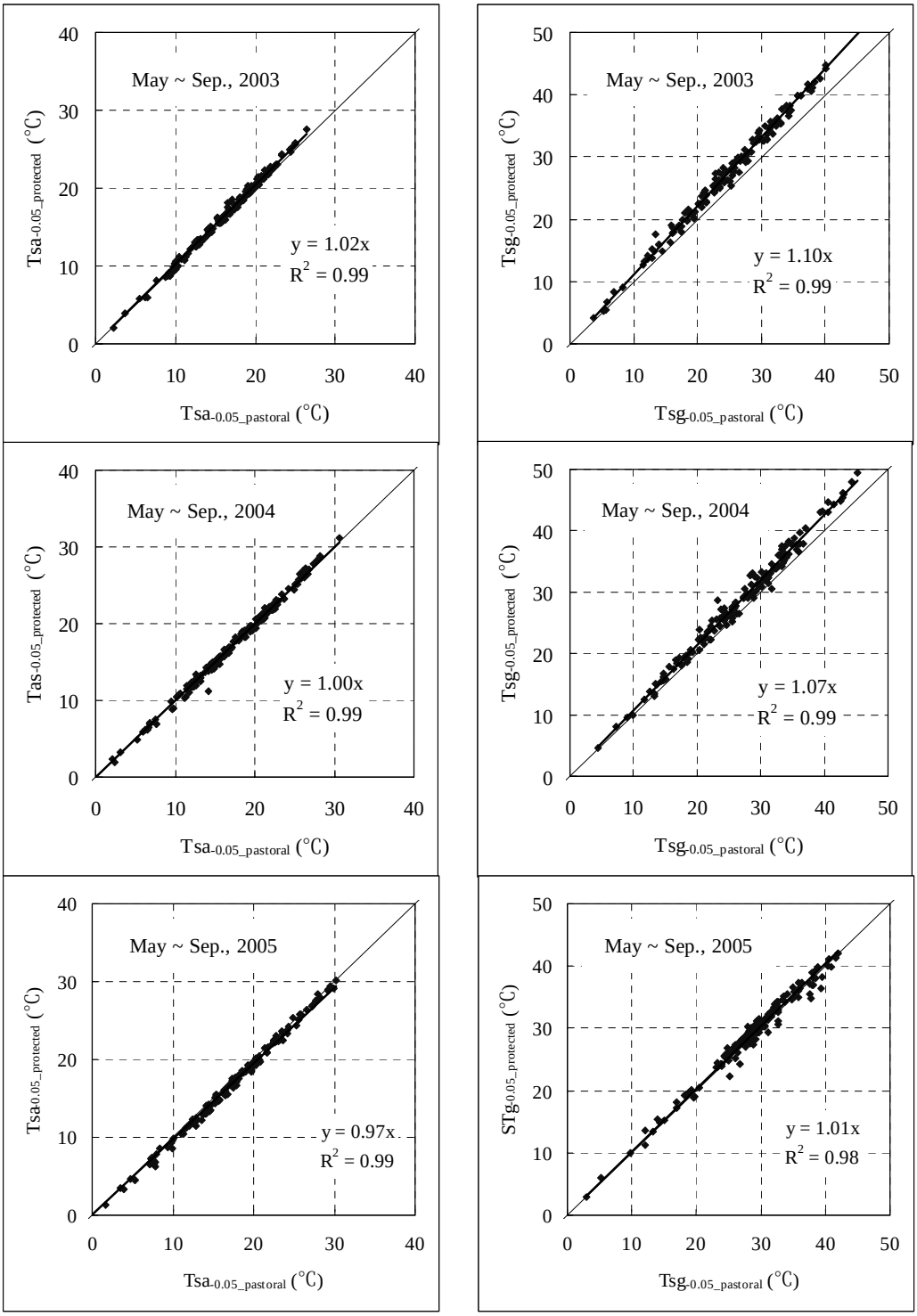


Fig. 3-6 A comparison between $\underline{T_{sa}}$ and $T_{sg}$ of 5-month data set (from May to September). $\underline{T_{sa}}$: daily-average surface soil temperature, $T_{sg}$: the difference of 30-minute average surface soil temperature values between daily-maximum and daily-minimum. Subscripts denote measurement areas. The straight lines are regression lines.

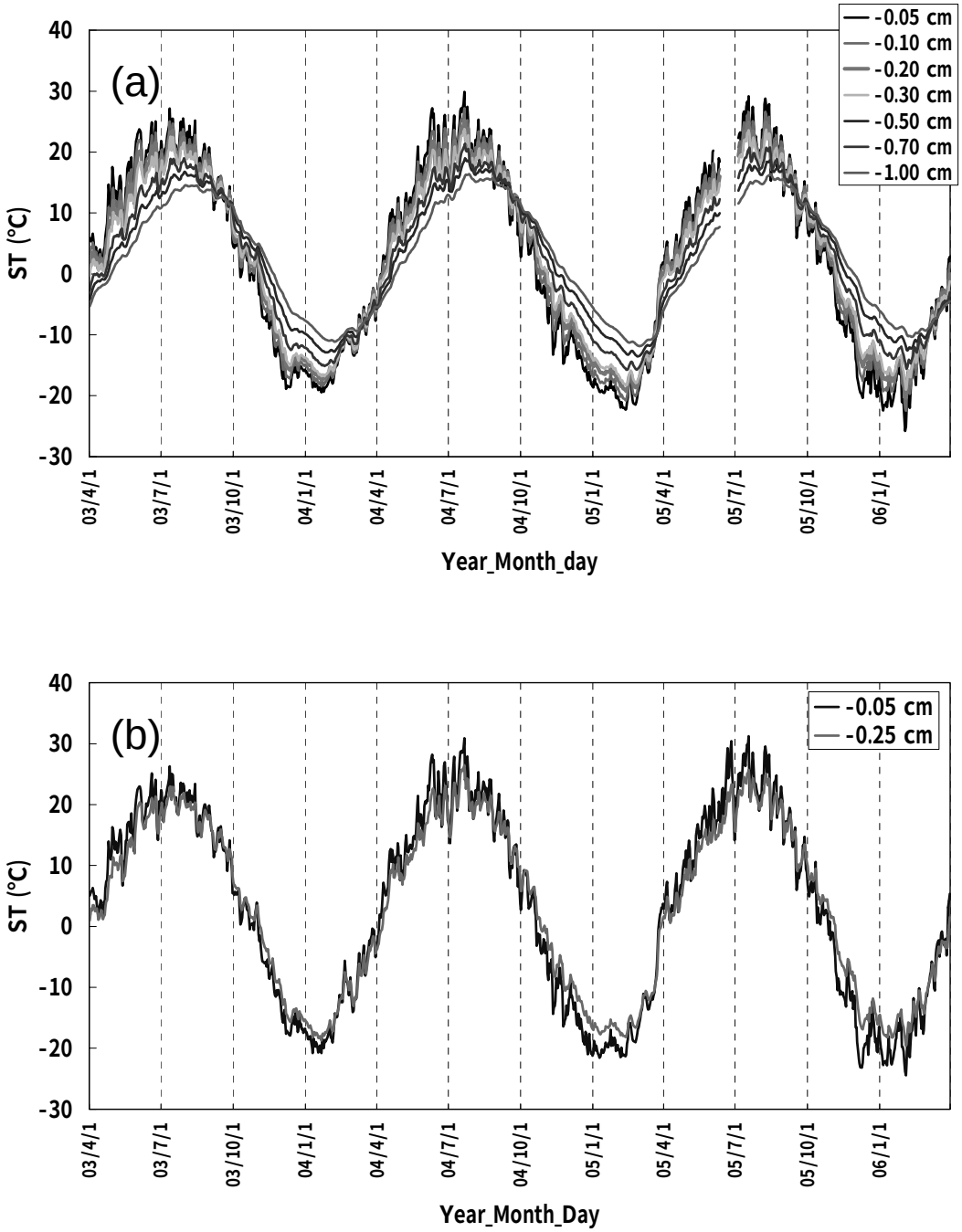


Fig. 3-7 The seasonal change of ST (soil temperature). (a): pastoral station, (b): protected station.

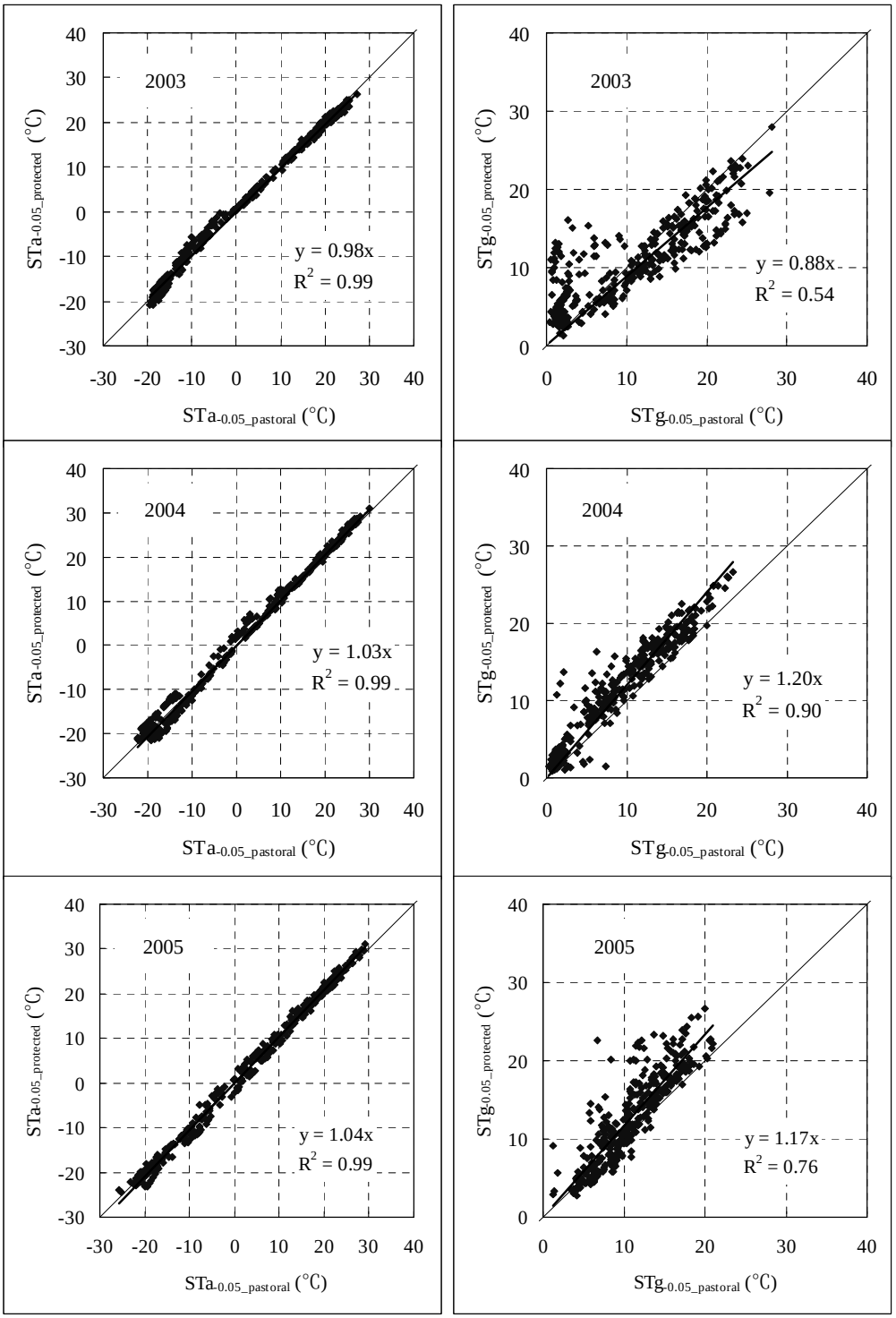


Fig. 3-8 A comparison between $STa_{-0.05}$ and $STg_{-0.05}$ of annual data set. $STa_{-0.05}$: daily-average soil temperature at depth of 5 cm, $STg_{-0.05}$: the difference of 30-minute average soil temperature values between daily-maximum and daily-minimum. Subscripts denote measurement areas. The straight lines are regression lines.

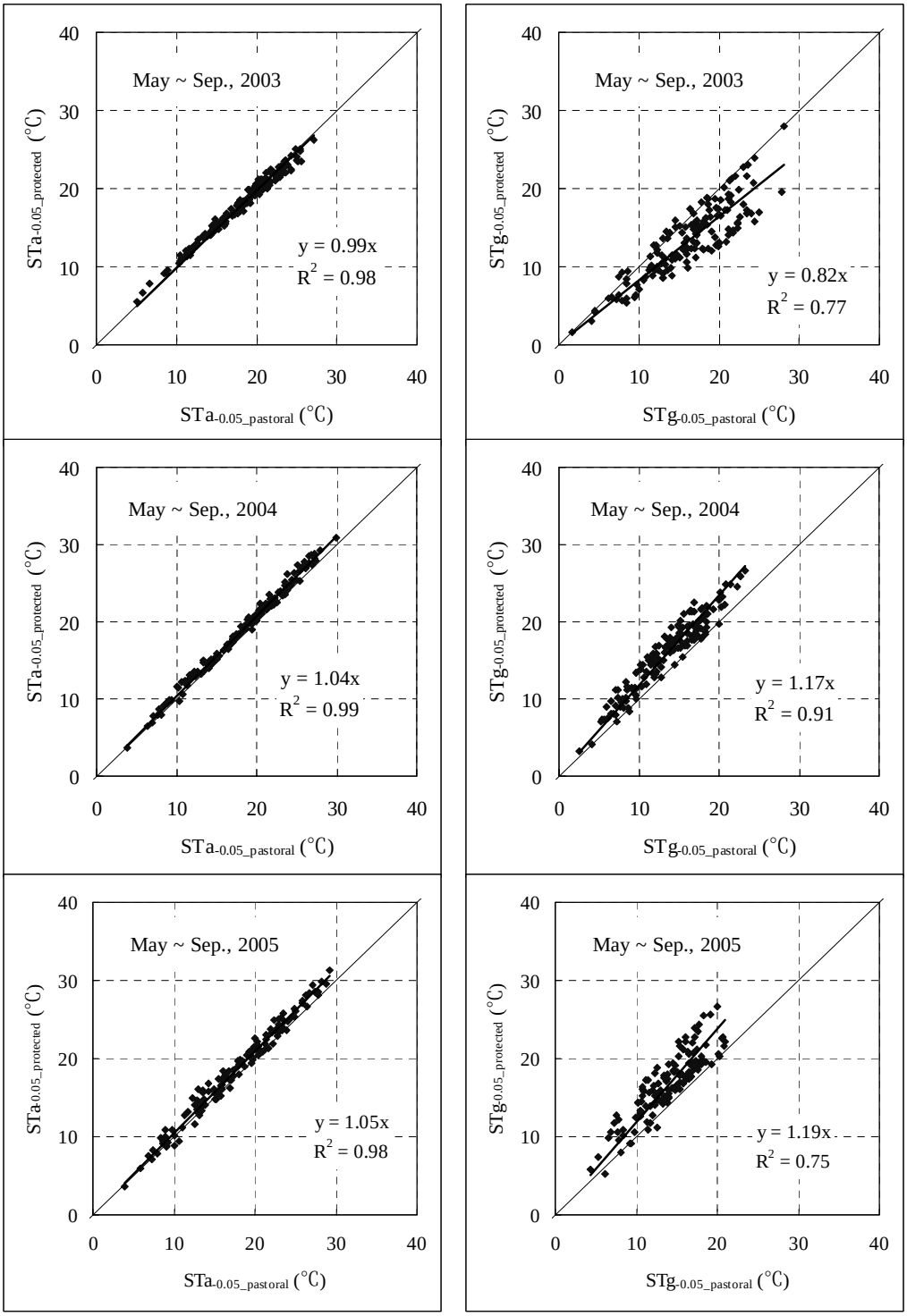


Fig. 3-9 A comparison between $STa_{-0.05}$ and $STg_{-0.05}$ of 5-month data set (from May to September). $STa_{-0.05}$: daily-average soil temperature at depth of 5 cm, $STg_{-0.05}$: the difference of 30-minute average soil temperature values between daily-maximum and daily-minimum. Subscripts denote measurement areas. The straight lines are regression lines.

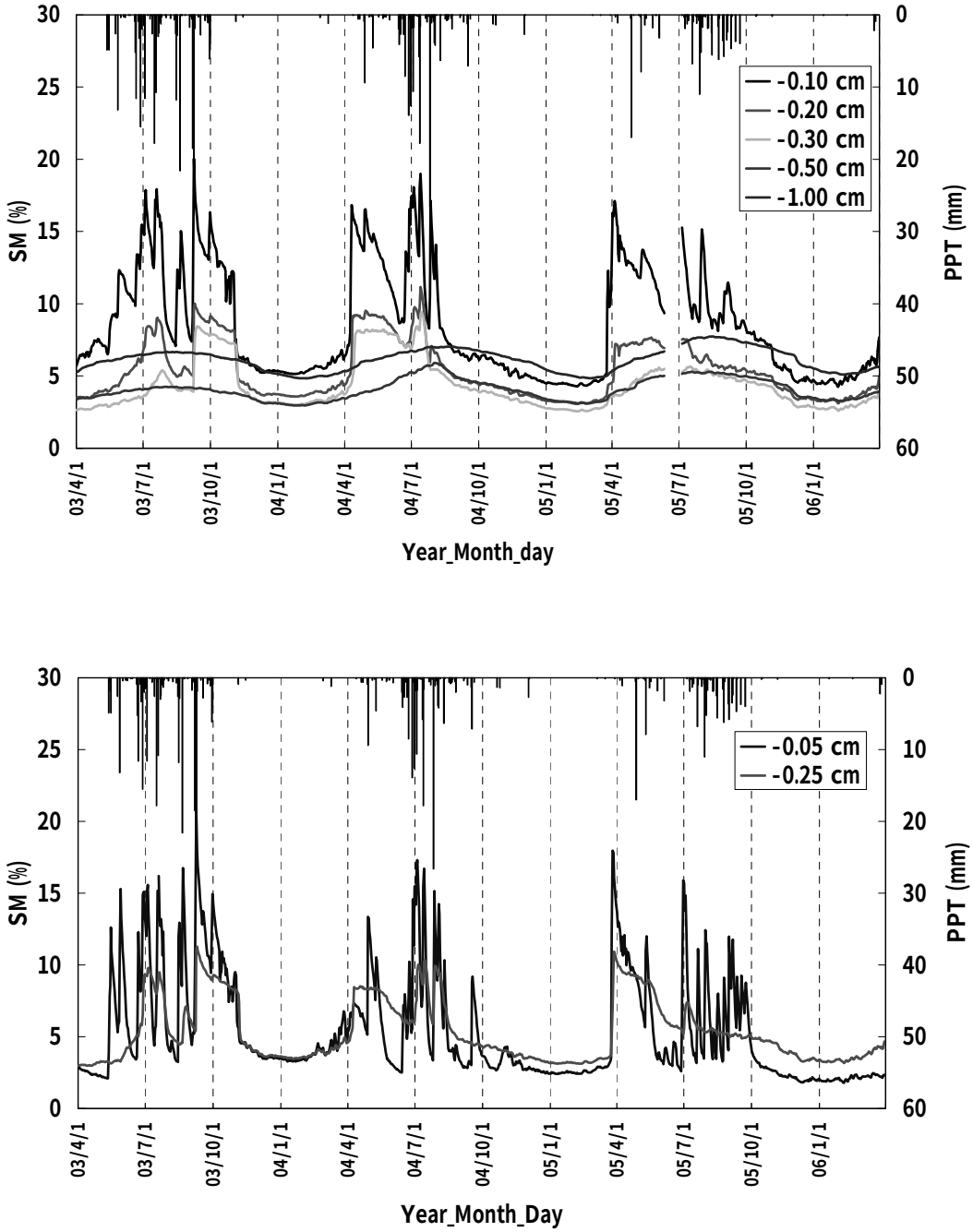


Fig. 3-10 The seasonal change of SM (soil moisture) and PPT (precipitation). (a): pastoral station, (b): protected station.

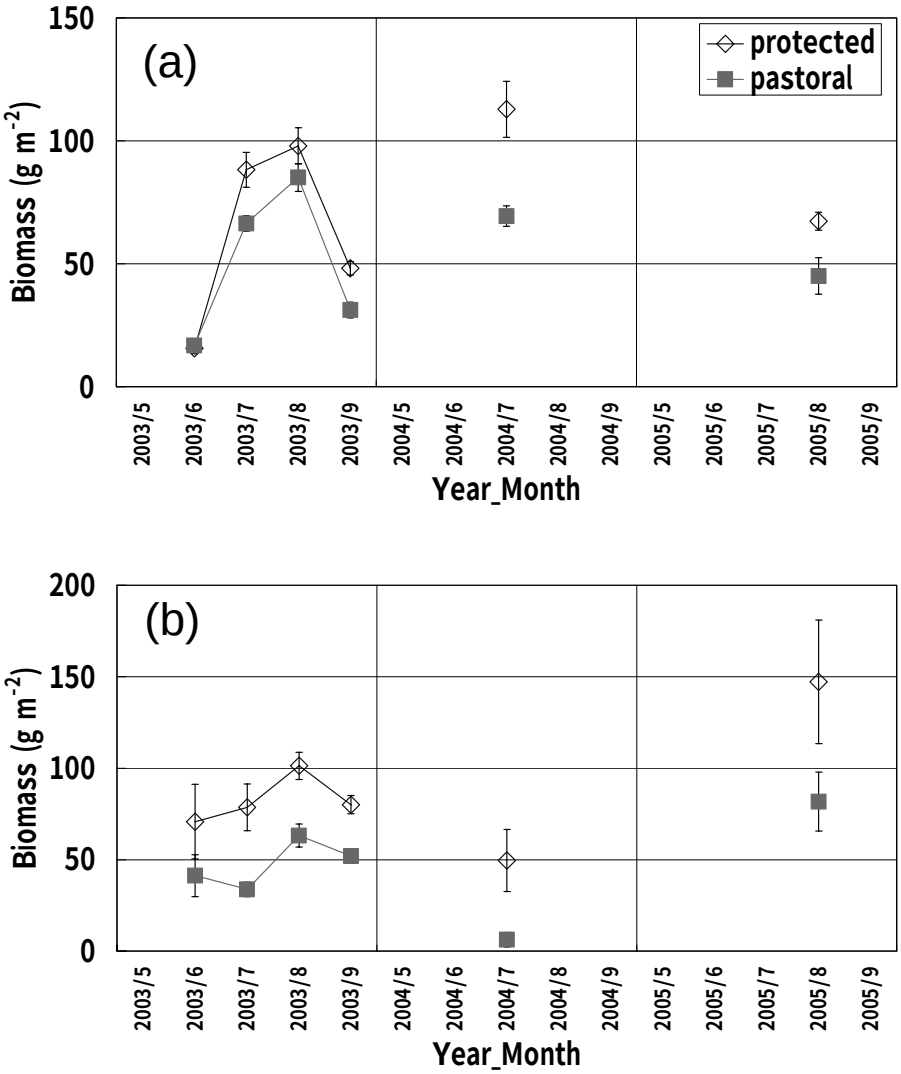


Fig. 3-11 The seasonal change of AGB (a) and ADB (b). AGB: aboveground green biomass, ADB: aboveground dead-vegetation biomass.

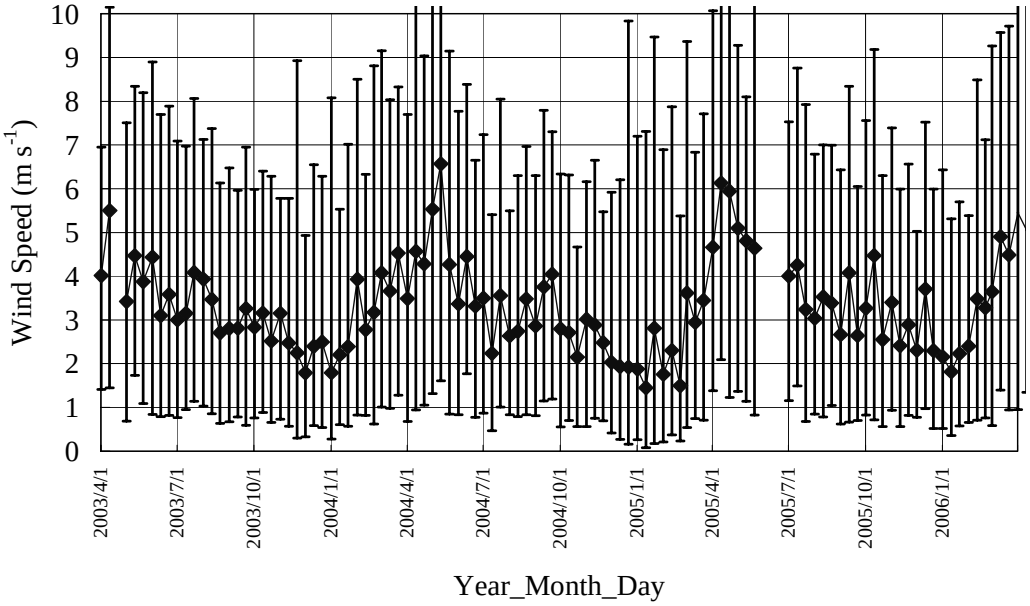


Fig. 3-12 The seasonal change of wind speed in KBU. The values are the 10-day average. Error bar shows the 10-day average of the daily maximum and minimum.

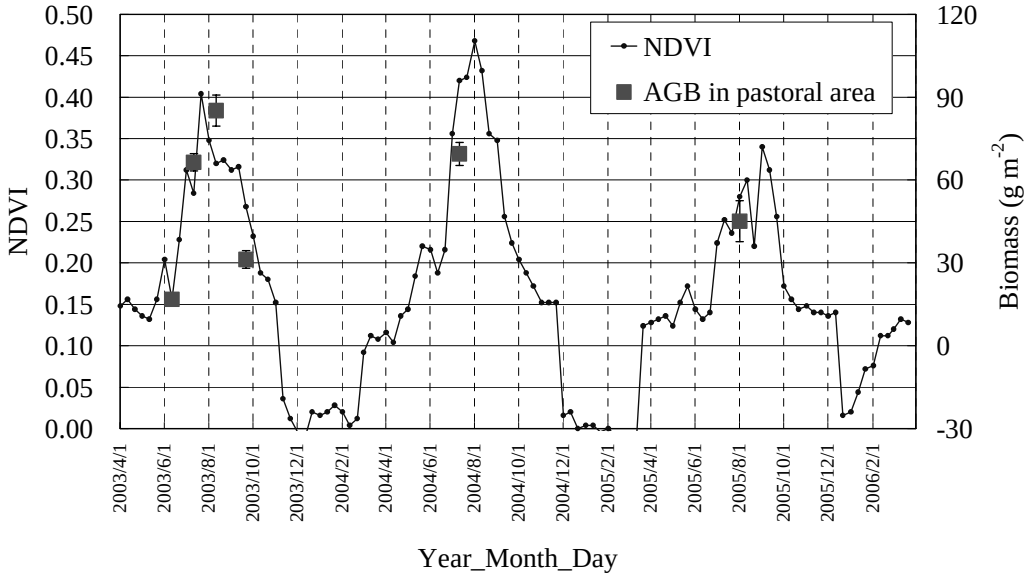


Fig. 3-13 The seasonal change of NDVI and AGB. AGB: aboveground green biomass.

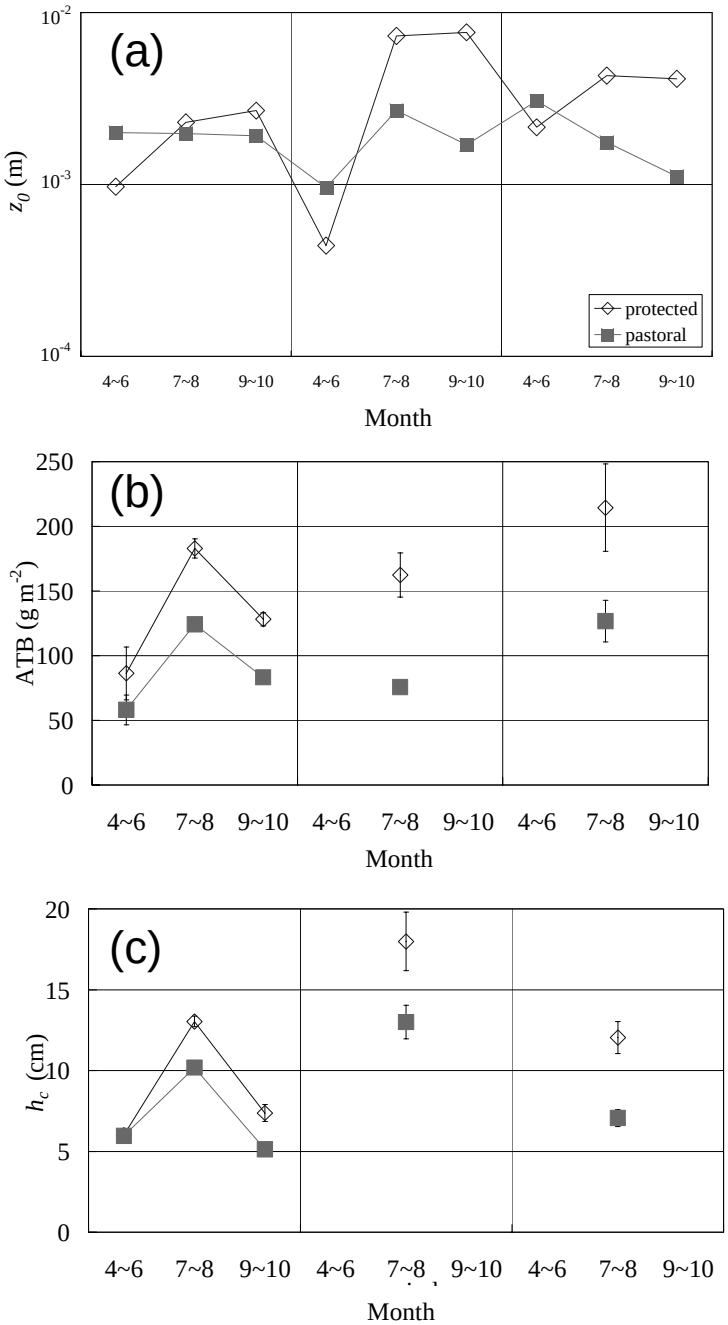


Fig. 3-14 The seasonal change of $z_0$ (a), ATB (b) and $h_c$ (c). $z_0$: roughness length, ATB: AGB + ADB, AGB: aboveground green biomass, ADB: aboveground dead-vegetation biomass, $h_c$: vegetation height .

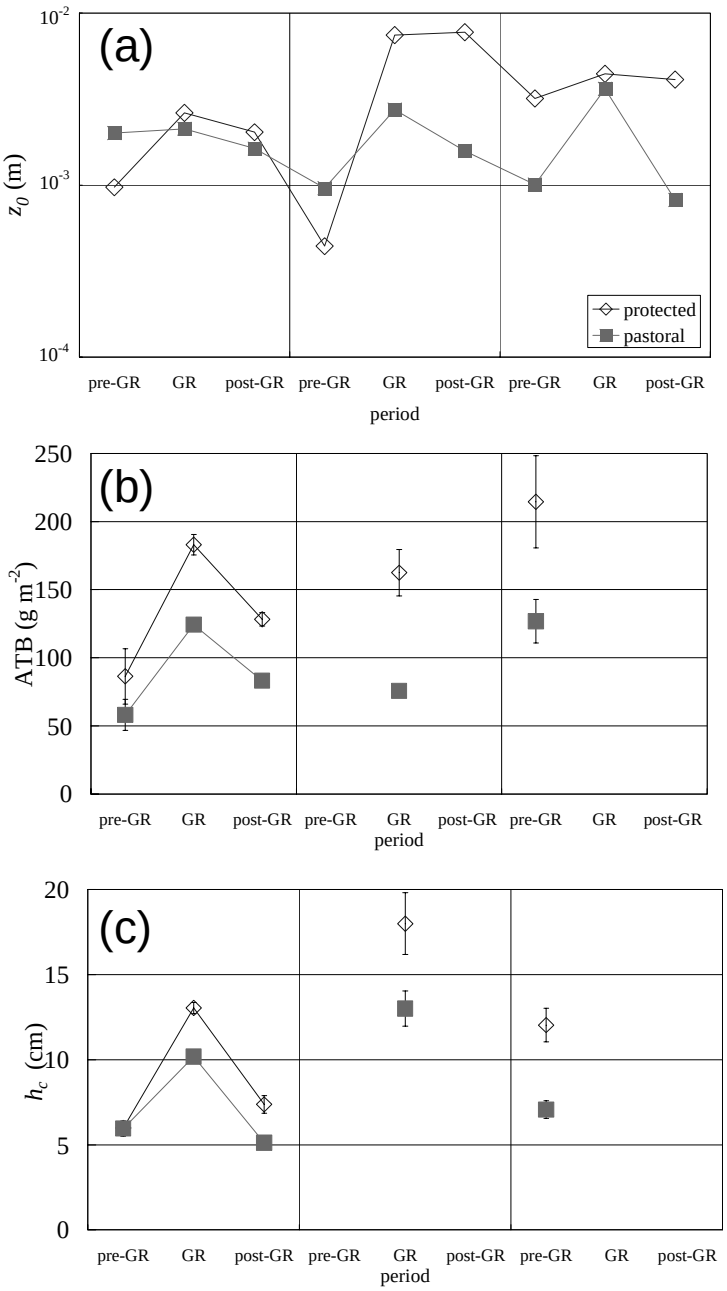


Fig. 3-15 The seasonal change of $z_0$ (a), ATB (b) and $h_c$ (c). $z_0$: roughness length, ATB: AGB + ADB, AGB: aboveground green biomass, ADB: aboveground dead-vegetation biomass, $h_c$: vegetation height . GR: growing season (NDVI > 0.3), pre-GR: the period before GR, post-GR: the period after GR.

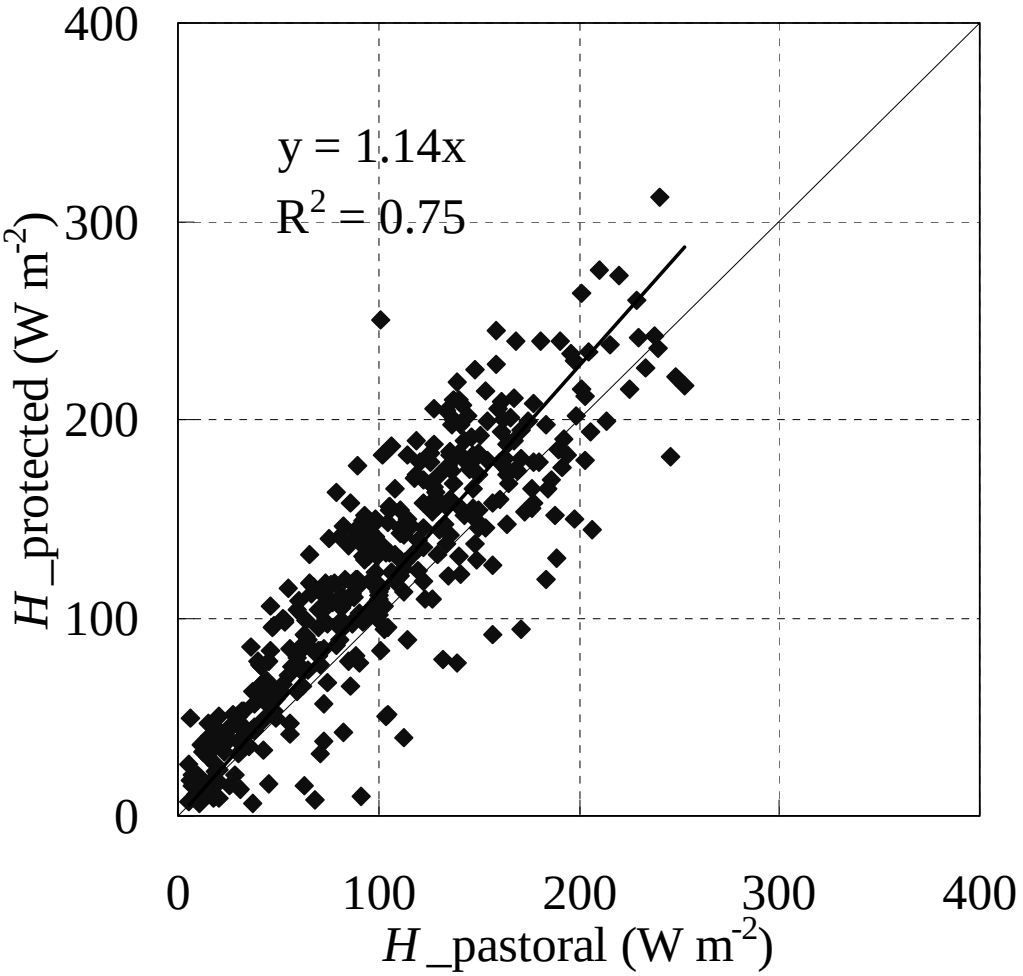


Fig. 3-16 An example of the figure in order to compare the components of the heat balance of the two stations (GR (Growing season) of 2003). *H*_pastoral: *H* (sensible heat flux) of pastoral area, *H*_protected: *H* of protected area,

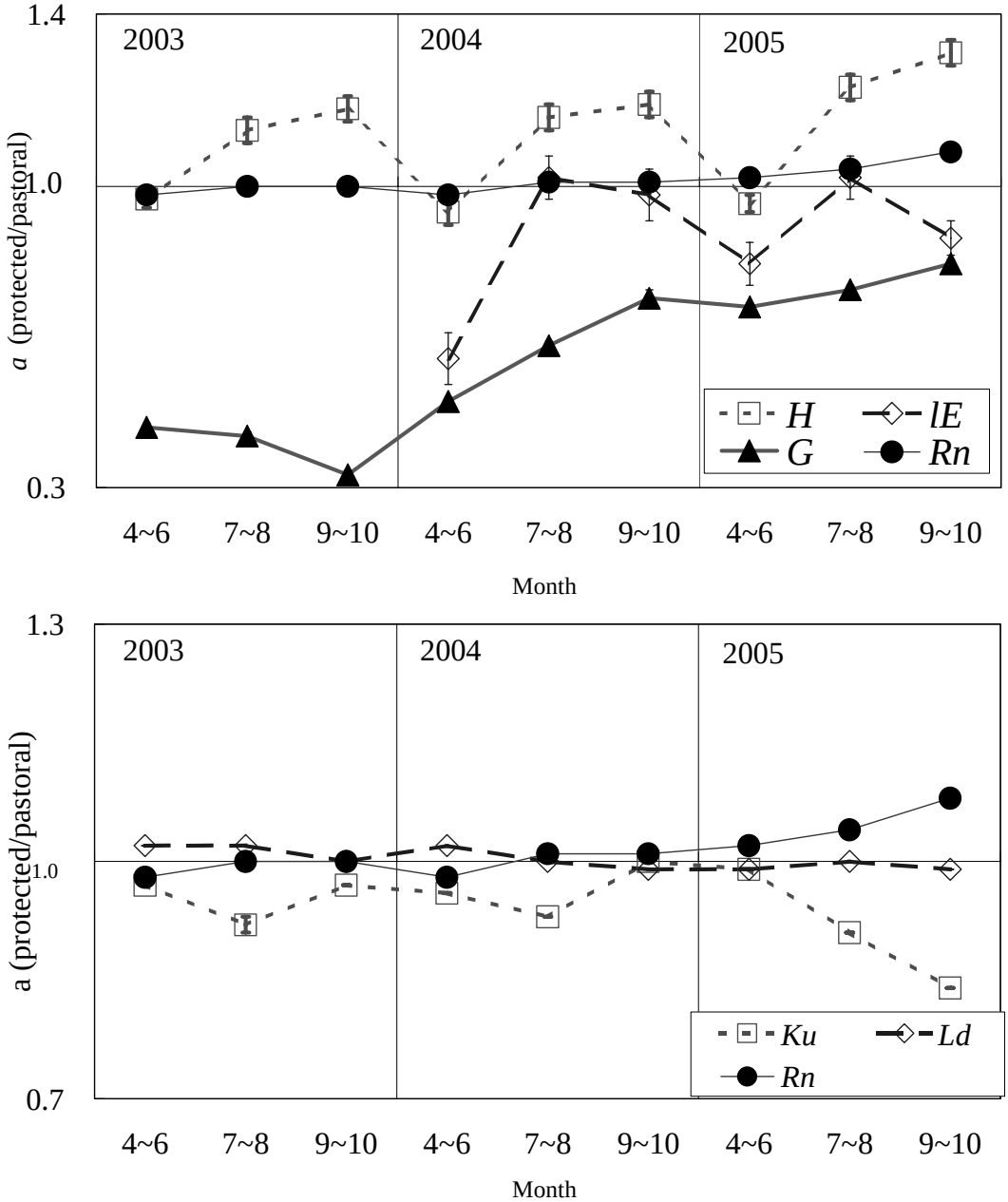


Fig. 3-17 The seasonal change of *a* of the components of the radiation and heat budget. *a*: $F_{protected} = a\ F_{pastoral}$, *F*: energy flux, $K_u$: upward shortwave radiation, $L_u$: upward longwave radiation, $R_n$: net radiation, *G*: soil heat flux, *H*: sensible heat flux, *lE*: latent heat flux.

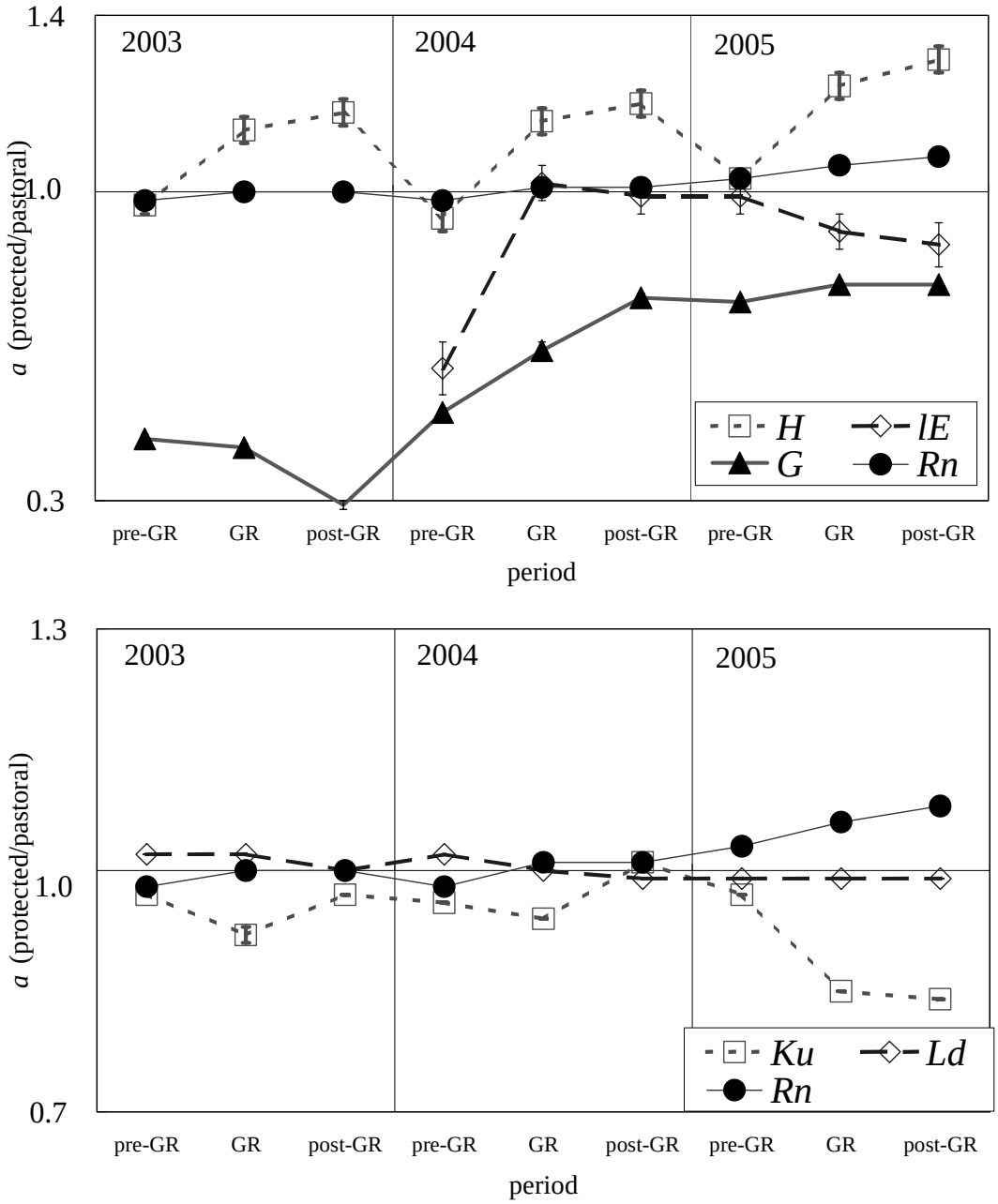


Fig. 3-18 The seasonal change of *a* of the components of the radiation and heat budget. *a*: $F_{protected} = a\ F_{pastoral}$, *F*: energy flux, $K_u$: upward shortwave radiation, $L_u$: upward longwave radiation, $R_n$: net radiation, *G*: soil heat flux, *H*: sensible heat flux, *lE*: latent heat flux. GR: growing season (NDVI > 0.3), pre-GR: the period before GR, post-GR: the period after GR.

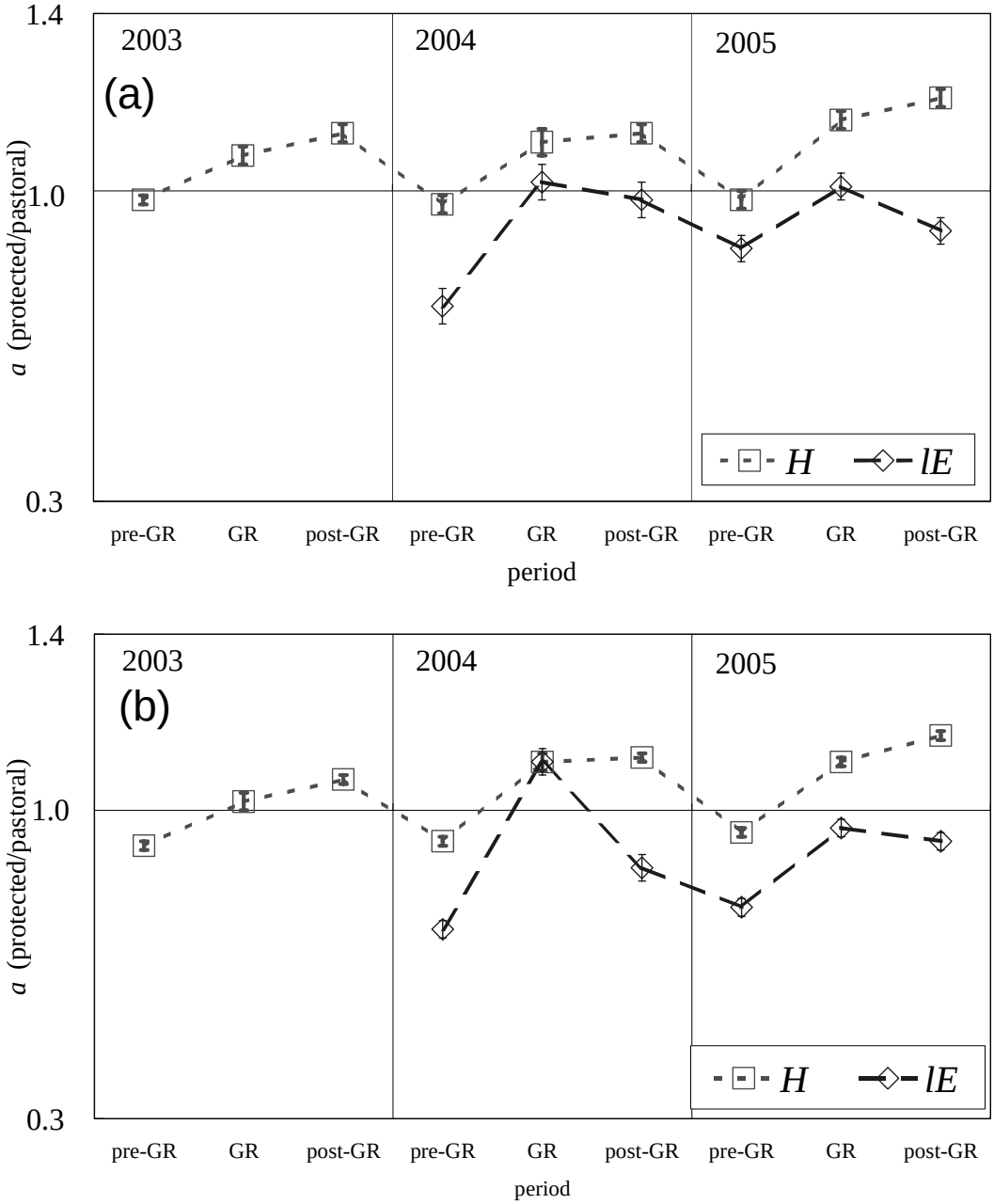


Fig. 3-19 The seasonal change of *a* of turbulent heat flux. (a): the data set wasn't done the correction to consider upwind area. (b): the data set wasn't done the data selection for wind direction and the correction. *a*: $F_{protected} = a\ F_{pastoral}$. GR: growing season (NDVI> 0.3), pre-GR: the period before GR and post-GR: the period after GR, *H*: sensible heat flux, *lE*: latent heat flux.

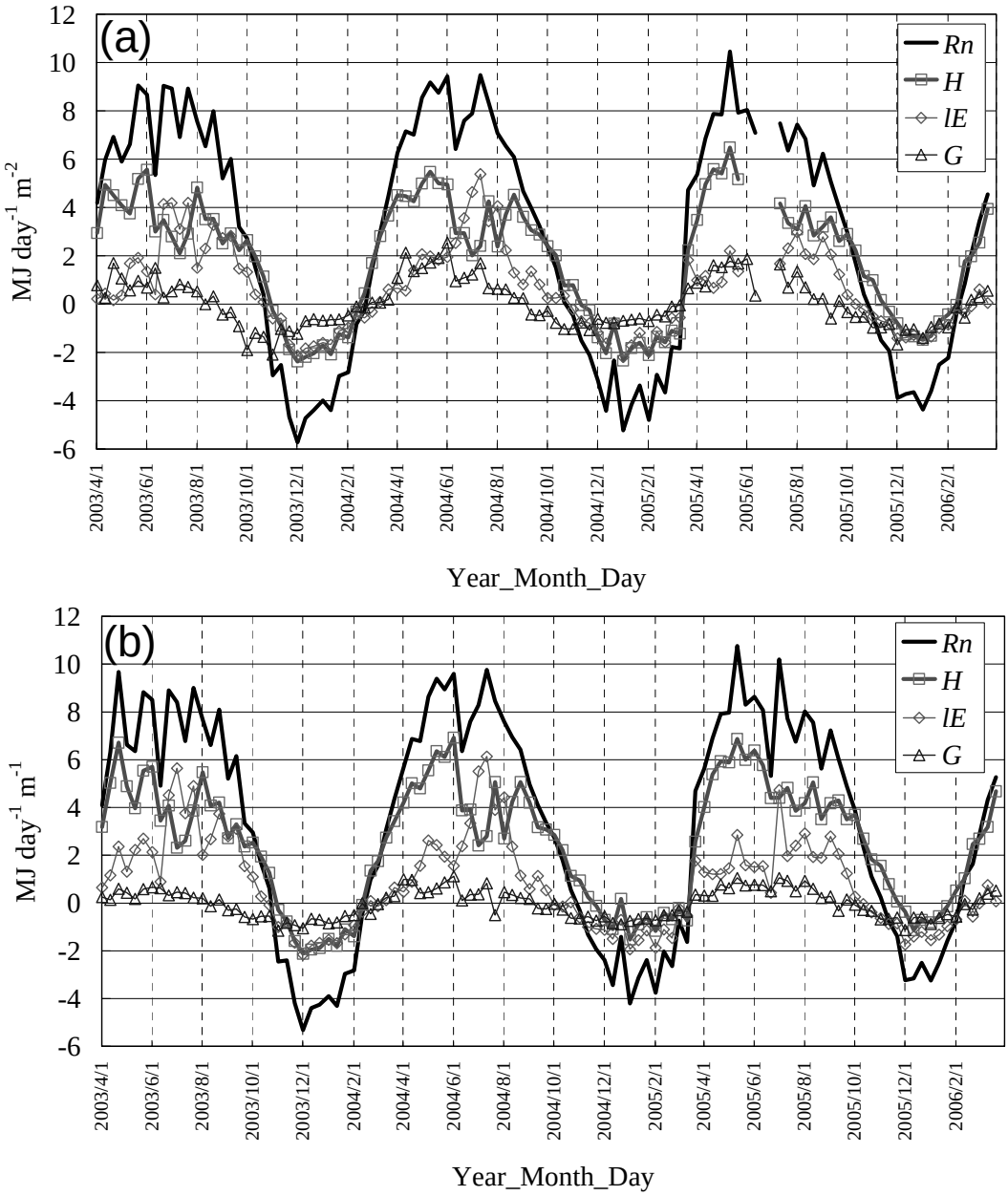


Fig. 3-20 The seasonal change of daily-integrated values of surface heat balance. $R_n$: net radiation, $G$: soil heat flux, $H$: sensible heat flux, $lE$: latent heat flux. (a) and (b) were the data sets in pastoral area and protected area, respectively.

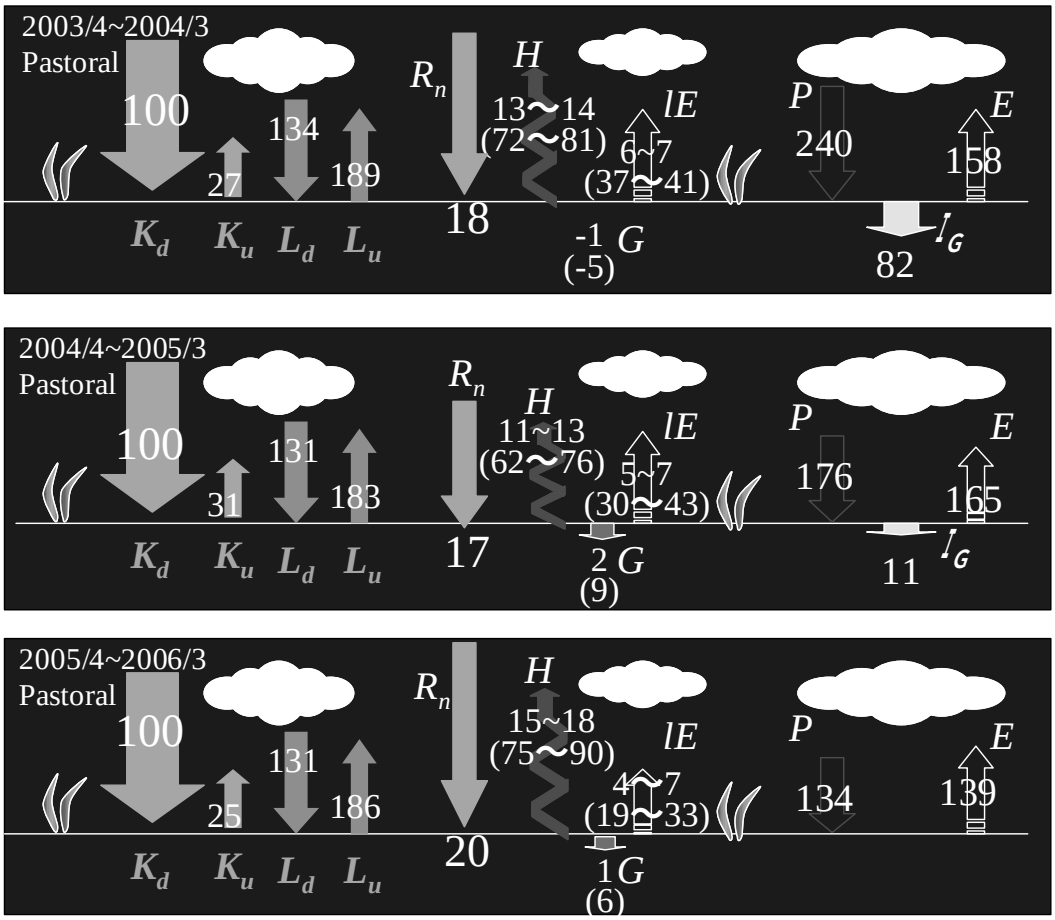


Fig. 3-21 The annual integrated values of surface energy balance (the ratio of downward short wave $K_d$) and water balance (mm) in the pastoral area. $K_u$: upward shortwave radiation, $L_u$: upward longwave radiation, $L_d$: downward longwave radiation, $R_n$: net radiation, $G$: soil heat flux, $H$: sensible heat flux, $lE$: latent heat flux, $P$: precipitation, $E$: transevaporation, $I_G$: Infiltration (= $P$ - $E$). The numbers in parentheses denote the ratio of $R_n$.

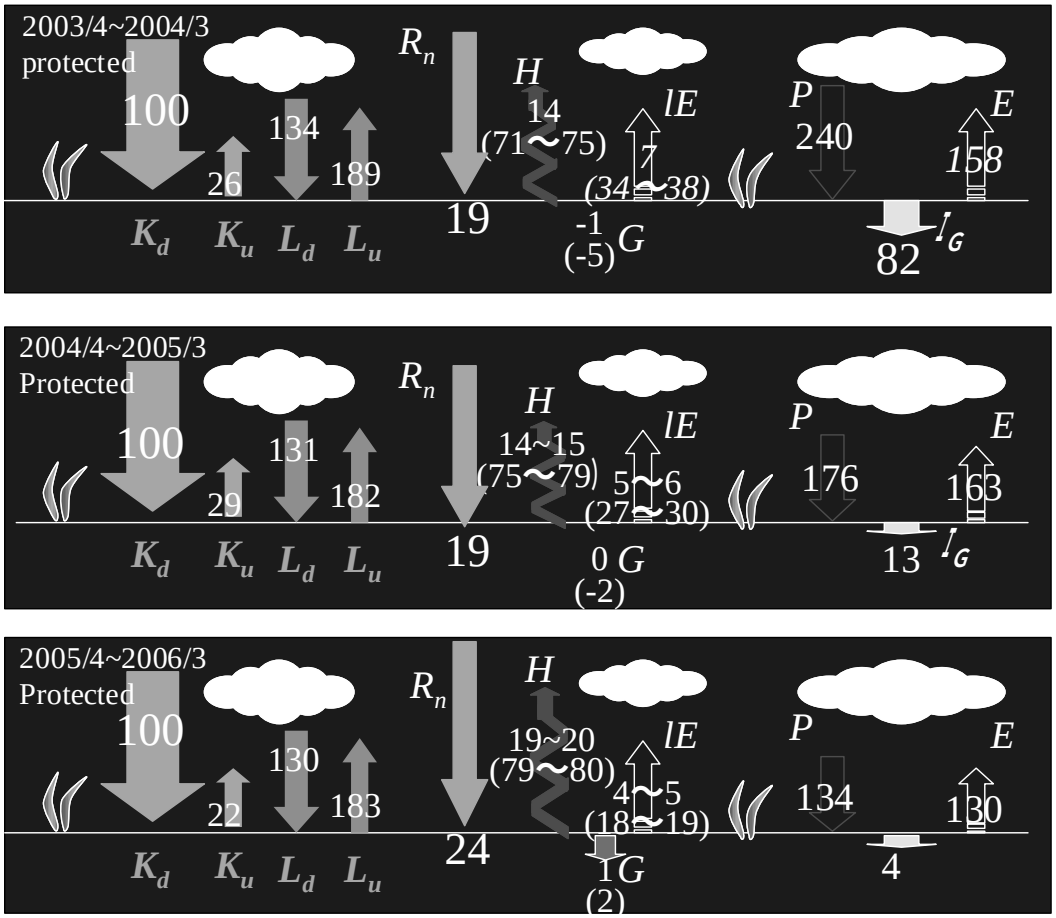


Fig. 3-22 The annual integrated values of surface energy balance (the ratio of downward short wave $K_d$) and water balance (mm) in the protected area. $K_u$: upward shortwave radiation, $L_u$: upward longwave radiation, $L_d$: downward longwave radiation, $R_n$: net radiation, $G$: soil heat flux, $H$: sensible heat flux, $lE$: latent heat flux, $P$: precipitation, $E$: transevaporation, $I_G$: Infiltration (= $P$ - $E$). $E$ value in 2003, which was not measured, was assumed to be same as that of pastoral area on the grounds that there would be significant difference in first year. The numbers in parentheses denote the ratio of $R_n$.

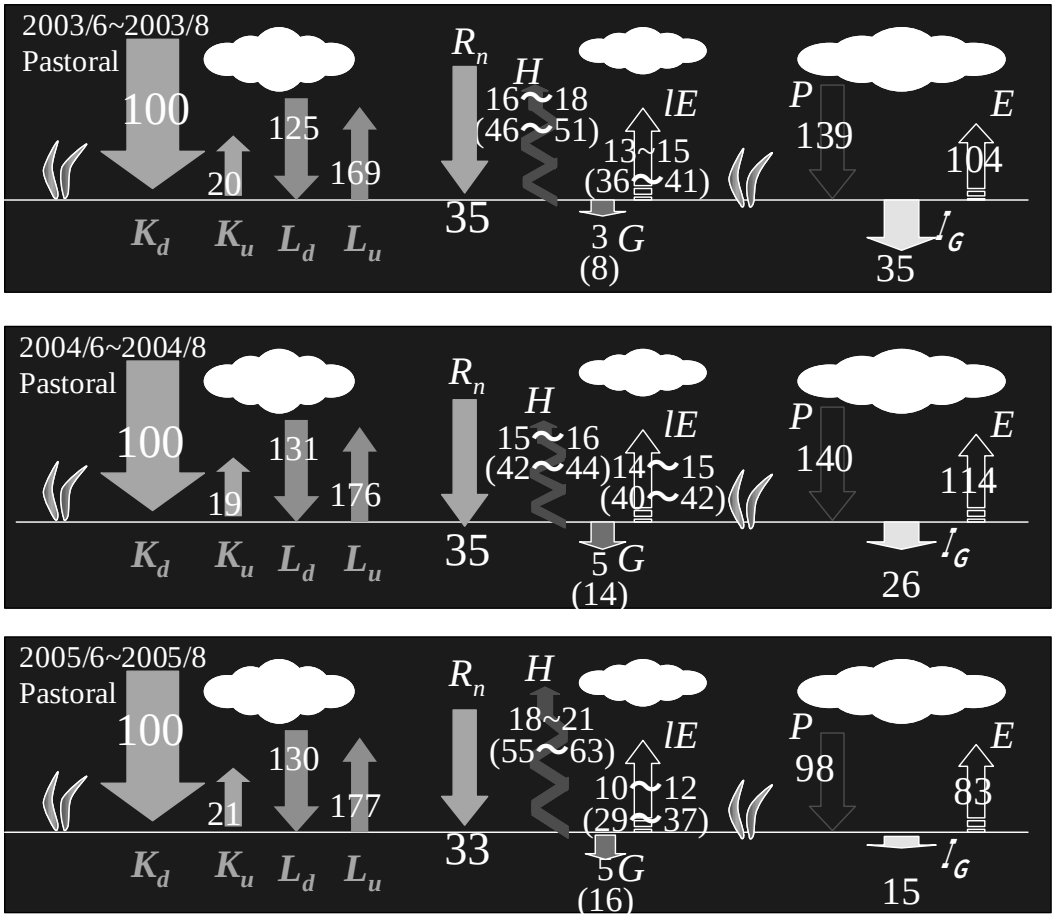


Fig. 3-23 The integrated values of surface energy balance (the ratio of downward short wave $K_d$) and water balance (mm) in the pastoral area during June to August. $K_u$: upward shortwave radiation, $L_u$: upward longwave radiation, $L_d$: downward longwave radiation, $R_n$: net radiation, $G$: soil heat flux, $H$: sensible heat flux, $lE$: latent heat flux, $P$: precipitation, $E$: transevaporation, $I_G$: Infiltration (= $P$ - $E$). The numbers in parentheses denote the ratio of $R_n$.

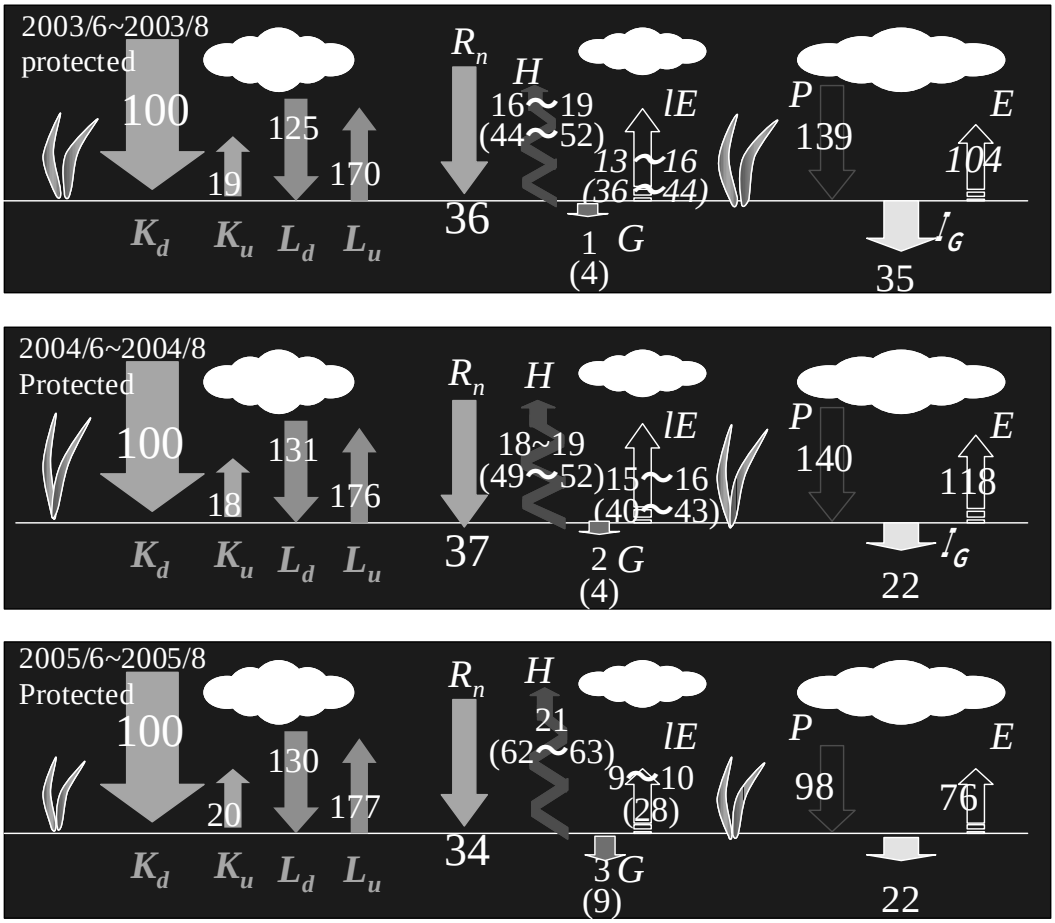


Fig. 3-24 The integrated values of surface energy balance (the ratio of downward short wave $K_d$) and water balance (mm) in the protected area during June to August. $K_u$: upward shortwave radiation, $L_u$: upward longwave radiation, $L_d$: downward longwave radiation, $R_n$: net radiation, $G$: soil heat flux, $H$: sensible heat flux, $lE$: latent heat flux, $P$: precipitation, $E$: transevaporation, $I_G$: Infiltration (= $P$ - $E$). $E$ value in 2003, which was not measured, was assumed to be same as that of pastoral area on the grounds that there would be significant difference in first year. The numbers in parentheses denote the ratio of $R_n$.

## Chapter 4

# Conclusions

The present study was conducted in order to assess influence of grazing on semi-arid grassland over the Mongolian steppe through a three-year observation. First, grazing effect appeared vegetation, and the results of vegetation change effected the energy balance, especially net radiation and sensible heat flux values. However latent heat flux (evapotranspiration) was not affected.

The results are summarized as follows (Fig. 4-1);

(1) Vegetation and roughness length

AGB (aboveground green biomass) results show that to protect the grassland from grazing caused a favorable condition for the growth of vegetation. ADG (aboveground dead-vegetation biomass) in the protected area was always larger than that in the pastoral area, because vegetation was consumed by livestock. This is why the roughness length $z_0$ of the protected area in GR and post-GR was larger than that of the pastoral area.

(2) The seasonal change of energy balance

In the protected area, the larger ATB (aboveground total biomass, ATB = AGB + ADG) caused upward shortwave radiation $K_u$ to be smaller, which resulted in the larger net radiation $R_n$ of the protected area. The increased part of $R_n$ was divided to soil heat flux $G$ and sensible heat flux $H$. For $H$ values in the protected area, the larger $z_0$ values because of the larger values of biomass, also contributed to the higher fluxes.

(3) The annual change of energy and water balance

There is no significant difference of the annual integrated $E$ values between two areas. The result agrees with the simulated study by Chen *et al*. (2006); the reduction of the

transpiration by grazing in the pastoral area is largely compensated by the increase of evaporation.

As shown above, there was influence of grazing on Mongolian steppe. However, compared with previous studies at overgrazed grassland, the effect was moderate. For example, there wasn't significant difference of soil surface temperature and evapotranspiration. This tends to imply that the grazing intensity of this region is not that heavy. This was confirmed from the fact that grazing intensity of KBU was smaller than the maximum sustainable values suggested by Chen *et al*. (2006). Fujita (2003) suggested that grazing maintained vegetation diversity. From this stand point, proper grazing is essential to maintain the steppe are. Similarly, there may be the unfavorable effect of grassland without vegetation. One example is that too much dead vegetation remained without grazing disturbed the vegetation growth in the protected area. Therefore it may not always be better for Mongolian steppe to stop grazing. Reasonable land use management including moderate grazing may be essential.

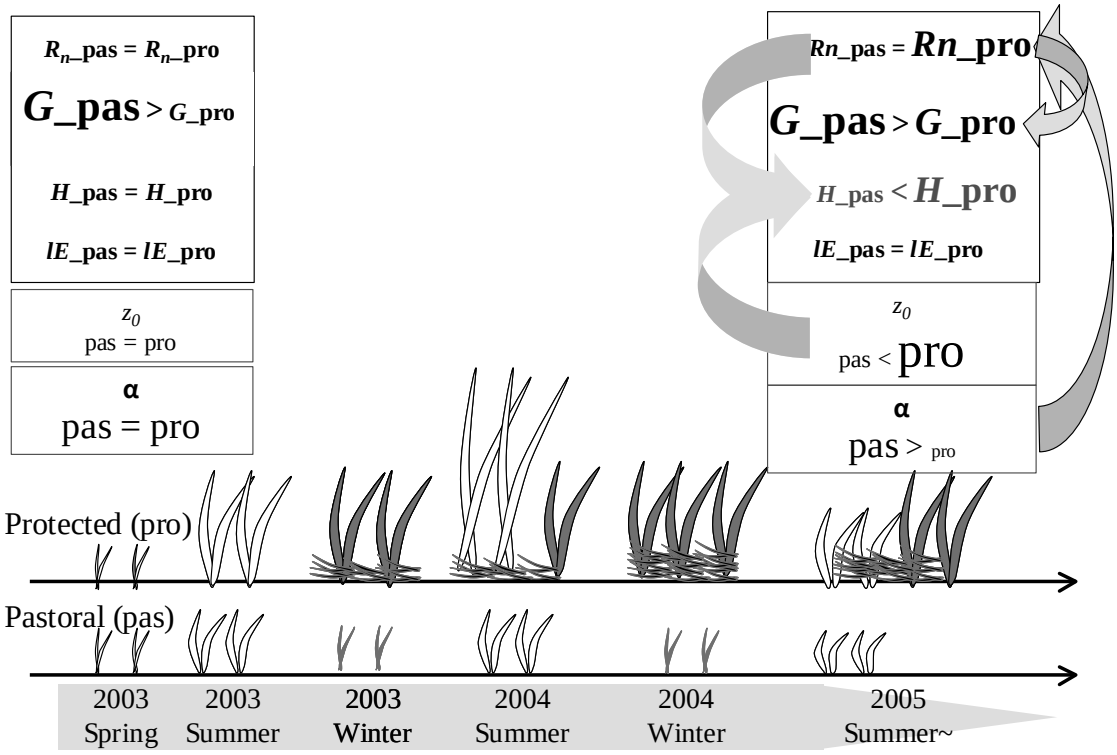


Fig. 4-1 The annual change of surface energy balance. $K_d$: downward shortwave radiation, $K_u$: upward shortwave radiation, $L_u$: upward longwave radiation, $L_d$: downward longwave radiation, $R_n$: net radiation, $G$: soil heat flux, $H$: sensible heat flux, $lE$: latent heat flux, $z_0$: roughness length, *á*:albedo.

## Acknowledgement

I wish to express my sincere gratitude to my academic adviser, Professor Michiaki Sugita, Associate Professor Jun Asanuma and Dr. Maki Tsujimura, Graduate School of Life and Environmental Sciences, University of Tsukuba, for their continuing guidance and encouragement. They gave me a chance to study on the topic of this thesis.

Special thanks are expended to Professor Tadashi Tanaka, Professor Norio Tase, Professor Hiroshi Okura, Dr. Tsutomu Yamanaka, Graduate School of Life and Environmental Sciences, University of Tsukuba, and Dr. Ayumi Kotani, Japan Science and Technology Agency, for their guidance.

I give my thanks to Mr. Hiroaki Kato, Ms. Maki Asano, Mr. Tadaaki Urano in Doctoral Program in Graduate School of Life and Environmental Sciences, University of Tsukuba, and Ms. Aki Hoshino for their advice and friendships.

Many thanks to my colleagues Ms. Aya Tanaka, Mr. Byanbahuu, Doctoral Program in Geoenvironmental Science, the University of Tsukuba, all the RAISE members and Mongolian people who helped me in the field work. I feel appreciating Professor Sheng Gong Li, Synthesis Research Center of Chinese Ecosystem Research Network, Institute of Geographic Sciences and Natural Resources Research, Chinese Academy of Sciences, Dr. Dambaravjaa Oyunbaartar, Institute of Meteorology and Hydorology, Mongolia, Mr. Hisanori Tanaka, Climatec Inc. and Ms. Kanae Sakaguchi in Master Program in Education, the University of Tsukuba for their corporation in my graduate work. And also thanks to all of the staff and students in hydrology group.

Finally I express special thanks my family to give me a chance to study and continuous encouragements.

This work has been supported by a CREST project (The Rangelands Atmosphere -Hydrosphere - Biosphere Interaction Study Experiment in Northeastern Asia) of JST (Japan Science and Technology Agency).

# Reference


Baldocchi, D. D.,and L. Xu and N. Kiang. (2004): How plant functional-type, weather, seasonal drought, and soil physical properties alter water and energy fluxes of an oak–grass savanna and an annual grassland. *Agricultural and Forest Meteorol*. **123**, 13–39.

Batima, P., Dagvadori, D. (2000): Climate change and its impact in Mongolia. *JEMR Publishing*, Ulaanbaatar, 227pp.

Batjargal, Z. (1997): Desertification of Mongolia. *RALA Report*. **200**, 107-113.

Bremer, D., Auen, L., Ham, J.and Owensby, C. (2001): Evaporation in a prairie ecosystem: effects of grazing by cattle. *Agron. J*. **93**, 338–348.

Bryant, N. A., L. F. Johnson, A. J. Brazel, R. C. Balling, C. F. Hutchinson and L. R. Beck. (1990): Measuring the effect of overgrazing in the Sonoran Desert. *Climate Change*. **17**, 243-264.

Businger, J. (1988): A note on the Businger-Dyer profiles. *Boundary Layer Moteorol.* **42**, 145-151.

Chen, Y., G., Lee, P., Lee, T., Oikawa (2006): Simulating root responses to grazing of a Mongolian grassland ecosystem. *Plant Ecol.* **183**, 265-275.

Chen, Y., G., Lee, P., Lee, T., Oikawa (2007): Model analysis of grazing effect on above-ground biomass and above-ground net primary production of a Mongolian grassland ecosystem. *J. Hydrol*. **333**, 155-164.

Cui, X., Y. Wang, H. Niu, J. Wu, S. Wang, E. Schnug, J. Rogasik, J. Fleckenstein and Y. Tang (2005): Effect of long-term grazing on soil organic carbon content in semiarid steppes in Inner Mongolia. *Ecol. Res.* **20**, 519-527.

Dyer, A. J. (1974): A review of flux-profile relationships. *Boundary layer Meteorol.*, **7**, 363-372.

Fernández-Giménez, M. and Allen-Diaz, B. (1999): Testing a non-equilibrium model of rangeland vegetation dynamics in Mongolia. *J. Appl. Ecol*. **36**, 871-885.

Fernández-Giménez, M. and D. M. Swift (2003): Strategies for sustainable grazing management in the developing world. *Proceedings of the VIIth International Rangelands Congress*. 821-831.

Falge, E., D. Baldocchi, R. Olson, P. Anthoni, M. Aubinet, C. Bernhofer, G. Burba, R. Ceulemans, R. Clement, H. Dolman, A. Granier, P. Gross, T. Grünwald, D. Hollinger, N. –O. Jensen, G. Katul, P. Keronen, A. Kowalski, C. T. Lai, B. E. Law, T. Meyers, J. Moncrieff, E. Moors, J. W. Munger, K. Pilegaard, Ü. Rannik, C. Rebmann, A. Suyker, J. Tenhunen, K. Tu, S. Verma, T. Vesala, K. Wilson and S. Wofsy (2001a): Gap filling strategies for defensible annual sums of net ecosystem exchange. *Agricultural and Forest Meteorol*. **107**, 43–69.

Falge, E., D. Baldocchi, R. Olson, P. Anthoni, M. Aubinet, C. Bernhofer, G. Burba, R. Ceulemans, R. Clement, H. Dolman, A. Granier, P. Gross, T. Grünwald, D. Hollinger, N. –O. Jensen, G. Katul, P. Keronen, A. Kowalski, C. T. Lai, B. E. Law, T. Meyers, J. Moncrieff, E. Moors, J. W. Munger, K. Pilegaard, Ü. Rannik, C. Rebmann, A. Suyker, J. Tenhunen, K. Tu, S. Verma, T. Vesala, K. Wilson and S. Wofsy (2001b): Gap filling strategies for long term energy flux data sets. *Agricultural and Forest Meteorol*. **107**, 71–77.

Free VEGETATION Products: http://free.vgt.vito.be/

Fujita, N. (2003): Ecology of Steppe and Sustainable management of pastoral land, *Sci. J., Kagaku*. **73**, (5), 563-569. (in Japanese).

Grace, J., Ford, E.D., Jarvis, P.G. (1981): Plants and Their Atmospheric Environment. 21st Symposium of the British Ecological Society. Blackwell Scientific Publications, Oxford, London.

Iida, S. (2000): Seasonal Changes of Stem Water Storage and its Role in Transpiration

Processes of a Japanese Red Pine. MS Thesis, University of Tsukuba, 128pp.

Kawata, K., T. Urano, G. Lee, S. Mariko and T. Nakamura. (2007): Structure of a plant community and variance of biomass under over-grazed environment in Kherlen Bayan-Ulaan, Mongolia. *J. Arid Land Studies*. in press. (in Japanese).

Kayane, I. (1980): Hydrology. *Daimyodo*, Tokyo, 272pp. (in Japanese).

Kojima, T. (2004): The Investigation on the Factors Which Govern Evapotranspiration of Kherlen River Basin in Mongolia. MS Thesis, University of Tsukuba, 85pp. (in Japanese).

Komonen, M., A. Komonen and A. Otgonsuren (2002): Daurian pikas (*Ochotona daurica*) and grassland condition in eastern Mongolia. *J. Zoology*. **259**, 281-288.

Kondo, J. (1994): Atmospheric Science near the Ground Surface. *University of Tokyo Press.* Tokyo, 324pp. (in Japanese).

Kneizys, F. X., E. P. Shettle, L. W. Abreu, J. H. Chetwynd, G. P. Anderson, W. O. Gallery, J. E. A. Selby and A. A. Clough (1988): Users guide to Lowtran 7. Air Force geophysics laboratory Report, No AFGL-TR-88-0177, Hanscom AFB, Ma, 137pp.

Kustas, P. W., Prueger, J. H., Hatfield, J. L., Ramalingam, K. and Hipps, L. E. (2000): Variability in soil heat flux from a mesquite dune site. *Agricultural and Forest Meteorology*. **103**, 249-264.

Lecain, D., Morgan, J., Schuman, G., Reeder, J. and Hart, R. (2000): Carbon exchange rates in grazed and ungrazed pastures of Wyoming. *J. Range Sci*. **53**, 199–206.

Li, S.-G., Harazono, Y., Oikawa, T., Ha, L, Z., Z-, Y-, He. And Xue, L, C. (2000): Grassland desertification by grazing and the resulting micrometeoroligocal changes in Inner Mongolia. *Agricultural and Forest Meteorol.* **102**, 125-137.

Li, S.-G., Asanuma, J., Eugster, W., Kotani, A., Liu, J.-J., Urano, T., Oikawa, T., Davaa, G., Oyunbaatar, D., Sugita, M., (2005): Net ecosystem carbon dioxide exchange over grazed steppe in central Mongolia. *Global Change Biol.* **11**, 1941–1955.

Lloyd, C. R. (1995): The effect of heterogeneous terrain on micrometeorological flux measurements: a case study from HAPEX-Sahel. *Agricultural and Forest Meteorol.* **73**, 209-216.

Manabe, S., Wetherald, R.T. (1986): Reduction in summer soil wetness induced by an increase in atmospheric carbon dioxide. *Sci*. **232**, 626–628.

Nachinshonkhor, U. G.., Tserendash, S., Jagalsaikhan, L., Tsooj, Sh., Tsendeekhuu, Ts., Dugarjav, Ch. and Hirose, T. (2003): productivity of Plant communities and Type of Animal Husbandry in the Mongolian Grassland, *Bulletin of JAMS*. **33**. (in Japanese).

National Agency for Meteorology, Hydrology and Environment Monitoring (2001): Mongolia's Initial National Communication, Ulaanbaatar.

Nobre, C.A., Sellers, P.J., Shukla, J. (1991): Amazonian deforestation and regional climate change. *J. Climate*. **4**, 957–988.

Saandar, M. and Sugita, M. (2004): Digital Atlas of Mongolian Natural Environments, (1) Vegetation, Soil, Ecology and Water, CD-ROM, Monmap Engineering Service Co., Ltd, Ulaanbaatar 210646, Mongolia.

Shukla, J., Nobre, C., Sellers, P. (1990): Amazon deforestation and climate change. *Science*. 247, 1322–1325.

Sugita, M., Asanuma, J., Tsujimura, M., Mariko, M., Lu, M., Kimura, F., D. Azzaya, and Ts. Adyasuren. (2007): An overview of the rangelands atmosphere-hydrosphere-biosphere interaction study experiment in northeastern Asia (RAISE), *J. Hydrol*. **333**, 3-20.

Sugita, M. (2003): Interactions of water cycle processes and ecology. *Sci. J., KAGAKU*, **15**, 559-562. (in Japanese).

Suzuki, K. (2003): Present situation of agriculture in Mongolia. *Sci. J., Kagaku*. **73**, (5), 549-553. (in Japanese).

Toda, M. and Sugita, M. (2003): Single level turbulence measurements to determine

roughness parameters of complex terrain. *J. Geophys. Res.* **108(D12)**, 4363, doi:10.1029/2002JD002573.

Twine, T. E., W.P. Kustas, J.M. Norman, D.R. Cook, P.R. Houser, T.P. Meyers, J.H. Prueger, P.J. Starks, M.L. Wesely (2000): Correcting eddy-covariance flux underestimates over a grassland. *Agricultural and Forest Meteorol*. **103**, 279-300.

Urano, T.(2005): Seasonal Dynamics of Biomass and Carbon Dioxide Fluxes in a Mongolian Grassland. MS Thesis, University of Tsukuba, 45pp.

USDA Natural Resources Conservation Service (1997): National Range and Pasture Handbook.

Wesche, K. and Retzer, V. (2005): Is degradation a major problem in semi-desert environments of the Gobi region in southern Mongolia? *Erforsch. biol. Res. Mongolia*. **9**, 133–146.

Wright, I.R., Gash, J.H.C., Da Rocha, H.R., Shuttleworth, W.J., Nobre, C.A., Maitelli, G.T., Zamparoni, C.A.G.P., Carvalho, P.R.A. (1992): Dry season micrometeorology of central Amazonian ranchland. *Quart. J. Roy. Meteorol. Society*. **118**, 1083–1099.

Yatagai, A., and Yasunari, T. (1994): Trends and decadal-scale fluctuations of surface air temperature and precipitation over China and Mongolia during the recent 40 year period (1951-1990). *J. Meteorol. Society of Japan*. **72**, 937-957.

Zhu, Z.D., Wang, T. (1992): Theory and practice on sandy desertification in China. *J. Quat. Sci*. **2**, 97–106 (in Chinese with English abstract).